# DISSERTATION | DOCTORAL THESIS

Titel | Title

Long-term soil warming effects on root tissue and root exudate metabolic profiles and microbial necromass carbon in a temperate mountain forest

verfasst von | submitted by

Xiaofei Liu

angestrebter akademischer Grad | in partial fulfilment of the requirements for the degree of

Doctor of Philosophy (PhD)

Wien | Vienna, 2024

| | |
|---|---|
| Studienkennzahl lt. Studienblatt \| Degree programme code as it appears on the student record sheet: | UA 794 685 437 |
| Dissertationsgebiet lt. Studienblatt \| Field of study as it appears on the student record sheet: | Biologie |
| Betreut von \| Supervisor: | Univ.-Prof. Mag. Dr. Wolfgang Wanek |

# Table of Contents

Acknowledgments ..... 5

Abstract ..... 7

Zusammenfassung ..... 9

Overview of manuscripts ..... 11

Chapter I ..... 13

General introduction, thesis outline and main goals ..... 13

General introduction ..... 14

Thesis outline and main goals ..... 22

References ..... 24

Chapter II ..... 31

Long-term soil warming changes the profile of primary metabolites in fine roots of Norway Spruce in a temperate montane forest ..... 31

Abstract ..... 33

1 Introduction ..... 34

2 Materials and methods ..... 37

3 Results ..... 42

4 Discussion ..... 46

References ..... 53

Supplementary Material ..... 66

Chapter III ..... 75

The quantity and biochemical composition of root exudates is not affected by long-term soil warming in a temperate forest ..... 75

Abstract ..... 77

Introduction ..... 78

Materials and Methods ..... 83

Results ..... 89

Discussion ..... 91

Conclusion ..... 98

References ..... 100
Supplement material ..... 113
Chapter IV ..... 119
Long-term soil warming decreases soil microbial necromass carbon by adversely affecting its production and decomposition ..... 119
Abstract ..... 121
Introduction ..... 122
Materials and methods ..... 125
Results ..... 131
Discussion ..... 133
Conclusion ..... 139
Reference ..... 140
Supplementary Material ..... 152
Chapter V ..... 156
Summary ..... 156

# Acknowledgments

First and foremost, I would like to express my deepest gratitude to my advisor, Prof. Wolfgang Wanek, for giving me the opportunity to complete my doctoral research within his group. His guidance, insight, and unwavering support were instrumental in the completion of this dissertation. His expertise and dedication to my academic development have been invaluable, and I am immensely grateful for his encouragement during challenging times.

I am also thankful to my dissertation committee members, Dr. Frank Hagedorn and Dr. Dagmar Woebken, for their constructive feedback and thought-provoking questions, which significantly contributed to improving the quality of this research.

Special thanks to my colleagues and friends in the Achenkirch soil warming project. Their camaraderie and willingness to collaborate have been crucial in fostering a productive and supportive environment that enabled my professional and personal growth throughout the experiment's conduction and the manuscript writing process.

I am deeply grateful for the opportunity to work in the Terrestrial Ecosystem Research lab (TER). My heartfelt thanks go out to all the TERies for collaboratively creating an exceptional work environment, making lab work seamless, and developing and sharing methodologies that have enabled me to build upon the achievements of giants. Their dedication to scientific discussions broadened my perspective, and their supportive and welcoming atmosphere provided me with strong professional relationships and lasting friendships that enriched my Ph.D. work.

I also want to express my heartfelt gratitude to my dear friends Xu, Mengyuan, Min, Tao, and Yuhua in Vienna. They provided me with the best emotional support when I encountered both happy and challenging moments in my work and life.

Lastly, I am incredibly fortunate to have a loving family that has supported me unconditionally throughout this journey. Thank you to my wife, Dandan Bai, and my daughter, Tongyou Liu, for believing in me and instilling the values of perseverance and dedication that have shaped my academic pursuits. You've both been my rock, providing unwavering patience, understanding, and motivation every step of the way. To my mom, thank you for your countless help with my small family, especially by caring for my daughter while I pursued my Ph.D. in Vienna.

# Abstract

Climate warming significantly challenges temperate forests, impacting tree root metabolism and altering the release of primary metabolites in root exudates, essential for plant growth and rhizosphere interactions and highly sensitive to temperature variations. This warming may also affect the fate of microbial necromass carbon, a substantial part of soil organic carbon in forest ecosystems, but the full extent and implications of these changes are yet to be completely understood. We conducted a study to explore the effects of long-term soil warming (>14 years, with a temperature increase of +4 °C) on the metabolome of fine root tissues and root exudates in an old spruce forest located in Achenkirch, a temperate region of the Austrian Alps. Covering three seasons (spring, summer, and autumn) across two years (2020 and 2021), this study utilized a liquid chromatography-mass spectrometry platform for primary metabolite analysis. Additionally, we examined the dynamics of microbial necromass carbon in 0-10 cm and 10-20 cm soil layers. We found that soil warming led to a considerable increase in the concentration of amino acids (15%) and sugars (21%) in root tissue metabolites, but not organic acids. This suggests that trees under warming conditions sustain enhanced growth, respiration, and nutrient uptake without down-regulation of primary metabolism. Notably, the changes in primary metabolite profiles were not driven by single compounds but by a general up- or downregulation of most primary metabolites. Regarding root exudates, we observed that their rates and profiles showed no significant response to long-term soil warming, though seasonal variations were evident. Root exudates profiles could be partly predicted by soil temperature, root diameter, and specific root length, indicating a complex interaction between root tissue metabolism and environmental factors. Furthermore, our study revealed that soil warming resulted in a notable decrease in microbial necromass carbon, with reductions of 11% in the upper soil layer (0-10 cm) and 33% in the lower layer (10-20 cm). This reduction is primarily attributed to a decline in microbial biomass carbon and microbial carbon use efficiency, exacerbated by limited soil phosphorus availability. Additionally, warming increased the activity of specific soil extracellular enzymes, accelerating microbial necromass carbon decomposition. These results indicate a decoupling of microbial necromass carbon formation and decomposition under climate

warming, potentially impacting soil organic carbon content in temperate forests. Overall, our research provides critical insights into the complex effects of long-term soil warming on different aspects of tree root tissue and root exudates metabolism and microbial necromass carbon dynamics in temperate forest ecosystems, highlighting the intricate responses of these systems to climate warming.

# Zusammenfassung

Die Klimaerwärmung stellt gemäßigte Wälder vor erhebliche Herausforderungen. Er beeinträchtigt u.a. den Stoffwechsel der Baumwurzeln und verändert die Freisetzung primärer Metaboliten in Wurzelexsudaten, die für das Pflanzenwachstum und die Wechselwirkungen in der Rhizosphäre essenziell sind. Diese Metaboliten reagieren äußerst empfindlich auf Temperaturschwankungen. Diese Erwärmung kann auch das Schicksal von mikrobiellem Nekromasse Kohlenstoff beeinflussen, einem wesentlichen Bestandteil des organischen Kohlenstoffs im Boden von Waldökosystemen. Jedoch sind die vollen Ausmaße und die Auswirkungen dieser Veränderungen noch nicht vollständig verstanden. In unserer Studie untersuchten wir die Auswirkungen einer langfristigen Bodenerwärmung (>14 Jahre, mit einer Temperaturerhöhung von +4 °C) auf das Metabolom von Feinwurzelgewebe und Wurzelexsudaten in einem alten Fichtenwald in Achenkirch, einer gemäßigten Region der österreichischen Alpen. Die Studie umfasste drei Jahreszeiten (Frühling, Sommer und Herbst) über zwei Jahre (2020 und 2021) und nutzte eine Flüssigchromatographie-Massenspektrometrie-Plattform zur Analyse primärer Metaboliten. Zusätzlich untersuchten wir die Dynamik des mikrobiellen Nekromasse Kohlenstoffs in den Bodenhorizonten von 0-10 cm und 10-20 cm Tiefe. Unsere Ergebnisse zeigten, dass die Bodenerwärmung zu einem erheblichen Anstieg des Gehalts an Aminosäuren (15 %) und Zuckern (21 %) in den Metaboliten des Wurzelgewebes führte, nicht jedoch an organischen Säuren. Dies legt nahe, dass Bäume unter Erwärmungsbedingungen ein gesteigertes Wachstum, eine erhöhte Atmung und eine verbesserte Nährstoffaufnahme aufrechterhalten, ohne den primären Stoffwechsel herunterzufahren. Bemerkenswert war, dass die Veränderungen im Metabolitenprofil nicht durch einzelne Verbindungen, sondern durch eine allgemeine Auf- oder Abregulierung der meisten primären Metaboliten bedingt waren. In Bezug auf die Wurzelexsudate stellten wir fest, dass ihre Raten und Zusammensetzung keine signifikante Reaktion auf die langfristige Bodenerwärmung zeigten, obwohl saisonale Schwankungen offensichtlich waren. Die Zusammensetzung der Wurzelexsudate ließ sich teilweise durch die Bodentemperatur, den Wurzeldurchmesser und die spezifische Wurzellänge vorhersagen, was auf eine komplexe Interaktion zwischen dem Stoffwechsel des Wurzelgewebes und Umweltfaktoren hinweist.

Darüber hinaus ergab unsere Studie, dass die Bodenerwärmung zu einem deutlichen Rückgang des mikrobiellen Nekromasse-Kohlenstoffs führte, mit einer Reduktion von 11 % in der oberen Bodenschicht (0-10 cm) und 33 % in der unteren Schicht (10-20 cm). Dieser Rückgang ist in erster Linie auf einen Rückgang der mikrobiellen Biomasse und der mikrobiellen Kohlenstoffnutzungseffizienz zurückzuführen, was durch einen begrenzten Phosphoranteil im Boden verstärkt wird. Zudem erhöhte die Erwärmung die Aktivität bestimmter extrazellulärer Enzyme im Boden, wodurch der Abbau des mikrobiellen Nekromasse-Kohlenstoffs beschleunigt wurde. Diese Ergebnisse weisen auf eine Entkopplung der mikrobiellen Nekromasse-Kohlenstoffbildung und des -abbaus unter Klimaerwärmung hin, was sich möglicherweise auf den organischen Kohlenstoffgehalt im Boden gemäßigter Wälder auswirkt. Insgesamt bietet unsere Forschung entscheidende Einblicke in die komplexen Auswirkungen einer langfristigen Bodenerwärmung auf verschiedene Aspekte des Stoffwechsels von Baumwurzelgewebe und Wurzelexsudaten sowie der Dynamik des mikrobiellen Nekromasse-Kohlenstoffs in gemäßigten Waldökosystemen und hebt die komplexen Reaktionen dieser Systeme auf die Klimaerwärmung hervor.

# Overview of manuscripts

**Chapter II**

**Manuscript title:** Long-term soil warming changes the profile of primary metabolites in fine roots of Norway Spruce in a temperate montane forest

**Authors:** Xiaofei Liu, Jakob Heinzle, Ye Tian, Erika Salas, Steve Kwatcho-Kengdo, Werner Borken, Andreas Schindlbacher, Wolfgang Wanek

**Reference:** Submitted manuscript

**Author contributions:** WW, AS, and WB designed the study. XF, JH, YT, SKK, WW, AS, and WB implemented the field experiment. XF, ES, and WW conducted the lab experiment. XF performed data analysis and wrote the manuscript, with the contributions of all co-authors.

**Chapter III**

**Manuscript title:** The quantity and biochemical composition of root exudates is not affected by long-term soil warming in a temperate forest

**Authors:** Xiaofei Liu, Jakob Heinzle, Ye Tian, Erika Salas, Steve Kwatcho-Kengdo, Werner Borken, Andreas Schindlbacher, Wolfgang Wanek

**Reference:** Draft manuscript

**Author contributions:** WW, AS, and WB designed the study. XF, JH, YT, SKK, WW, AS, and WB implemented the field experiment. XF, ES, and WW conducted the lab experiment. XF performed data analysis and wrote the manuscript, with the contributions of all co-authors.

**Chapter IV**

**Manuscript title:** Long-term soil warming decreases soil microbial necromass carbon by adversely affecting its production and decomposition

**Authors:** Xiaofei Liu, Jakob Heinzle, Ye Tian, Erika Salas, Steve Kwatcho-Kengdo, Werner Borken, Andreas Schindlbacher, Wolfgang Wanek

**Reference:** Submitted manuscript

**Author contributions:** WW, AS, and WB designed the study. XF, JH, YT, SKK, WW, AS, and WB implemented the field experiment. XF, ES, and WW conducted the lab experiment. XF performed data analysis and wrote the manuscript, with the contributions of all co-authors.

# Chapter I

# General introduction, thesis outline and main goals

## General introduction

### 1. The response of temperate forest ecosystems to climate warming

Temperate forests represent 25% of the earth's forests area and encompass 14% of the global forest carbon (C) stocks (Pan et al., 2011; Adams et al., 2019). They provide a suite of important ecosystem services, including timber products, clean water, and plant C sequestration that depend on underlying ecosystem processes related to C, water, and nutrient cycling (Pan et al., 2011; FAO, 2018; Manning et al., 2018). The Sixth IPCC Assessment Report projects a global surface temperature increase of 1.5 °C to 2 °C by the 21st century's end and a 1-2 °C rise in temperate forests from 1990 to 2050 (IPCC, 2023). In response to climate warming, plants can adjustment their physiological and phenological traits, such as development, photosynthesis, respiration, and metabolic rates, to cope with the stress environment (Gargallo-Garriga et al., 2015; Aidoo et al., 2016; Richardson et al., 2018; Drake et al., 2019; Dusenge et al., 2019; Furze et al., 2019; Nagele et al., 2022; Jiang et al., 2023). This alteration in plant physiology not only affects the C sink capacity of forests but also influences the quality and quantity of C input into soils through litterfall, root turnover, and root exudates, key inputs of fresh organic C to the soil organic C (SOC) pool (Lu et al., 2013; Giardina et al., 2014; Hartmann et al., 2020). Such changes in plants can have cascading effects on soil microbial communities and the decomposition of soil organic matter, including microbial necromass C (Figure 1).

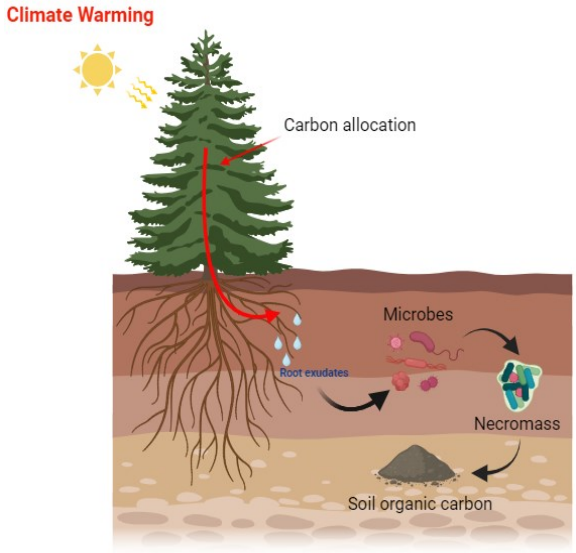


**Figure 1** A schematic of tree-soil-microbe interactions in response to climate warming

Many experimental studies have been using *in situ* (i.e., heat lamps, buried resistance cables or open top chambers) or *ex situ* (i.e., greenhouses and growth chambers) manipulations to better understand the potential effects of rising temperatures on temperate forest ecosystem processes, such as forest biomass accumulation (Reich et al., 2016; Lim et al., 2019), microbial community composition (Schindlbacher et al., 2011; DeAngelis et al., 2015), soil nutrient availability (Ueda et al., 2013; Tian et al., 2023b), and soil C dynamics on different timescales (Melillo et al., 2017). While these studies have provided crucial data on the impacts of climate warming on temperate forest ecosystems, there remains a gap in our understanding of specific ecosystem processes (Gargallo-Garriga et al., 2015; Berini et al., 2018), especially those occurring at the plant root-soil interface. The dynamics of metabolite composition of root tissues and root exudates and their subsequent influence on soil C pool dynamics, including the production and decomposition of microbial necromass C, are less explored (Jing et al., 2019). These processes are pivotal in regulating the SOC pool and the overall C budget of forest ecosystems. Comprehensive research focusing on these underrepresented processes is essential to predict the future role of temperate forests in global C cycling accurately. Such knowledge could lead to the development of targeted strategies to bolster the resilience of these forests through adaptive management practices that optimize C sequestration while maintaining ecosystem health and productivity.

## 2. Climate warming effects on primary metabolites in plant roots

Plants encounter a variety of biotic and abiotic stresses throughout their life cycle, with climate warming representing a significant environmental challenge (Atkin and Tjoelker, 2003; Anzano et al., 2022; Hong et al., 2022). This stress profoundly impacts plant metabolism, prompting an adaptive response through the modulation of metabolic pathways and the synthesis of a diverse array of chemical compounds (Dusenge et al., 2019; Sardans et al., 2020). These metabolites, classified into primary and secondary categories, play crucial roles in plant adaptation (Obata, 2019; Erb and Kliebenstein, 2020). Primary metabolites like sugars, amino acids, and organic acids are fundamental to plant growth, energy storage, and nutrient assimilation (Erb and Kliebenstein, 2020; Sardans et al., 2020). Secondary metabolites, including phenolics, flavonoids, and terpenoids, play a pivotal role in plant

defense mechanisms (Erb and Kliebenstein, 2020; Anzano et al., 2022). These phytochemicals serve as physical and chemical barriers against pathogens and herbivores, act as signaling molecules in plant interactions, and modulate relationships with various soil organisms.

In response to rising temperatures, plants engage in a warming response mechanism that encompasses alterations in gene expression, protein translation, and changes in metabolite and cell membrane lipid compositions (Escandon et al., 2018; Carrera et al., 2021; Li and Gaquerel, 2021). While numerous experimental studies, both *in situ* (using heat lamps and buried resistance cables) (Gargallo-Garriga et al., 2015; Gargallo-Garriga et al., 2017; Berini et al., 2018; Birami et al., 2020) and *ex situ* (in greenhouses, pots and growth chambers) (Escandon et al., 2017; Mokochinski et al., 2018), have focused on the effects of increased temperatures on the aboveground parts of plants with well-documented responses, the influence and response of plant roots to such temperature changes have received much less attention (Gargallo-Garriga et al., 2015). Recent research highlights the evolution of a "cry-for-help" strategy in plant roots, involving the recruitment of beneficial soil microorganisms to mitigate environmental stress damage (Rizaludin et al., 2021). Hence, a comprehensive understanding of how the metabolism of plant roots responds to climate change is crucial for developing strategies to improve plant resilience in changing climates. This is also important to understand whole plant performance, given that plant belowground C allocation is a plastic and key process of ecosystem C fluxes and that roots serve as the conduit to meet the plants demands for limiting belowground resources, particularly water and nutrients. On the other hand, roots link plant responses with soil (microbial) processes, therefore shaping a key interface in terrestrial ecosystems.

Elevated temperatures can stimulate root growth and activity (Jiang et al., 2022; Kwatcho Kengdo et al., 2022), leading to changes in the production and allocation of primary metabolites. Increased root growth under warming conditions is often associated with a greater demand for energy and C, resulting in altered carbohydrate metabolism in roots (Jiang et al., 2023). For instance, the levels of sugars like glucose and fructose in root tissues may increase to support enhanced growth and metabolic activities (Saddhe et al., 2021). This change in sugar concentration can also influence the osmotic potential of root cells, aiding in

maintaining water uptake under warming conditions (Nagele et al., 2022; Long and Adams, 2023). Amino acids, vital for protein synthesis and nitrogen metabolism, are also affected by climate warming (Aidoo et al., 2016; Galili et al., 2016). Elevated temperatures can alter the nitrogen assimilation pathways in plants, impacting the synthesis and distribution of amino acids in root tissues (Calleja-Cabrera et al., 2020). This change can influence root growth and function, as well as the plant's overall nitrogen use efficiency. Organic acids in roots, essential for amino acid and energy metabolism, and for nutrient uptake and soil interactions, may also show altered patterns under warming conditions (Lopez-Bucio et al., 2000; Jones et al., 2003). For instance, the production of organic acids like citrate and malate can be influenced by temperature-induced changes in soil nutrient availability, particularly in the availability of phosphorus and micronutrients (Yu et al., 2012). These organic acids play a critical role in mobilizing nutrients from the soil, and their altered production and exudation can affect nutrient dynamics in forest ecosystems. Moreover, climate warming can indirectly influence root primary metabolites through its impact on soil moisture and microbial communities (Berini et al., 2018). Changes in soil moisture due to increased evapotranspiration under warmer conditions can affect root water uptake and thus influence metabolic processes. Additionally, altered microbial activity in the soil can impact nutrient cycling, further influencing root metabolite profiles.

Understanding the effects of climate warming on root primary metabolites is therefore crucial, as these changes can have cascading effects on plant health, soil fertility, and ecosystem functioning. Ongoing research in this area is essential to predict and manage the impacts of climate change on plant-soil interactions in various ecosystems.

## 3. Climate warming effects on primary metabolites in plant root exudates

Plants allocate 20-40% of their freshly synthesized photosynthetic C to the soil in the form of root exudates (Badri and Vivanco, 2009; Brunn et al., 2022). These exudates are crucial for the soil ecosystems, as they impact soil nutrient cycling, microbial biomass, and their composition, and influence the overall soil C storage (Badri and Vivanco, 2009; Guyonnet et al., 2017; Canarini et al., 2019). Root exudates are a mix of a wide variety of compounds, including primary and secondary metabolites (see above) (Badri and Vivanco, 2009; Erb and

Kliebenstein, 2020). Research has made significant strides in identifying and quantifying these metabolites across various plant species, such as cottongrass (*Eriophorum vaginatum*) (Proctor and He, 2017), rice (Tawaraya et al., 2018), and *Ranunculus acris* (Williams et al., 2022). These studies have primarily focused on herbaceous plants and shrubs, while investigations involving woody species are comparatively sparse, with notable exceptions being Chinese fir (*Cunninghamia lanceolata*) (Xiong et al., 2023), *Quercus serrata* (Sun et al., 2021) and *Cinnamomum camphora* (Weinhold et al., 2021). The scarcity of research on the metabolite composition of root exudates from woody species underscores a crucial gap in our knowledge of root exudate composition dynamics in forest ecosystems. Considering the vital ecological roles of woody plants in terrestrial C sequestration and biodiversity (Pan et al., 2011; Adams et al., 2019), it is essential to undertake more extensive studies to better understand the diverse metabolites released by woody species under different environmental conditions.

The quantity and quality of root exudates can be affected by various abiotic and biological factors (Badri and Vivanco, 2009; Yin et al., 2013; Gargallo-Garriga et al., 2018; Sun et al., 2021; Williams et al., 2022; Rathore et al., 2023). One of the most studied abiotic factors influencing root exudates is temperature (Yin et al., 2013; Heinzle et al., 2023; Xiong et al., 2023), as it affects processes like photosynthesis, translocation, and respiration in plants (Cavaleri et al., 2015; Reich et al., 2018; Dusenge et al., 2019; Prescott et al., 2020). Research indicates that warmer temperatures can lead to a change in the release of certain metabolites from plant roots. For example, under heat stress maize roots showed a reduction in amino acid exudation but an increase in organic acid exudation (Tiziani et al., 2022). These organic acids are crucial for nutrient solubilization and chelation, making nutrients more available to plants (Lopez-Bucio et al., 2000; Jones et al., 2003) and potentially influencing the soil microbial community, as these compounds serve as energy sources for soil microorganisms (Badri and Vivanco, 2009; Guyonnet et al., 2017). However, most research has focused on specific metabolites and qualitative aspects (Escandon et al., 2018; Birami et al., 2020; Xiong et al., 2023), rather than studying the whole exudate metabolome quantitatively, particularly in comparison to the root metabolome composition (Gargallo-Garriga et al., 2015). Moreover, while previous studies have contributed to our knowledge of

the effects of warming on secondary metabolites in root exudates, our understanding of effects on primary metabolites, which have strong effects on soil organic matter decomposition by soil microbes, remains limited. Therefore, the role of primary metabolites in root exudates under climate warming deserves more attention. As we deepen our understanding of these processes, we can better predict and potentially mitigate the impacts of climate change on terrestrial ecosystems.

Acknowledging the influence of C supply in roots on the release of root exudates (Farrar et al., 2003; Dilkes et al., 2004; Canarini et al., 2019), there is still a gap in understanding the link between specific primary metabolites in root tissues and the composition of root exudates in the context of climate warming. Primary metabolites perform various functions in roots, such as osmotic regulation and energy production (Nagele et al., 2022; Long and Adams, 2023), while in exudates, they are essential for supporting microbial processes and facilitating nutrient mobilization (Badri and Vivanco, 2009; Canarini et al., 2019). The intricate dynamics between these metabolites in both root tissues and root exudates, particularly in response to climate warming, represent an important yet underexplored field for future research.

## 4. Climate warming effects on soil microbial necromass carbon

Microbial necromass carbon (MNC) in soil, primarily comprising the remains of fungi and bacteria, is a crucial precursor in the formation and stabilization of SOC, accounting for more than half of the SOC (Joergensen, 2018; Liang et al., 2019; Buckeridge et al., 2022). Given this substantial contribution, understanding the dynamics of MNC in response to climate change is essential for a comprehensive comprehension of SOC cycling in a warming world (Joergensen, 2018; Kästner et al., 2021; Buckeridge et al., 2022; Whalen et al., 2022).

Climate warming significantly impacts soil nutrient availability, especially N and phosphorus (P), and soil extracellular enzyme activity (EEA) (Bai et al., 2013; Fanin et al., 2022; Tian et al., 2023b), all of which can profoundly influence MNC dynamics. The alteration in soil N and P availability due to warming can either constrain or promote microbial activity, thereby affecting MNC accumulation (Ma et al., 2023; Wang et al., 2023; Zhang et al., 2023a). Furthermore, warming affects key microbial physiological traits such as

carbon use efficiency (CUE) and growth rate (Dove et al., 2021; Tian et al., 2023a; Zhang et al., 2023b), which are integral to the balance between MNC formation and decomposition (Buckeridge et al., 2022; Craig et al., 2022). Typically, microorganisms with higher CUE and faster turnover rates are promoting MNC accumulation (Prommer et al., 2020). However, these traits can also expedite MNC decomposition via priming effects, underscoring the intricate relationship between microbial physiology and MNC dynamics (Craig et al., 2022). Additionally, lab and field studies have observed that elevated temperatures increase maintenance costs for microbes, potentially reducing their CUE (Zhang et al., 2022). Soil EEA, particularly enzymes like N-acetylglucosaminidase which break down microbial residues, play a significant role in MNC decomposition (Fanin et al., 2022). Research has shown that soil enzymes in colder regions exhibit greater sensitivity to temperature increases compared to those in warmer regions, suggesting a latitude-specific response of soil EEA to climate warming (Chen et al., 2018; Fanin et al., 2022). However, the direct relationship between soil enzymes and MNC in the context of climate warming remains to be more comprehensively understood.

Overall, climate warming affects MNC through alterations in microbial physiology, nutrient availability, and soil enzyme activities. These changes underscore the need for further research to elucidate the nuanced relationships between these factors and MNC in the context of a warming climate.

## 5. Forest tree metabolomics approaches for global change studies

Metabolomics studies of trees have garnered momentum in recent years for their potential to elucidate tree responses to environmental stressors (Moore et al., 2014; Carrera et al., 2021; Jamloki et al., 2021; Walker et al., 2022). Specifically, in ecometabolomics, metabolomic techniques are applied to unravel molecular mechanisms governing the interactions of species with their abiotic and biotic environment across different spatial and temporal scales (Uthe et al., 2021). This field primarily relies on mass spectrometry (MS) techniques, notably gas chromatography-mass spectrometry (GC-MS) (Maridueña-Zavala et al., 2017) and liquid chromatography-mass spectrometry (LC-MS) (Liu and Rochfort, 2013), alongside with capillary electrophoresis (CE)-MS (Sato et al., 2004), Fourier-transform ion cyclotron

resonance (FT-ICR)-MS (Maia et al., 2023), and mass spectrometry imaging (MSI) (Bjarnholt et al., 2014). These methodologies enable extensive and in-depth metabolite analysis in diverse biological samples. Challenges in metabolomics include dealing with the diversity, complexity, and dynamic nature of metabolites in biological systems (Erb and Kliebenstein, 2020; Carrera et al., 2021; Hong et al., 2022; Walker et al., 2022). A key objective in plant metabolomics is to identify and quantify these complex compounds to reveal how plants respond to environmental changes, such as drought, temperature, and biotic stressors like pathogen and pest attacks (Escandon et al., 2017; Gargallo-Garriga et al., 2018; Birami et al., 2020; Tiziani et al., 2022). Analyses of primary metabolites and secondary metabolites have helped in constructing a detailed picture of how plants adapt to environmental pressures.

Climate warming, a key aspect of climate change, significantly threatens global forest productivity by affecting tree growth and survival (Reich et al., 2018; Furze et al., 2019; Pennisi, 2020). This situation underscores the importance of understanding the effects of climate warming on tree physiology and performance, which are intricately driven by and based on molecular networks (Gargallo-Garriga et al., 2015; Berini et al., 2018; Mokochinski et al., 2018; Jamloki et al., 2021). A growing body of work has employed targeted and/or non-targeted metabolomics techniques to investigate the metabolic adjustments in photosynthetic tissues and roots in plants under climate warming conditions (Gargallo-Garriga et al., 2015; Escandon et al., 2017; Berini et al., 2018; Mokochinski et al., 2018; Birami et al., 2020; Xiong et al., 2023). A common response across various plant species to warming or heat stress is the increased concentration of soluble sugars and amino acids (Gargallo-Garriga et al., 2015; Furze et al., 2019; Birami et al., 2020). The accumulation of primary metabolites, such as carbohydrates, in response to climate warming plays a crucial role in promoting the stability of protein structures and cell membrane bilayers under warming conditions (Birami et al., 2020; Hong et al., 2022; Long and Adams, 2023). While existing studies have shed light on how plant metabolite profiles change with warming, they have primarily utilized untargeted methods (Yu et al., 2012; Gargallo-Garriga et al., 2015; Escandon et al., 2017; Mokochinski et al., 2018; Birami et al., 2020; Xiong et al., 2023). These methods offer qualitative insights but lack often compound identification and

quantitative information, and they often focus more on secondary metabolites (Escandon et al., 2017; Berini et al., 2018; Mokochinski et al., 2018). This gap highlights the need for future research employing targeted metabolomic approaches to obtain robust quantitative multi-metabolite information. Such approaches could provide more precise, quantitative data on primary metabolites, offering a deeper understanding of the specific metabolic shifts and adaptations in plants due to climate warming. This direction in research is vital for developing comprehensive strategies to mitigate the impact of climate change on plant ecosystems, especially in forested areas.

In conclusion, ecometabolomics has emerged as a vital tool for understanding plant responses to global climatic changes and for identifying traits that could be crucial for future forest plant seedling selection. Moreover, ecometabolomic studies contribute significantly to predictions about potential shifts in plant community composition by comparing the acclimation capabilities of different species to environmental changes. These studies are increasingly becoming indispensable for ecologists and environmentalists, offering substantial insights and advancements in the field.

**Thesis outline and main goals**

The overall goal of this Ph.D. thesis is based on the second longest (>14 years) temperate forest soil warming manipulation experiment, which is located in Achenkirch, Tyrol, Austria, which will allow us to better understand how the primary metabolites of root tissues and root exudates respond and interact with long-term soil warming and season by targeted metabolomics, and how this affects the microbial necromass C response to long-term warming.

In the first sub-project (**Chapter 2**), we explored how long-term soil warming influences the primary metabolite profiles in the roots of mature spruce trees (*Picea abies* L.) in a temperate forest. Employing a targeted ecometabolomics approach, we assessed changes in both the concentration and profiles of root metabolites, such as amino acids, organic acids, and sugars. Our study objectives included determining if soil warming modifies the concentration of these metabolites as a reaction to altered temperature, root growth, respiration, and nutrient demand, and if it impacts the composition of these metabolites,

indicating stress adaptation pathways and highlighting specific metabolic pathways that are up-regulated or down-regulated in response to soil warming. This investigation aimed to advance our understanding of the adaptive responses of tree root systems to environmental changes, particularly to soil warming.

In the second sub-project (**Chapter 3**), we focused on how extended soil warming affects the rates and profiles of primary metabolites in root exudates. Our study had three main objectives: first, to determine if soil warming leads to an increase in the rates of primary metabolites in root exudates, such as organic acids, particularly since long-term soil warming reduced soil total P pools and subsequently soil P availability. Second, we aimed to explore whether variations in root exudation could be predicted based on changes in root morphology. Lastly, we hypothesized that root tissue and root exudates would exhibit distinct but correlated metabolite profiles, reflecting complex metabolic interactions that are affected by prolonged soil warming. This investigation sought to elucidate the adaptive mechanisms of root systems in response to long-term changes in soil temperature and nutrient availability.

In the third sub-project (**Chapter 4**), we examined the effects of long-term soil warming (over 14 years) on microbial necromass C dynamics and the underlying processes. In assessing microbial necromass C, we consider the impact of long-term soil warming on soil microbial traits (microbial biomass C, CUE, and turnover time), soil nutrients (N and P), and soil EEA to provide a depth-informed understanding of MNC dynamics. This investigation aimed to provide a deeper understanding of how prolonged soil warming influences microbial necromass C dynamics and the associated microbial processes in forest ecosystems.

## References


Adams, M.B., Kelly, C., Kabrick, J., Schuler, J., 2019. Chapter 6 - Temperate forests and soils, In: Busse, M., Giardina, C.P., Morris, D.M., Page-Dumroese, D.S. (Eds.), Developments in Soil Science. Elsevier, pp. 83-108.

Aidoo, M.K., Bdolach, E., Fait, A., Lazarovitch, N., Rachmilevitch, S., 2016. Tolerance to high soil temperature in foxtail millet (Setaria italica L.) is related to shoot and root growth and metabolism. Plant Physiology and Biochemistry 106, 73-81.

Anzano, A., Bonanomi, G., Mazzoleni, S., Lanzotti, V., 2022. Plant metabolomics in biotic and abiotic stress: a critical overview. Phytochemistry Reviews 21, 503-524.

Atkin, O.K., Tjoelker, M.G., 2003. Thermal acclimation and the dynamic response of plant respiration to temperature. Trends in Plant Science 8, 343-351.

Badri, D.V., Vivanco, J.M., 2009. Regulation and function of root exudates. Plant Cell Environment 32, 666-681.

Bai, E., Li, S., Xu, W., Li, W., Dai, W., Jiang, P., 2013. A meta-analysis of experimental warming effects on terrestrial nitrogen pools and dynamics. New phytologist 199, 441-451.

Berini, J.L., Brockman, S.A., Hegeman, A.D., Reich, P.B., Muthukrishnan, R., Montgomery, R.A., Forester, J.D., 2018. Combinations of Abiotic Factors Differentially Alter Production of Plant Secondary Metabolites in Five Woody Plant Species in the Boreal-Temperate Transition Zone. Frontiers in Plant Science 9, 1257.

Birami, B., Nagele, T., Gattmann, M., Preisler, Y., Gast, A., Arneth, A., Ruehr, N.K., 2020. Hot drought reduces the effects of elevated $CO_2$ on tree water-use efficiency and carbon metabolism. New phytologist 226, 1607-1621.

Bjarnholt, N., Li, B., D'Alvise, J., Janfelt, C., 2014. Mass spectrometry imaging of plant metabolites–principles and possibilities. Natural Product Reports 31, 818-837.

Brunn, M., Hafner, B.D., Zwetsloot, M.J., Weikl, F., Pritsch, K., Hikino, K., Ruehr, N.K., Sayer, E.J., Bauerle, T.L., 2022. Carbon allocation to root exudates is maintained in mature temperate tree species under drought. New phytologist 235, 965-977.

Buckeridge, K.M., Creamer, C., Whitaker, J., 2022. Deconstructing the microbial necromass continuum to inform soil carbon sequestration. Functional Ecology 36, 1396-1410.

Calleja-Cabrera, J., Boter, M., Oñate-Sánchez, L., Pernas, M., 2020. Root Growth Adaptation to Climate Change in Crops. Frontiers in Plant Science 11.

Canarini, A., Kaiser, C., Merchant, A., Richter, A., Wanek, W., 2019. Root Exudation of Primary Metabolites: Mechanisms and Their Roles in Plant Responses to Environmental Stimuli. Frontires in Plant Science 10, 157.

Carrera, F.P., Noceda, C., Maridueña-Zavala, M.G., Cevallos-Cevallos, J.M., 2021. Metabolomics, a Powerful Tool for Understanding Plant Abiotic Stress. Agronomy-Basel 11, 824.

Cavaleri, M.A., Reed, S.C., Smith, W.K., Wood, T.E., 2015. Urgent need for warming experiments in tropical forests. Global Change Biology 21, 2111-2121.

Chen, J., Luo, Y., Garcia-Palacios, P., Cao, J., Dacal, M., Zhou, X., Li, J., Xia, J., Niu, S., Yang, H., Shelton, S., Guo, W., van Groenigen, K.J., 2018. Differential responses of carbon-degrading enzyme activities to warming: Implications for soil respiration. Global Change Biology 24, 4816-4826.

Craig, M.E., Geyer, K.M., Beidler, K.V., Brzostek, E.R., Frey, S.D., Stuart Grandy, A., Liang, C., Phillips, R.P., 2022. Fast-decaying plant litter enhances soil carbon in temperate forests but not through microbial physiological traits. Nature Communications 13, 1229.

DeAngelis, K.M., Pold, G., Topcuoglu, B.D., van_Diepen, L.T.A., Varney, R.M., Blanchard, J., Melillo, J., Frey, S., 2015. Long-term forest soil warming alters microbial communities in temperate forest soils. Frontiers in Microbiology 6, 104.

Dilkes, N.B., Jones, D.L., Farrar, J., 2004. Temporal dynamics of carbon partitioning and rhizodeposition in wheat. Plant Physiology 134, 706-715.

Dove, N.C., Torn, M.S., Hart, S.C., Tas, N., 2021. Metabolic capabilities mute positive response to direct and indirect impacts of warming throughout the soil profile. Nature Communications 12, 2089.

Drake, J.E., Furze, M.E., Tjoelker, M.G., Carrillo, Y., Barton, C.V.M., Pendall, E., 2019. Climate warming and tree carbon use efficiency in a whole-tree $^{13}CO_2$ tracer study. New phytologist 222, 1313-1324.

Dusenge, M.E., Duarte, A.G., Way, D.A., 2019. Plant carbon metabolism and climate change: elevated $CO_2$ and temperature impacts on photosynthesis, photorespiration and respiration. New phytologist 221, 32-49.

Erb, M., Kliebenstein, D.J., 2020. Plant Secondary Metabolites as Defenses, Regulators, and Primary Metabolites: The Blurred Functional Trichotomy. Plant Physiology 184, 39-52.

Escandon, M., Meijon, M., Valledor, L., Pascual, J., Pinto, G., Canal, M.J., 2018. Metabolome Integrated Analysis of High-Temperature Response in Pinus radiata. Frontiers in Plant Science 9, 485.

Escandon, M., Valledor, L., Pascual, J., Pinto, G., Canal, M.J., Meijon, M., 2017. System-wide analysis of short-term response to high temperature in Pinus radiata. Journal of Experimental Botany 68, 3629-3641.

Fanin, N., Mooshammer, M., Sauvadet, M., Meng, C., Alvarez, G., Bernard, L., Bertrand, I., Blagodatskaya, E., Bon, L., Fontaine, S., Niu, S.L., Lashermes, G., Maxwell, T.L., Weintraub, M.N., Wingate, L., Moorhead, D., Nottingham, A.T., 2022. Soil enzymes in response to climate warming: Mechanisms and feedbacks. Functional Ecology 36, 1378-1395.

FAO, F., 2018. The state of the world's forests 2018—forest pathways to sustainable development. UN.

Farrar, J., Hawes, M., Jones, D., Lindow, S., 2003. How roots control the flux of carbon to the rhizosphere. Ecology 84, 827-837.

Furze, M.E., Huggett, B.A., Aubrecht, D.M., Stolz, C.D., Carbone, M.S., Richardson, A.D., 2019. Whole-tree nonstructural carbohydrate storage and seasonal dynamics in five temperate species. New phytologist 221, 1466-1477.

Galili, G., Amir, R., Fernie, A.R., 2016. The Regulation of Essential Amino Acid Synthesis and Accumulation in Plants. Annual Review of Plant Biology 67, 153-178.

Gargallo-Garriga, A., Ayala-Roque, M., Sardans, J., Bartrons, M., Granda, V., Sigurdsson, B.D., Leblans, N.I.W., Oravec, M., Urban, O., Janssens, I.A., Penuelas, J., 2017. Impact of Soil Warming on the Plant Metabolome of Icelandic Grasslands. Metabolites 7, 44.

Gargallo-Garriga, A., Preece, C., Sardans, J., Oravec, M., Urban, O., Penuelas, J., 2018. Root exudate metabolomes change under drought and show limited capacity for recovery. Scientific reports 8, 12696.

Gargallo-Garriga, A., Sardans, J., Perez-Trujillo, M., Oravec, M., Urban, O., Jentsch, A., Kreyling, J., Beierkuhnlein, C., Parella, T., Penuelas, J., 2015. Warming differentially influences the effects of drought on stoichiometry and metabolomics in shoots and roots. New phytologist 207, 591-603.

Giardina, C.P., Litton, C.M., Crow, S.E., Asner, G.P., 2014. Warming-related increases in soil CO2 efflux are explained by increased below-ground carbon flux. Nature Climate Change 4, 822-827.

Guyonnet, J.P., Vautrin, F., Meiffren, G., Labois, C., Cantarel, A.A.M., Michalet, S., Comte, G., Haichar, F.E.Z., 2017. The effects of plant nutritional strategy on soil microbial denitrification activity through rhizosphere primary metabolites. FEMS Microbiology Ecology 93.

Hartmann, H., Bahn, M., Carbone, M., Richardson, A.D., 2020. Plant carbon allocation in a changing world - challenges and progress: introduction to a Virtual Issue on carbon allocation: Introduction to a virtual issue on carbon allocation. New phytologist 227, 981-988.

Heinzle, J., Liu, X.F., Tian, Y., Kengdo, S.K., Heinze, B., Nirschi, A., Borken, W., Inselsbacher, E., Wanek, W., Schindlbacher, A., 2023. Increase in fine root biomass enhances root exudation by long-term soil warming in a temperate forest. Frontiers in Forests and Global Change 6.

Hong, Y., Zhou, Q., Hao, Y., Huang, A.C., 2022. Crafting the plant root metabolome for improved microbe-assisted stress resilience. New phytologist 234, 1945-1950.

IPCC, 2023. Climate Change 2022 - Mitigation of Climate Change: Working Group III Contribution to the Sixth Assessment Report of the Intergovernmental Panel on Climate Change. Cambridge University Press, Cambridge.

Jamloki, A., Bhattacharyya, M., Nautiyal, M.C., Patni, B., 2021. Elucidating the relevance of high temperature and elevated $CO_2$ in plant secondary metabolites (PSMs) production. Heliyon 7, e07709.

Jiang, Q., Jia, L., Chen, Y., Yang, Z., Chen, S., Xiong, D., Liu, X., Wang, X., Yao, X., Chen, T., Fan, A., Wu, D., Chen, G., Yang, Y., 2023. Substrate and adenylate limit subtropical tree fine-root respiration under soil warming. Plant Cell Environment 46, 2827-2840.

Jiang, Q., Jia, L.Q., Wang, X.H., Chen, W.Y., Xiong, D.C., Chen, S.D., Liu, X.F., Yang, Z.J., Yao, X.D., Chen, T.T., Fan, A.L., Chen, G.S., Yang, Y.S., 2022. Soil warming alters fine root lifespan, phenology, and architecture in a Cunninghamia lanceolata plantation. Agricultural and Forest Meteorology 327, 109201.

Jing, Y.L., Wang, Y., Liu, S.R., Zhang, X.D., Wang, Q.K., Liu, K., Yin, Y., Deng, J.F., 2019. Interactive effects of soil warming, throughfall reduction, and root exclusion on soil microbial community and residues in warm-temperate oak forests. Applied Soil Ecology 142, 52-58.

Joergensen, R.G., 2018. Amino sugars as specific indices for fungal and bacterial residues in soil. Biology and Fertility of Soils 54, 559-568.

Jones, D.L., Dennis, P.G., Owen, A.G., van Hees, P.A.W., 2003. Organic acid behavior in soils – misconceptions and knowledge gaps. Plant and Soil 248, 31-41.

Kästner, M., Miltner, A., Thiele-Bruhn, S., Liang, C., 2021. Microbial Necromass in Soils—Linking Microbes to Soil Processes and Carbon Turnover. Frontiers in Environmental Science 9.

Kwatcho Kengdo, S., Persoh, D., Schindlbacher, A., Heinzle, J., Tian, Y., Wanek, W., Borken, W., 2022. Long-term soil warming alters fine root dynamics and morphology, and their ectomycorrhizal fungal community in a temperate forest soil. Global Change Biology 28, 3441-3458.

Li, D., Gaquerel, E., 2021. Next-Generation Mass Spectrometry Metabolomics Revives the Functional Analysis of Plant Metabolic Diversity. Annual Review of Plant Biology 72, 867-891.

Liang, C., Amelung, W., Lehmann, J., Kastner, M., 2019. Quantitative assessment of microbial necromass contribution to soil organic matter. Global Change Biology 25, 3578-3590.

Lim, H., Oren, R., Näsholm, T., Strömgren, M., Lundmark, T., Grip, H., Linder, S., 2019. Boreal forest biomass accumulation is not increased by two decades of soil warming. Nature Climate Change 9, 49-52.

Liu, Z., Rochfort, S., 2013. A fast liquid chromatography-mass spectrometry (LC-MS) method for quantification of major polar metabolites in plants. Journal of Chromatography B 912, 8-15.

Long, R.W., Adams, H.D., 2023. The osmotic balancing act: When sugars matter for more than metabolism in woody plants. Global Change Biology 29, 1684-1687.

Lopez-Bucio, J., Nieto-Jacobo, M.F., Ramirez-Rodriguez, V.V., Herrera-Estrella, L., 2000. Organic acid metabolism in plants: from adaptive physiology to transgenic varieties for cultivation in extreme soils. Plant Science 160, 1-13.

Lu, M., Zhou, X., Yang, Q., Hui Li, Luo, Y., Fang, C., Chen, J., Yang, X., Li, B., 2013. Responses of ecosystem carbon cycle to experimental warming: a meta-analysis. Ecology 94, 726-738.

Ma, T., Yang, Z.Y., Shi, B.W., Gao, W.J., Li, Y.F., Zhu, J.X., He, J.S., 2023. Phosphorus supply suppressed microbial necromass but stimulated plant lignin phenols accumulation in soils of alpine grassland on the Tibetan Plateau. Geoderma 431, 116376.

Maia, M., Figueiredo, A., Cordeiro, C., Sousa Silva, M., 2023. FT-ICR-MS-based metabolomics: A deep dive into plant metabolism. Mass Spectrometry Reviews 42, 1535-1556.

Manning, P., van der Plas, F., Soliveres, S., Allan, E., Maestre, F.T., Mace, G., Whittingham, M.J., Fischer, M., 2018. Redefining ecosystem multifunctionality. Nature Ecology & Evolution 2, 427-436.

Maridueña-Zavala, M.G., Freire-Peñaherrera, A., Cevallos-Cevallos, J.M., Peralta, E.L., 2017. GC-MS metabolite profiling of Phytophthora infestans resistant to metalaxyl. European Journal of Plant Pathology 149, 563-574.

Melillo, J.M., Frey, S.D., DeAngelis, K.M., Werner, W.J., Bernard, M.J., Bowles, F.P., Pold, G., Knorr, M.A., Grandy, A.S., 2017. Long-term pattern and magnitude of soil carbon feedback to the climate system in a warming world. Science 358, 101-105.

Mokochinski, J.B., Mazzafera, P., Sawaya, A., Mumm, R., de Vos, R.C.H., Hall, R.D., 2018. Metabolic responses of Eucalyptus species to different temperature regimes. J Integr Plant Biol 60, 397-411.

Moore, B.D., Andrew, R.L., Kulheim, C., Foley, W.J., 2014. Explaining intraspecific diversity in plant secondary metabolites in an ecological context. New phytologist 201, 733-750.

Nagele, T., Gibon, Y., Le Hir, R., 2022. Plant sugar metabolism, transport and signalling in challenging environments. Physiologia plantarum 174, e13768.

Obata, T., 2019. Metabolons in plant primary and secondary metabolism. Phytochemistry Reviews 18, 1483-1507.

Pan, Y., Birdsey, R.A., Fang, J., Houghton, R., Kauppi, P.E., Kurz, W.A., Phillips, O.L., Shvidenko, A., Lewis, S.L., Canadell, J.G., Ciais, P., Jackson, R.B., Pacala, S.W., McGuire, A.D., Piao, S., Rautiainen, A., Sitch, S., Hayes, D., 2011. A large and persistent carbon sink in the world's forests. Science 333, 988-993.

Pennisi, E., 2020. Tropical forests store carbon despite warming. Science 368, 813.

Prescott, C.E., Grayston, S.J., Helmisaari, H.S., Kastovska, E., Korner, C., Lambers, H., Meier, I.C., Millard, P., Ostonen, I., 2020. Surplus Carbon Drives Allocation and Plant-Soil Interactions. Trends in ecology & evolution 35, 1110-1118.

Proctor, C., He, Y.H., 2017. Quantifying root extracts and exudates of sedge and shrub in relation to root morphology. Soil Biology and Biochemistry 114, 168-180.

Prommer, J., Walker, T.W.N., Wanek, W., Braun, J., Zezula, D., Hu, Y., Hofhansl, F., Richter, A., 2020. Increased microbial growth, biomass, and turnover drive soil organic carbon accumulation at higher plant diversity. Global Change Biology 26, 669-681.

Rathore, N., Hanzelkova, V., Dostalek, T., Semerad, J., Schnablova, R., Cajthaml, T., Munzbergova, Z., 2023. Species phylogeny, ecology, and root traits as predictors of root exudate composition. New phytologist 239, 1212-1224.

Reich, P.B., Sendall, K.M., Stefanski, A., Rich, R.L., Hobbie, S.E., Montgomery, R.A., 2018. Effects of climate warming on photosynthesis in boreal tree species depend on soil moisture. Nature 562, 263-267.

Reich, P.B., Sendall, K.M., Stefanski, A., Wei, X., Rich, R.L., Montgomery, R.A., 2016. Boreal and temperate trees show strong acclimation of respiration to warming. Nature 531, 633–636.

Richardson, A.D., Hufkens, K., Milliman, T., Aubrecht, D.M., Furze, M.E., Seyednasrollah, B., Krassovski, M.B., Latimer, J.M., Nettles, W.R., Heiderman, R.R., Warren, J.M., Hanson, P.J., 2018. Ecosystem warming extends vegetation activity but heightens vulnerability to cold temperatures. Nature 560, 368-371.

Rizaludin, M.S., Stopnisek, N., Raaijmakers, J.M., Garbeva, P., 2021. The Chemistry of Stress: Understanding the 'Cry for Help' of Plant Roots. Metabolites 11, 357.

Saddhe, A.A., Manuka, R., Penna, S., 2021. Plant sugars: Homeostasis and transport under abiotic stress in plants. Physiologia plantarum 171, 739-755.

Sardans, J., Gargallo-Garriga, A., Urban, O., Klem, K., Walker, T.W.N., Holub, P., Janssens, I.A., Penuelas, J., 2020. Ecometabolomics for a Better Understanding of Plant Responses and Acclimation to Abiotic Factors Linked to Global Change. Metabolites 10, 239.

Sato, S., Soga, T., Nishioka, T., Tomita, M., 2004. Simultaneous determination of the main metabolites in rice leaves using capillary electrophoresis mass spectrometry and capillary electrophoresis diode array detection. The Plant Journal 40, 151-163.

Schindlbacher, A., Rodler, A., Kuffner, M., Kitzler, B., Sessitsch, A., Zechmeister-Boltenstern, S., 2011. Experimental warming effects on the microbial community of a temperate mountain forest soil. Soil Biology and Biochemistry 43, 1417-1425.

Sun, L.J., Ataka, M., Kominami, Y., Yoshimura, K., Kitayama, K., 2021. Similar release pattern of two major groups of primary metabolites in root exudates of four coexisting canopy species. Rhizosphere 20, 100425.

Tawaraya, K., Horie, R., Wagatsuma, T., Saito, K., Oikawa, A., 2018. Metabolite profiling of shoot extract, root extract, and root exudate of rice under nitrogen and phosphorus deficiency. Soil Science and Plant Nutrition 64, 312-322.

Tian, Y., Schindlbacher, A., Malo, C.U., Shi, C.P., Heinzle, J., Kengdo, S.K., Inselsbacher, E., Borken, W., Wanek, W., 2023a. Long-term warming of a forest soil reduces microbial biomass and its carbon and nitrogen use efficiencies. Soil Biol Biochem 184, 109109.

Tian, Y., Shi, C., Malo, C.U., Kwatcho Kengdo, S., Heinzle, J., Inselsbacher, E., Ottner, F., Borken, W., Michel, K., Schindlbacher, A., Wanek, W., 2023b. Long-term soil warming decreases microbial phosphorus utilization by increasing abiotic phosphorus sorption and phosphorus losses. Nature Communications 14, 864.

Tiziani, R., Miras-Moreno, B., Malacrinò, A., Vescio, R., Lucini, L., Mimmo, T., Cesco, S., Sorgonà, A., 2022. Drought, heat, and their combination impact the root exudation patterns and rhizosphere microbiome in maize roots. Environmental and Experimental Botany 203, 105071.

Ueda, M.U., Muller, O., Nakamura, M., Nakaji, T., Hiura, T., 2013. Soil warming decreases inorganic and dissolved organic nitrogen pools by preventing the soil from freezing in a cool temperate forest. Soil Biology and Biochemistry 61, 105-108.

Uthe, H., van Dam, N.M., Hervé, M.R., Sorokina, M., Peters, K., Weinhold, A., 2021. Chapter Six - A practical guide to implementing metabolomics in plant ecology and biodiversity research, In: Pétriacq, P., Bouchereau, A. (Eds.), Advances in Botanical Research. Academic Press, pp. 163-203.

Walker, T.W.N., Alexander, J.M., Allard, P.-M., Baines, O., Baldy, V., Bardgett, R.D., Capdevila, P., Coley, P.D., David, B., Defossez, E., Endara, M.-J., Ernst, M., Fernandez, C., Forrister, D., Gargallo-Garriga, A., Jassey, V.E.J., Marr, S., Neumann, S., Pellissier, L., Peñuelas, J., Peters, K., Rasmann, S., Roessner, U., Sardans, J., Schrodt, F., Schuman, M.C., Soule, A., Uthe, H., Weckwerth, W., Wolfender, J.-L., van Dam, N.M., Salguero-Gómez, R., 2022. Functional Traits 2.0: The power of the metabolome for ecology. Journal of Ecology 110, 4-20.

Wang, K.K., Ren, T., Yan, J.Y., Lu, Z.F., Cong, R.H., Li, X.K., Lu, J.W., 2023. Soil phosphorus availability alters the effects of straw carbon on microbial mediated phosphorus conversion. Plant and Soil 491, 575-590.

Weinhold, A., Döll, S., Liu, M., Schedl, A., Pöschl, Y., Xu, X., Neumann, S., van Dam, N.M., 2021. Tree species richness differentially affects the chemical composition of leaves, roots and root exudates in four subtropical tree species. Journal of Ecology 110, 97-116.

Whalen, E.D., Grandy, A.S., Sokol, N.W., Keiluweit, M., Ernakovich, J., Smith, R.G., Frey, S.D., 2022. Clarifying the evidence for microbial- and plant-derived soil organic matter, and the path toward a more quantitative understanding. Global Change Biology 28, 7167-7185.

Williams, A., Langridge, H., Straathof, A.L., Muhamadali, H., Hollywood, K.A., Goodacre, R., de Vries, F.T., 2022. Root functional traits explain root exudation rate and composition across a range of grassland species. Journal of Ecology 110, 21-33.

Xiong, D.C., Huang, J.X., Lin, T.C., Liu, X.F., Xu, C., Chen, S.D., Yang, Z.J., Chen, G.S., Yang, Y.S., 2023. Warming Increased Metabolite Composition and Pathways in Root Exudates of Chinese Fir Saplings in Subtropical China. Journal of Soil Science and Plant Nutrition 23, 2545-2565.

Yin, H., Li, Y., Xiao, J., Xu, Z., Cheng, X., Liu, Q., 2013. Enhanced root exudation stimulates soil nitrogen transformations in a subalpine coniferous forest under experimental warming. Global Change Biology 19, 2158-2167.

Yu, J.J., Du, H.M., Xu, M., Huang, B.R., 2012. Metabolic Responses to Heat Stress under Elevated Atmospheric $CO_2$ Concentration in a Cool-season Grass Species. Journal of the American Society for Horticultural Science 137, 221-228.

Zhang, H.R., Yang, T., Wu, X.J., Zhang, J.W., Yu, X.Y., Zhou, J.X., Herath, S., Peng, X.W., 2023a. Phosphorus addition increases microbial necromass by increasing N availability in China: A meta-analysis. Applied Soil Ecology 190, 105009.

Zhang, Q., Qin, W., Feng, J., Li, X., Zhang, Z., He, J.-S., Schimel, J.P., Zhu, B., 2023b. Whole-soil-profile warming does not change microbial carbon use efficiency in surface and deep soils. Proceedings of the National Academy of Sciences 120, e2302190120.

Zhang, Q., Qin, W., Feng, J., Zhu, B., 2022. Responses of soil microbial carbon use efficiency to warming: Review and prospects. Soil Ecology Letters 4, 307-318.

# Chapter II

# Long-term soil warming changes the profile of primary metabolites in fine roots of Norway Spruce in a temperate montane forest

# Long-term soil warming changes the profile of primary metabolites in fine roots of Norway Spruce in a temperate montane forest

Xiaofei Liu[1,2,3], Jakob Heinzle[4], Ye Tian[1], Erika Salas[1], Steve Kwatcho-Kengdo[5], Werner Borken[5], Andreas Schindlbacher[4], Wolfgang Wanek[1]

[1]Division of Terrestrial Ecosystem Research, Department of Microbiology and Ecosystem Science, Center of Microbiology and Environmental Systems Science, University of Vienna, Djerassiplatz 1, 1030 Vienna, Austria;

[2]Doctoral School in Microbiology and Environmental Science, University of Vienna, Djerassiplatz 1, A-1030 Vienna, Austria;

[3]Key Laboratory of Humid Subtropical Eco-geographical Process of Ministry of Education, School of Geographical Sciences, Fujian Normal University, Fuzhou 350117, China;

[4]Department of Forest Ecology and Soils, Federal Research and Training Centre for Forests, Natural Hazards and Landscape-BFW, Seckendorff-Gudent Weg 8, 1131 Vienna, Austria;

[5]Department of Soil Ecology, Bayreuth Center of Ecology and Environmental Research (BAYCEER), University of Bayreuth, Dr.-Hans-Frisch-Straße 1-3, 95448, Bayreuth, Germany

**Abstract**

Climate warming poses major threats to temperate forests, but the response of tree root metabolism has largely remained unclear. We examined the impact of long-term soil warming (>14 years, +4 °C) on the fine root metabolome across three seasons for two years in an old spruce forest, using a liquid chromatography-mass spectrometry platform for primary metabolite analysis. A total of 44 primary metabolites were identified in roots (19 amino acids, 12 organic acids, and 13 sugars). Warming increased the concentration of total amino acids and of total sugars by 15% and 21%, respectively, but not organic acids. We found that soil warming and sampling date, along with their interaction, directly influenced the primary metabolite profiles. Specifically, in warming plots, concentrations of arginine, glycine, lysine, threonine, tryptophan, mannose, ribose, fructose, glucose, and oxaloacetic acid increased by 51.4%, 19.9%, 21.5%, 19.3%, 22.1%, 23.0%, 38.0%, 40.7%, 19.8%, and 16.7%, respectively. Rather than being driven by single compounds, changes in metabolite profiles reflected a general up- or downregulation of most metabolic pathway network. This emphasizes the importance of metabolomics approaches in investigating root metabolic pathways and understanding the effects of climate change on tree root metabolism.

**Keywords:** Soil warming, root metabolism, primary metabolites, temperate forest, sugars, amino acids, organic acids.

## 1 Introduction

Temperate forests cover approximately 16% of the global forest area and comprise 14% of global forest carbon (C) storage, with half of this C stored in the soil (Hansen et al., 2010; Pan et al., 2011). They provide valuable ecosystem services by acting as a net sink of atmospheric carbon dioxide ($CO_2$) thereby contributing to the mitigation of global climate warming. However, the impact of rising global temperatures on plant photosynthesis (Dusenge et al., 2019), C allocation (Furze et al., 2019), tree growth, and tree mortality (Yi et al., 2022) can have profound effects on forest structure, functioning, primary productivity, and C storage (Hansen et al., 2010; Dusenge et al., 2019). To cope with stress situations, plants have evolved a range of efficient mechanisms to rapidly respond to temperature changes (Abedini et al., 2021; Jamloki et al., 2021). For example, plants adapt to higher temperatures by synthesizing heat shock proteins to protect cellular proteins, adjusting membrane lipid compositions for cellular integrity, and accumulating osmoprotectants like proline and sugars for osmotic balance and protein stabilization (Simon & Adamczyk, 2019; Erb & Kliebenstein, 2020; Sardans et al., 2020). These strategies significantly impact the biosynthesis and regulation of primary metabolites—key to plant stress response—including essential amino acids, sugars, and organic acids (Gargallo-Garriga et al., 2017). This interplay between physiological adaptations and primary metabolite regulation is crucial for understanding plant responses to climate warming and predicting the adaptability of tree metabolic processes and forest ecosystems to future environmental challenges (Abedini et al., 2021; Jamloki et al., 2021). Insights into these dynamics can reveal critical aspects of tree physiology and the importance of metabolic flexibility in sustaining ecosystem resilience amidst climate change.

Recent studies suggested that primary metabolite profiles are sensitive to climate warming, but their response varied depending on plant species, plant organ, compound type, and the duration of warming exposure (Gargallo-Garriga et al., 2015; Gargallo-Garriga et al., 2017; Birami et al., 2020; Sytiuk et al.,2023). For instance, grass and herb metabolomes responded to moderate warming in subarctic grasslands by increases in malate and some amino acids (e.g. glutamic acid, glutamine, lysine, isoleucine) while sugars tended to decrease (Peñuelas

et al., 2013; Gargallo-Garriga et al., 2017). Interestingly, plant leaves (shoots) and roots exhibit markedly different responses to warming, a phenomenon rooted in their fundamentally different roles. Roots, acting as photosynthetic C sinks and being heterotrophic, absorb nutrients and water and, under conditions of (intermediate) warming, showed an increase in the concentrations of proteinogenic amino acids. Conversely, leaves (shoots), which function as photosynthetic C sources and being autotrophic, exhibited elevated levels of organic acids involved in energy metabolism in response to warming (Gargallo-Garriga et al., 2015; Birami et al., 2020). Moreover, seasonal changes significantly influence plant metabolite profiles. For instance, soluble sugars accumulated in response to diminished water availability in tropical regions during drier periods (Budzinski et al.,2016). Conversely, in periods of rapid growth like during summer or in the rainy season, plants increase the production of energy compounds by supporting processes like glycolysis, citric acid cycle and the mitochondrial electron transport chain (Budzinski et al.,2016; Prinsloo and Nogemane, 2018; Sytiuk et al.,2023).

While a range of studies have provided insight into how climate change affects plant primary metabolite profiles, they have largely focused on grasses, herbs, moss, and crops, and particularly on their photosynthetic tissues (Escandon et al., 2018; Jamloki et al., 2021; Rodrigues et al., 2021; Sytiuk et al.,2023). Therefore, there is a lack of understanding regarding how warming affects plant primary metabolite profiles in root tissues, and this particularly in woody species (Gargallo-Garriga et al., 2015), though they are key for forest C sequestration, forest ecosystem stability, and global climate change mitigation (Pan et al., 2011; Furze et al., 2019). Furthermore, the majority of these studies were conducted in lab incubation or pot experiments (Escandon et al., 2018; Rodrigues et al., 2021), which may not accurately reflect the response of plant primary metabolite profiles to warming under natural conditions. Despite the importance, no field warming experiments in forests have studied the warming effects on plant primary metabolite profiles in root tissues, and as such, there is a significant gap in knowledge on this topic.

Metabolomic techniques, such as gas chromatography-mass spectrometry (GC-MS) and liquid chromatography-mass spectrometry (LC-MS), are powerful tools for investigating the response of plants to environmental change at the metabolite level (Simon & Adamczyk, 2019; Sardans et al., 2020; Carrera et al., 2021; Escolà Casas & Matamoros, 2021), but have been underutilized in climate change research (Gargallo-Garriga et al., 2015; Berini et al., 2018; Escandon et al., 2018; Sardans et al., 2020; Rodrigues et al., 2021). So far most of these studies were performed with an untargeted metabolomics approach, which provides qualitative and relative quantitative data but not absolute quantification (Gargallo-Garriga et al., 2015; Gargallo-Garriga et al., 2017; Escandon et al., 2018). The complexity of analyzing a wide range of metabolites requires multiple analysis platforms and extensive chemical methods (Wang et al., 2018; Zhou et al., 2019). Here, targeted analysis using commercially available standards can provide reliable and sensitive identification, precise quantification, and combined with stable isotope tracing, flux measurements of specific compounds (Liu & Locasale, 2017; Carrera et al., 2021). Therefore, targeted metabolomics analysis can offer deeper insights into the specific responses of primary (and secondary) metabolism to global change drivers based on absolute quantitation, helping to better understand how plants regulate primary metabolism in response to climate change.

In this study, we used a targeted ecometabolomics approach to investigate how long-term soil warming affects the primary metabolite profiles in the fine roots of mature Norway spruce trees (*Picea abies* L. Karst) in a temperate mountain forest. Norway spruce is recognized as one of Europe's most important tree species due to its economic and ecological importance and exhibits considerable sensitivity to climate change, such as warming and drought (Hanewinkel et al., 2013; Bosela et al., 2021). Specifically, our research aimed to test two hypotheses: firstly, that soil warming leads to an increase in the concentration of primary root metabolites (amino acids, organic acids, and sugars) reflecting a general upregulation of plant primary metabolism under elevated temperatures (*H1*); and secondly, that soil warming selectively enhances specific metabolic pathways, resulting in a differentiated increase in certain primary metabolites (*H2*), to cope with altered nutrient and soil water constraints induced by soil warming.

## 2 Materials and methods

### 2.1 Study location and experimental design

This study was conducted in the Achenkirch soil warming experiment in a temperate montane forest located in the Austrian Alps (11°38′21″E; 47°34′50″N) at an elevation of 910 m a.s.l. The region, characterized by a temperate continental climate, had an average annual temperature of 7 °C and mean precipitation of 1698 mm from 2000-2019. In 2020, these values were 7 °C and 1580 mm, and 6 °C and 1844 mm in 2021 (Figure **S1**). The soils in the area have been classified as shallow Rendzic Leptosols, and the dominant tree species in the 140-year-old forest is Norway spruce (*Picea abies* L. H. *Karst.*), with subdominant European beech (*Fagus sylvatica* L.).

We utilized a paired plot design, with twelve paired 2 m x 2 m plots (warmed and unwarmed control) grouped into six blocks. Three blocks were established in 2004 and the other three in 2007. The two treatments, ambient temperature (control) and warming by +4 °C, were assigned to each pair of plots in each block. Soil warming cables (Etherma, Salzburg, Austria) were installed at a soil depth of 3 cm with 7.5 cm spacing in the warmed plots and in the control plots. Dummy cables were installed in control plots to mimic the disturbance effect created by cable installation. Soil temperature was recorded at half-hourly intervals at depths of 5 and 15 cm below the soil surface in control and warmed plots. Throughout the snow-free period (~April-December), the soil temperature in the warming plots was maintained at a constant 4.1 ± 0.1 °C higher than in the paired control plots at 5 cm soil depth across all sampling dates (Heinzle et al., 2023). After 14 years of soil warming, fine root biomass (FRB) and fine root production increased by 17% and 128%, respectively, while the total soil C, nitrogen (N), and phosphorus (P) levels decreased (Kwatcho Kengdo et al., 2022; Tian et al.,2023a, b).

### 2.2 Root sampling and root morphological measurements

Fine roots were collected in the spring (May 2021 and April 2022), summer (July 2021 and 2022), and autumn (October 2020 and 2021). In brief, during each sampling campaign two terminal fine root branches per plot, consisting of first to third order fine roots < 2 mm diameter and of 5–10 cm length, were excavated from the mineral soil depth of 3–5 cm,

carefully cleaned from soil and washed with deionized water. The roots were then used to measure root exudation in situ (Heinzle et al., 2023), thereafter cut, frozen on dry ice, transported to the laboratory in Vienna on dry ice, and immediately freeze-dried. A subsample of the same root branch adjacent to the root segment studied above was collected for genetic analysis of tree species affiliation. More than 95% of all fine root samples were assigned to Norway spruce, the rest showing mixed spruce-beech signals or being unidentifiable (Heinzle et al., 2023). Although root exudation was measured as part of the broader study, the primary focus of this specific research was on the analysis of root metabolites in response to soil warming; therefore, detailed methods pertaining to root exudate collection are not included in this report but are given elsewhere (Heinzle et al. 2023).

Root morphological traits, including root length, surface area, and volume, were measured in the same samples and the data published elsewhere (Heinzle et al., 2023). Consequently, the methodologies of these measurements are briefly outlined here, and are more extensively documented in the aforementioned study. The scanning and data evaluation for root morphological traits was performed with WinRHIZO 2004b (Regents Instruments Inc., Quebec, Canada). Additionally, we calculated root biomass-specific traits such as specific root length (SRL), specific root area (SRA), and root tissue density (RTD), which were derived as ratios of root dry mass to root biomass, area, and volume, respectively.

### 2.3 Extraction of low molecular weight compounds from root tissues

For metabolite analysis, freeze-dried roots were cut in small pieces and then ground to a fine powder in a ball mill (Retsch MM2, Hanau, Germany). To extract the root material, 20-40 mg of the ground (<10 µm) root material was weighed into 2 ml polypropylene screw-cap reaction vials. The root material was then extracted with 1.5 ml methanol/chloroform/Milli Q water (MCW, 12:3:5, v:v:v) for 30 min at 70 °C, with occasional vortexing of the vials. After the samples had cooled to room temperature, they were centrifuged at 10,000 *g* for 5 min, and 800 µl of the supernatant was transferred with a pipette into a new 2.0 ml reaction vial. To induce phase separation, 800 µl MQ and 250 µl chloroform were added to the reaction vial followed by vigorous mixing. The vial was then centrifuged at 10,000 *g* for 5 min to separate the lower chloroform and the upper aqueous methanol-water phases. For further purification

of the aqueous phase, 1.2 ml of the upper phase was transferred into a new 2.0 ml reaction vial, and 500 µl chloroform was added, mixed vigorously, and centrifuged at 10,000 *g* for two min to separate the phases. Finally, 1.0 ml of the upper phase was transferred into a new reaction vial and dried in a centrifugal vacuum concentrator at approximately 100 mbar (Speed Vac, Savant, Thermo Fisher). The residue was then redissolved in 1.0 ml MQ and used for primary metabolite analysis.

### 2.4 Analysis of low molecular weight compounds

#### 2.4.1 Amino acids

Amino acids were analyzed using UPLC-ESI-MS/MS (Ultimate 3000 UPLC instrument coupled via an electrospray ionization (ESI) inlet to Q Exactive Orbitrap HRMS system, Thermo Scientific) after derivatization with 6-Aminochinolyl-N-hydroxysuccinimidylcarbamat (AQC) reagent (Waters Corp., Milford, U.S.A.). The derivatized amino acids were separated on a 2.1 × 100 mm, 1.7 µm C18 reverse-phase column (AccQ-Tag$^{TM}$ ULTRA, Waters, USA). The separation gradient was: 0-0.5 min (constant 0.1% B), 0.5-2.5 min (increase to 5.0% B), 2.5-8 min (increase to 20% B), 8-8.25 min (constant 20% B), 8.25-11 min (decrease to 10% B), 11-11.2 min (decrease to 0.1% B) and 11.2-15 min (constant 0.1% B). The working eluent A was 0.01% formic acid in Milli Q water, eluent B was 100% acetonitrile, and the column flow rate was 0.4 ml min$^{-1}$. The autosampler temperature was set at 25 °C and the column temperature at 55 °C. The sample injection volume was 1 µl. All samples were analyzed in the positive (+) ESI mode with the following Orbitrap parameters: spray voltage 3 kV, capillary temperature 320 °C, resolution 70,000, and mass scan range 50-750 m/z for full scan analysis.

#### 2.4.2 Organic acids

Organic acids were analyzed without derivatization, directly by separation on a Dionex ICS-5000 analytical ion chromatography system (Dionex, Thermo Scientific, Sunnyvale, CA) with conductivity detection and coupled to a Q Exactive Orbitrap mass spectrometer (Thermo Scientific, Waltham, MA, USA). Organic acids were separated on a Dionex IonPac AS11-HC analytical column (2 × 250 mm) with a Dionex IonPa AS11-HC Guard Column (2 × 50 mm),

using a gradient of 1 to 85 mM KOH at a flow rate of 0.3 ml $min^{-1}$ and a column temperature of 30 °C. The injection volume was set to 10 µl. The samples were analyzed in the negative (-) ESI mode with the following Orbitrap parameters: spray voltage 3 kV, capillary temperature 320 °C, resolution 70,000, and mass scan range 50-750 m/z for full scan analysis. Formic acid was quantified using conductivity detection through Chromeleon 7.2 software (Thermo Fisher Scientific) because its mass was lower than the Orbitrap lower mass detection limit of m/z 50, while other organic acids were quantified by mass spectrometry using Freestyle 1.7 software (Thermo Scientific).

### 2.4.3 Sugars

Sugars were analyzed using UPLC-ESI-MS/MS (Ultimate 3000 UPLC instrument coupled to a Q Exactive Orbitrap HRMS system, Thermo Scientific) after derivatization with 1-phenyl-3-methyl-5-pyrazolone (PMP) (Salas et al., 2023). Briefly, aliquots (100 µl) of sample or standard were derivatized by addition of 100 µl 0.5 M PMP. Derivatized samples were passed through 0.22 µm LC syringe filters with cellulose acetate membrane (VWR International™) for LC-MS analysis. The chromatographic separation was conducted on a 2.1 × 100 mm, 1.7 µm C18 reverse-phase column (AccQ-Tag$^{TM}$ ULTRA, Waters, USA), using a mobile phase of 20 mM ammonium acetate (solvent A) and acetonitrile (solvent B) at a flow rate of 0.3 ml $min^{-1}$. The injection volume was 2 µl, and the column temperature was set at 35 °C. The separation gradient used was: 0-0.5 min (constant 13% B), 0.5-2 min (increase to 16% B), 2-15 min (increase to 21% B), 15-16 min (increase to 60% B), 16-17 min (increase to 90% B), 17-20 min (decrease to 13% B) and 20-25 min (constant 13% B for column re-equilibration). The samples were analyzed in the positive (+) ESI mode with the following Orbitrap parameters: spray voltage 3.5 kV, capillary temperature 300 °C, resolution 70,000, and mass scan range 50-1000 m/z for full scan analysis.

Fructose, sucrose, and raffinose were analyzed separately using a Dionex ICS-5000 ion chromatography system (Thermo Scientific) without PMP derivatization, due to their non-reducing nature and lower keto group reactivity. These sugars were separated on a CarboPac PA20 column and quantified by pulsed amperometric detection. The separation gradient was as follows: 0-15 min (constant 20 mM KOH), 15-20 min (increase to 100 mM KOH), 20-25

min (constant 100 mM KOH) and 25-30 min (decrease to 20 mM KOH). The flow rate was 0.3 ml $min^{-1}$, the column temperature was 30 °C, and the injection volume was 10 µl.

### 2.5 Data analysis

Data processing and statistical analysis were conducted using R 4.0.3 (R Core team, 2019). The data on the concentration of metabolites were checked manually for outliers and if necessary, to obtain homoscedasticity and normality, log- or sqrt-transformation were applied. For analyzing the main and interactive effects of sampling date, year, and warming treatment, we applied linear mixed-effects models. We treated warming, sampling date, and year as fixed factors, while considering block and warming duration as random factors for all measured parameters. When interactions were statistically significant ($P < 0.05$), we employed Tukey post-hoc tests to investigate group-specific differences. To account for the false discovery rate (FDR) arising from multiple comparisons, we corrected the raw p-values using the Benjamini-Hochberg (BH) procedure via the R function '*p.adjust*()'.

To assess whether the primary metabolite profiles differed between control and warming treatments, we performed non-parametric analysis of dissimilarity using Permutational Multivariate Analysis of Variance (PERMANOVA), using the ADONIS procedure and Bray-Curtis distances. We chose PERMANOVA as it allows analysis of effects of multiple main effects including their interactions. Due to the sensitivity of PERMANOVA for inhomogeneities in dispersion among groups (similar to variance inhomogeneity), we analyzed the homogeneity of dispersions across treatments, employing a distance-based test (PERMDISP, Anderson., 2008). We measured dispersions as distances of points to the centroid, and each term in the analysis was subjected to 9999 permutations to test for differences in dispersion. Moreover, we used Non-metric Multidimensional Scaling (NMDS) to visualize differences of primary metabolite profiles in roots among treatments, sampling date. To analyze the compounds association to NMDS axes a spearman correlation was conducted between compound-specific values and the respective NMDS 1 and 2 axis scores. To examine the association between root morphological traits and soil environmental factors (soil temperature and soil moisture) with the metabolome ordination generated by NMDS, linear regression analyses were conducted. This analysis focused on assessing the relationship

between these biological and environmental variables and the scores derived from the first two axes (NMDS1 and NMDS2) of the NMDS analysis. All these analyses were conducted with the "vegan" and "corrplot" packages in R.

Metaboanalyst 5.0 (https://www.metaboanalyst.ca/MetaboAnalyst/ModuleView.xhtml) was used for pathway analysis using the *Arabidopsis thaliana* metabolic pathway database as a reference for the global test algorithm. The resultant metabolites were mapped on the Kyoto Encyclopedia of Genes and Genomes (KEGG) reference metabolic pathways using iPATH for the construction of biological pathways involving the identified metabolites. In order to eliminate the influence of sampling date and year on the root metabolites a mixed effects model, with sampling date and year as fixed factors, and with block and warming duration as random factors was calculated for each metabolite and only the model residuals of each metabolite then were used for pathway analysis of warming effects. A score for pathway impact was calculated as the sum of the importance measures of identified metabolites divided by the total sum of the importance measures of all the identified and unidentified metabolites in the pathway.

## 3 Results

### 3.1 Warming effects on the concentration of primary metabolites

In the root extracts we identified and quantified a total of 44 primary metabolites, including 19 amino acids, 12 organic acids, and 13 sugars, across six sampling dates in both the warmed and the control treatments (Table **S1**). A linear mixed-effects model revealed that warming ($F$=12.88, $P$<0.001, Table **S2**), sampling date ($F$=10.33, $P$<0.001, Table **S2**), and year ($F$=191.88, $P$<0.001, Table **S2**) significantly affected the concentration of total primary metabolites (TPM in Table **S2**). Moreover, warming and sampling date ($F$=3.77, $P$=0.025, Table **S2**) and sampling date and year ($F$=27.05, $P$<0.001, Table **S2**) showed significant interaction effects on the concentration of total primary metabolites. Amino acids, organic acids, and sugars represented 10.9%, 21.7%, and 67.5% of the root primary metabolites in the control treatment, and this proportion did not differ from the warming treatment (Figure **1B**).

A linear mixed-effects models demonstrated that the concentration of total amino acids (TAA) in root extracts was significantly affected by warming ($F$=5.91, $P$=0.016, Table **S2**),

sampling date ($F$=3.36, $P$=0.037, Table **S2**), year ($F$=22.42, $P$<0.001, Table **S2**), and by the interaction between sampling date and year ($F$=24.10, $P$<0.001, Table **S2**). Compared to the control, the concentration of total amino acids in root increased by 14.5% in the warming treatment (Figure **1A**, t=-2.54, $P$=0.019), particularly arginine, glycine, lysine, threonine and tryptophan (Figure **2A**, Table S2). For total organic acids (TOA), the concentration was influenced by sampling date ($F$=17.02, $P$<0.001, Table **S2**) and year ($F$=226.52, $P$<0.001, Table **S2**), but was not affected by warming ($F$=0.31, $P$=0.579) or the interaction between warming and sampling date ($F$=1.69, $P$=0.188). Only the concentration of oxaloacetic acid increased (by 16.7%) in the warming treatment, but it was not affected by sampling date or the interaction between warming and sampling date (Figure **2C**, Table **S2**). The concentration of total sugars (TS) was affected by warming ($F$=12.08, $P$=0.001), sampling date ($F$=23.06, $P$=0.001), year ($F$=115.76, $P$<0.001), and the interaction between warming and sampling date ($F$=3.37, $P$=0.037) and between sampling date and year ($F$=43.29, $P$<0.001). The total sugar concentration in roots increased by 20.8% across the six sampling dates in the warming treatment compared to the control (Figure **1A**, t=-2.82, $P$=0.011). Among the sugars, mannose, ribose, fructose, and glucose concentrations increased by 23.0%, 38.0%, 40.7%, and 19.8%, respectively, in the warming treatment (Figure **2D**, Table **S2**).

### 3.2 Warming effects on primary metabolite profiles

PERMANOVA (Adonis) analysis revealed that primary metabolite profiles significantly varied due to warming ($F$=5.79, $R^2$=0.016, $P$=0.002), season ($F$=29.83, $R^2$=0.17, $P$=0.001), and year ($F$=88.78, $R^2$=0.254, $P$=0.001). Although there was no evidence for a three-way interaction (warming × season × year, $P$=0.183), effects of treatment varied across seasons and seasonal effects changed between years (season × warming and season × year, $P$< 0.05) (Table 1). PERMDISP results showed no significant effect of warming ($F$=0.584, $P$=0.451) and year ($F$=2.174, $P$=0.240) on the dispersion within each group (Table 1), suggesting that the observed significant differences were due to warming or year effects, and not attributable to data (variance) heterogeneity. In comparison, the dispersion of primary metabolite profiles differed by season. NMDS 1 reflected the separation of metabolites between 2021 and 2022. Along NMDS 2, we found a separation of metabolite profiles between sampling date (Figure

**3A**). Most metabolites, independent of type (amino acid, organic acid, or sugar), were negatively associated with NMDS 1 and positively with NMDS 2. These included tricarboxylic acid cycle (TCA) compounds (i.e., citrate, succinate, fumarate, malate, oxaloacetate), aromatic amino acids (tryptophan, tyrosine, and phenylalanine), glutamate family amino acids (arginine and glutamate), and transport sugars (sucrose, raffinose) (Figure **3B**).

### 3.3 Linkages between metabolite profiles, soil environment, and root traits

We performed regression analyses to test for relationships between NMDS 1 (interannual separation of metabolite profiles) and NMDS 2 axis scores (interannual/sampling date of metabolite profiles) and soil temperature, soil moisture, and root morphological traits across the different sampling dates. Soil moisture (only in warmed plots) and specific root length had significant positive relationships with the primary metabolite profiles along NMDS 1(Figure **4b, d**), while soil temperature and root diameter had significant negative relationships with the primary metabolite profiles of NMDS 1(Figure **4a, c**). This relates to higher metabolite concentrations in 2020 (with negative NMDS1 scores but positive metabolite concentration scores, Figure **3B**) at higher soil temperature, lower soil moisture, and higher root diameter but specific root length. Only soil temperature had a significant, here positive, relationship with the profiles of primary metabolites along NMDS 2 in both treatments (Figure **4e**). This translates to high NMDS 2 scores indicating high metabolite concentrations in summer which was reflected by high summer temperatures, and seasonally lower temperatures being linked to lower primary metabolite levels during autumn and spring.

### 3.4. Pathway analysis of warming-induced responses in root metabolism

Table 2 presents the impact of soil warming on various metabolic pathways, quantified through pathway impact values and statistical significance, indicated by -log10(P) values. Pathways with a -log10(P) greater than 1.3 are statistically significantly ($P<0.05$) altered by soil warming (Figure **5** and **Table 2**). The pathways most robustly affected by the warming treatment included starch and sucrose metabolism (1), galactose metabolism (2), glycine, serine, and threonine metabolism (3), arginine and proline metabolism (4), arginine

biosynthesis (5), and tryptophan metabolism (6), followed by pyruvate metabolism (7), C fixation (8), glutathione metabolism (9) and glycolysis (10).

## 4 Discussion

### 4.1 Warming effects on the concentration of primary metabolites

Through two years of study, we observed that soil warming significantly altered primary metabolite profiles in fine roots, leading to a general increase in amino acid and sugar concentrations. This finding supports our initial hypothesis *(H1)* and aligns with findings from prior research (Gargallo-Garriga et al., 2015; Rodrigues et al., 2021), indicating an upregulation of the complex metabolic pathway network of roots under warmer conditions.

Amino acids not only serve as basic building blocks and N donors for the biosynthesis of proteins, nucleic acids, phospholipids and N-containing secondary compounds (e.g. alkaloids) but also play important roles in mediating cell osmosis in plants under both biotic and abiotic stress conditions (Galili et al., 2016; Yang et al., 2020; Trovato et al., 2021). In this study, we found an increase in root arginine concentrations in the warmed plots, indicating an upregulation of the glutamate pathway, and concomitant changes in arginine biosynthesis and arginine (and proline) metabolism, which is also supported by the metabolic pathway analysis. Arginine is a precursor of polyamines, which are associated with many biological processes, such as the protection of cells against osmotic stress (Kalamaki et al., 2009), which however did not play a role here. Moreover, lysine and threonine deriving from the aspartate pathway also increased in response to warming, both functioning as osmoregulation factors (Gargallo-Garriga et al., 2015; Zulfiqar et al., 2022). On the other hand, increased lysine concentrations can also affect other metabolic pathways, for instance, lysine affects tryptophan metabolism in transgenic rice (*Oryza sativa L.*) (Yang et al., 2018). We also found significantly increased tryptophan concentrations and upregulated tryptophan metabolism in roots of warmed plots.

Roots in warmed plots were observed to accumulate total soluble sugars, as well as specifically of glucose, fructose, mannose, and ribose. This finding is consistent with previous findings of increased sugar concentrations under warming, drought, and elevated $CO_2$ (Gargallo-Garriga et al., 2015; Furze et al., 2019; Birami et al., 2020; Rodrigues et al., 2021). Sugar accumulation is linked to enhanced root metabolism and osmoregulation, potentially driven by elevated root respiration due to higher soil temperatures, which promotes the breakdown of storage carbohydrates and the concomitant release of glucose (Huang et al., 2012; Hartmann & Trumbore, 2016). This is supported by increased root

respiration (approximately +40%) in warmed fine roots (Schindlbacher et al., 2009; Schindlbacher et al., 2012; Kwatcho Kengdo et al., 2023), suggesting a warming-induced modification of soluble sugar metabolism in roots. Despite the anticipated reduction in sucrose levels due to its cleavage into glucose and fructose (Hartmann & Trumbore, 2016), no significant decrease was observed in the concentration of sucrose in warmed roots in this study, possibly due to an accelerated transport of photosynthetic assimilates to the roots. The observed increase in soluble sugars during spring and summer with warming is noteworthy. However, this trend is not evident in autumn, which suggests that factors other than temperature influence the seasonal variation, particularly in the latter season. This aligns with prior research, which posits seasonal dependence of warming effects due to variations in temperature extremes and soil moisture (Prieto et al.,2009) or due to seasonal changes in substrate availability or limitations (Maxwell et al.,2022). It's hypothesized that during the growing season (April to August), elevated temperatures accelerate growth and root C allocation in warming treatments, being reflected in higher root sugar concentrations (Hartmann & Trumbore, 2016; Kuptz et al.,2011). Conversely, in the non-growing season (October), plants prioritize root C storage (as starch) instead of accumulating soluble sugars for the upcoming year.

In the present study, most organic acids in spruce roots, including tricarboxylic acid (TCA) cycle intermediates such as citric acid, malic acid, and succinic acid, remained unaltered under warming, except for oxaloacetic acid, which increased. This finding contradicts previous studies that have shown increased levels of total organic acids under drought combined with warming (Suseela et al., 2015; Kumari & Parida, 2018) and decreased levels after warming (Wang et al., 2020). These studies suggest that a potential decrease and/or increase in TCA cycle activity depends on cellular energy demand and on the demand for C skeletons derived from the TCA cycle for amino acid biosynthesis. One possible explanation for the observed increase in oxaloacetic acid could be that increased root respiration and energy production under warming could stimulate organic acid production to balance the increased demand for energy. Metabolic pathway analysis also showed that warming influenced the TCA cycle via pyruvate metabolism. Another possible explanation is that warming may have increased the flow of amino-N through aspartic acid, the product of

transamination of oxaloacetic acid with alanine or glutamine as an amino group donor (Yoneyama & Suzuki, 2020).

Our study demonstrated that plant roots adapt to long-term soil warming by enhancing primary metabolite concentrations to restore homeostasis. Increased levels of metabolites such as amino acids and sugars likely support higher respiration rates, potentially leading to a negative C balance under warming conditions (Cong et al.,2022; Huang et al., 2021; Petrík et al.,2024). They may also sustain higher levels of fine root growth as found recently in the same forest (Kwatcho Kengdo et al., 2023). The whole tree and ecosystem implications of our findings are, however, uncertain. For instance, it remains unclear whether these changes in primary metabolites directly result from shifts in C allocation between aboveground and belowground parts, or between primary metabolite groups, due to the limited scope of our experimental setup. Increased root metabolite levels (this study) and concurrently stimulated root growth and respiration (Kwatcho Kengdo et al., 2023; Schindlbacher unpublished data) in response to warming will only be sustained when whole trees respond alike, by increasing belowground C allocation under whole-system warming. Our warming experiment was confined to a small plot size (2 m by 2 m, warming only parts of a tree's root system) and followed soil warming only, while the above-ground portions of the trees were exposed to ambient temperatures. Thus, our findings should not be extrapolated to whole trees or ecosystems. In contrast, the Spruce and Peatland Responses under Changing Environments (SPRUCE) experiment in northern Minnesota, USA, offers a more comprehensive view of ecosystem-level responses (Hanson et al., 2017). Despite these limitations, our study provides important insights into the potential long-term impacts of warming on tree root metabolism, but predicting how above-ground physiological changes due to climate warming will influence below-ground C allocation and root metabolism remains a significant challenge.

### 4.2 Warming effects on the primary metabolite profile

This study supports the hypothesis (*H2*) that soil warming alters root primary metabolite profiles, as evidenced by PERMANOVA and in line with earlier observations in Icelandic grasslands under long-term soil warming (Gargallo-Garriga et al., 2017) and *Pinus halepensis* seedlings under short-term (10 days) heat stress (Birami et al., 2020), indicating a shift in

plant metabolomes in response to warming. Notably, the plant response to heat stress differs from its response to climate warming (Wang et al., 2020; Jagadish et al., 2021). For example, under prolonged warming, Wang et al. (2020) found increases in the glycolysis pathway and inhibited TCA cycle activity in *Arabidopsis*, while heat stress caused accumulation of sugars and antioxidants but also inhibited the TCA cycle activity. Some previous studies have shown that plant metabolite profiles remain unchanged under moderate warming conditions as long as this is not accompanied by decreased water availability (Gargallo-Garriga et al., 2015; Suseela et al., 2015). Soil moisture was not reduced during root sampling in this study (Heinzle et al., 2023), hence the primary metabolite profiles of roots in warmed and control soil were not affected by decreased soil moisture. In addition, metabolite profiles were notably influenced by the interaction of season, warming and year. This could be due to varying precipitation patterns between the season, or due to changes in plant phenology (in autumn trees trigger a "suspended metabolism" program rendering all metabolite pools largely unresponsive to soil warming) (Proctor, 2000). Consequently, metabolite concentrations rose during spring and summer with warming, but not in autumn.

Our results show that the root metabolome had acclimated to long-term soil warming, indicated by consistent positive temperature correlations with metabolite profiles across seasons and by similar root exudation rates in both control and warmed roots by the same sampling campaign (Heinzle et al., 2023). This result contradicts previous findings at the same site which reported increases in soil and root respiration (Schindlbacher et al., 2009; Schindlbacher et al., 2012; Schindlbacher et al., 2015), as well as stimulation of fine root growth (Kwatcho Kengdo et al., 2023). Despite this, we observed increased concentrations of primary metabolites including amino acids, sugars, and oxaloacetic acid in roots, likely facilitating increased root respiration and fine root growth. The enhanced metabolite concentrations support a positive link between root growth and metabolite levels, driven by a need for faster biosynthesis of proteins, nucleic acids, and other biomolecules. The link between root growth and increased primary metabolite levels is evidenced by higher fine root growth (Kwatcho Kengdo et al., 2022) and metabolite concentrations in warmed plots, suggesting enhanced biosynthesis of essential biomolecules such as proteins, nucleic acids, and polysaccharides, and this needs greater production of their building blocks such as amino

acids and sugars. This further indicates a broad upregulation of primary metabolism rather than the accumulation of select metabolites typically seen in stress responses. Supporting these observations, research by Meyer et al. (2007) on *Arabidopsis thaliana* elucidates that accelerated plant growth is not attributable to isolated metabolites but rather to a concerted effect across essential metabolic pathways, including glycolysis, starch and sucrose metabolism, the oxidative pentose phosphate cycle, the TCA cycle, nitrogen assimilation, and lipid biosynthesis. Such adjustments are manifest in the raised levels of substrates and intermediates, corroborating our findings of a metabolic response to thermal warming.

### 4.3 Intra- and interannual patterns of primary metabolites

Plants undergo different growth phases in various seasons, which are often associated with intra-annual changes in their primary metabolite profiles (Rivas-Ubach et al., 2012; Gargallo-Garriga et al., 2015). We observed significant differences in primary metabolite concentrations between years and among the three seasons. Our NMDS analysis revealed that primary metabolite levels were highest in summer and lowest in spring, and that soil temperature was the main driving factor behind the changes in primary metabolite concentration among different seasons. Overall primary metabolite levels increased with soil temperature across seasons. Temperature has been confirmed as one of the most critical environmental factors that can affect the production and accumulation of primary metabolites in plants (Atkin et al., 2000; Huang et al., 2012). The favorable climatic conditions of summer, with high soil temperature and acceptable availability of soil moisture in this region, can increase enzyme and metabolic activities in roots and facilitate the uptake of water and nutrients from the soil, which thereby is likely reflected in increased root metabolism and root metabolite concentrations in summer.

The primary metabolite profiles showed notable interannual discrepancies between 2020 and 2021, with higher overall concentrations observed in 2020 than in 2021. The primary reasons behind these differences were identified as differences in morphology of the fine root branches during the two years. Root morphology has been linked to improved resource acquisition, where a larger root surface area and greater specific root length can facilitate the uptake of water and nutrients from the soil, leading to enhanced metabolic processes in roots

(Reich et al., 2008; Han & Zhu, 2021). A negative correlation was found between root respiration and root tissue density in woody species (Han & Zhu, 2021). Root tissue density was smaller in 2020 than in 2021 in this study, indicating higher root metabolic activity in 2020 than in 2021, which was reflected in overall higher primary metabolite levels. Furthermore, a comparative analysis of soil conditions between the two years reveals a lower soil temperature in 2021 compared to 2020, while 2021 exhibited enhanced soil moisture. This observation potentially offers a partial explanation for the described phenomena, given that root metabolite concentrations tend to rise with increasing soil temperature and diminish with higher soil moisture (Hartmann & Trumbore, 2016).

## 5 Conclusions

In summary, our study clearly illustrates how tree roots modulate the concentration and profile of primary metabolites in response to long-term soil warming across seasons. We observed a notable accumulation of sugars and amino acids in root tissues, which likely plays a critical osmoprotective role against warming stress. These findings underscore the high plasticity of plant root metabolism, evidenced by the up-regulation of specific metabolic pathway (e.g., amino acid biosynthesis and metabolism pathways) in response to climate warming. Moreover, our data suggest that long-term soil warming may facilitate thermal acclimation in root metabolism through an increase in the concentration of primary metabolites, thereby enhancing the roots' capacity for nutrient uptake and assimilation under changing climatic conditions. This research significantly contributes to our understanding of the impact of climate change on root metabolic processes in forest ecosystems. Looking forward, future research must consider whole tree or ecosystem level warming, for a more comprehensive assessment of warming effects beyond plant root metabolism and related tree root function, given yet unknown responses of tree growth and belowground C allocation to altered nutrient and soil water constraints.

## Conflict of interest

The authors have no conflicts of interest to declare.

**Funding**

This study was funded by the Austrian Science Fund (FWF; project I 3745) and China Scholarship Council (CSC) Grant (202008350128).

**Acknowledgements**

We sincerely thank Christian Holtermann for his invaluable contributions to maintaining the soil warming system in the field site, Ludwig Seidl for technical support on metabolite analysis.

**Author contributions**

WW, AS, and WB designed the study. XF, JH, YT, SKK, WW, AS, and WB implemented the field experiment. XF, ES, and WW conducted the lab experiment. XF performed data analysis and wrote the manuscript, with the contributions of all co-authors.

## References


Abedini, D., Jaupitre, S., Bouwmeester, H., & Dong, L. (2021). Metabolic interactions in beneficial microbe recruitment by plants. *Current Opinion in Biotechnology, 70*, 241-247.

Anderson, M. (2008). PERMANOVA+ for PRIMER: guide to software and statistical methods. Primer-E Limited.

Atkin, O. K., Edwards, E. J., & Loveys, B. R. (2000). Response of root respiration to changes in temperature and its relevance to global warming. *New Phytologist, 147*(1), 141-154.

Berini, J. L., Brockman, S. A., Hegeman, A. D., Reich, P. B., Muthukrishnan, R., Montgomery, R. A., & Forester, J. D. (2018). Combinations of Abiotic Factors Differentially Alter Production of Plant Secondary Metabolites in Five Woody Plant Species in the Boreal-Temperate Transition Zone. *Frontiers in Plant Science, 9*(1257), 1257.

Birami, B., Nagele, T., Gattmann, M., Preisler, Y., Gast, A., Arneth, A., & Ruehr, N. K. (2020). Hot drought reduces the effects of elevated $CO_2$ on tree water-use efficiency and carbon metabolism. *New Phytologist, 226*(6), 1607-1621.

Bosela, M., Tumajer, J., Cienciala, E., Dobor, L., Kulla, L., Marčiš, P., . . . Büntgen, U. (2021). Climate warming induced synchronous growth decline in Norway spruce populations across biogeographical gradients since 2000. *Science of the Total Environment*, 752, 141794.

Budzinski, I. G., Moon, D. H., Linden, P., Moritz, T., & Labate, C. A. (2016). Seasonal Variation of Carbon Metabolism in the Cambial Zone of Eucalyptus grandis. *Frontiers in Plant Science*, 7, 932.

Carrera, F. P., Noceda, C., Mariduena-Zavala, M. G., & Cevallos-Cevallos, J. M. (2021). Metabolomics, a Powerful Tool for Understanding Plant Abiotic Stress. *Agronomy-Basel, 11*(5), 824.

Cong, Y., Saurer, M., Bai, E., Siegwolf, R., Gessler, A., Liu, K., . . . Li, M.-H. (2022). In situ 13CO2 labeling reveals that alpine treeline trees allocate less photoassimilates to roots compared with low-elevation trees. *Tree physiology*, 42(10), 1943-1956.

Dusenge, M. E., Duarte, A. G., & Way, D. A. (2019). Plant carbon metabolism and climate change: elevated $CO_2$ and temperature impacts on photosynthesis, photorespiration and respiration. *New Phytologist, 221*(1), 32-49.

Erb, M., & Kliebenstein, D. J. (2020). Plant Secondary Metabolites as Defenses, Regulators, and Primary Metabolites: The Blurred Functional Trichotomy. *Plant Physiology, 184*(1), 39-52.

Escandon, M., Meijon, M., Valledor, L., Pascual, J., Pinto, G., & Canal, M. J. (2018). Metabolome Integrated Analysis of High-Temperature Response in Pinus radiata. *Frontiers in Plant Science, 9*(485), 485.

Escolà Casas, M., & Matamoros, V. (2021). Analytical challenges and solutions for performing metabolomic analysis of root exudates. *Trends in Environmental Analytical Chemistry, 31*, e00130.

Furze, M. E., Drake, J. E., Wiesenbauer, J., Richter, A., & Pendall, E. (2019). Carbon isotopic tracing of sugars throughout whole-trees exposed to climate warming. *Plant, Cell & Environment, 42*(12), 3253-3263.

Galili, G., Amir, R., & Fernie, A. R. (2016). The Regulation of Essential Amino Acid Synthesis and Accumulation in Plants. *Annual Review of Plant Biology, 67*(1), 153-178.

Gargallo-Garriga, A., Ayala-Roque, M., Sardans, J., Bartrons, M., Granda, V., Sigurdsson, B. D., . . . Penuelas, J. (2017). Impact of Soil Warming on the Plant Metabolome of Icelandic Grasslands. *Metabolites, 7*(3), 44.

Gargallo-Garriga, A., Sardans, J., Perez-Trujillo, M., Oravec, M., Urban, O., Jentsch, A., . . . Penuelas, J. (2015). Warming differentially influences the effects of drought on stoichiometry and metabolomics in shoots and roots. *New Phytologist, 207*(3), 591-603.

Han, M., & Zhu, B. (2021). Linking root respiration to chemistry and morphology across species. *Global Change Biology, 27*(1), 190-201.

Hanewinkel, M., Cullmann, D. A., Schelhaas, M.-J., Nabuurs, G.-J., & Zimmermann, N. E. (2013). Climate change may cause severe loss in the economic value of European forest land. *Nature Climate Change*, 3(3), 203-207.

Hansen, M. C., Stehman, S. V., & Potapov, P. V. (2010). Quantification of global gross forest cover loss. *Proceedings of the National Academy of Sciences, 107*(19), 8650-8655.

Hanson, P. J., Riggs, J. S., Nettles, W. R., Phillips, J. R., Krassovski, M. B., Hook, L. A., ... & Barbier, C. (2017). Attaining whole-ecosystem warming using air and deep-soil heating methods with an elevated $CO_2$ atmosphere. *Biogeosciences*, 14(4), 861-883.

Hartmann, H., & Trumbore, S. (2016). Understanding the roles of nonstructural carbohydrates in forest trees - from what we can measure to what we want to know. *New Phytologist, 211*(2), 386-403.

Heinzle, J., Liu, X. F., Tian, Y., Kengdo, S. K., Heinze, B., Nirschi, A., . . . Schindlbacher, A. (2023). Increase in fine root biomass enhances root exudation by long-term soil warming in a temperate forest. *Frontiers in Forests and Global Change, 6*.

Huang, J., Hammerbacher, A., Gershenzon, J., van Dam, N. M., Sala, A., McDowell, N. G., . . . Hartmann, H. (2021). Storage of carbon reserves in spruce trees is prioritized over growth in the face of carbon limitation. *Proceedings of the National Academy of Sciences*, 118(33), e2023297118.

Huang, B., Rachmilevitch, S., & Xu, J. (2012). Root carbon and protein metabolism associated with heat tolerance. *Journal of Experimental Botany, 63*(9), 3455-3465.

Jagadish, S. V. K., Way, D. A., & Sharkey, T. D. (2021). Plant heat stress: Concepts directing future research. *Plant, Cell & Environment, 44*(7), 1992-2005.

Jamloki, A., Bhattacharyya, M., Nautiyal, M. C., & Patni, B. (2021). Elucidating the relevance of high temperature and elevated $CO_2$ in plant secondary metabolites (PSMs) production. *Heliyon, 7*(8), e07709.

Kalamaki, M. S., Merkouropoulos, G., & Kanellis, A. K. (2009). Can ornithine accumulation modulate abiotic stress tolerance in Arabidopsis? *Plant Signaling & Behavior, 4*(11), 1099-1101.

Kuptz, D., Fleischmann, F., Matyssek, R. and Grams, T.E.E. (2011), Seasonal patterns of carbon allocation to respiratory pools in 60-yr-old deciduous (*Fagus sylvatica*) and evergreen (*Picea abies*) trees assessed via whole-tree stable carbon isotope labeling. *New Phytologist*, 191: 160-172.

Kumari, A., & Parida, A. K. (2018). Metabolomics and network analysis reveal the potential metabolites and biological pathways involved in salinity tolerance of the halophyte Salvadora persica. *Environmental and Experimental Botany, 148*, 85-99.

Kwatcho Kengdo, S., Persoh, D., Schindlbacher, A., Heinzle, J., Tian, Y., Wanek, W., & Borken, W. (2022). Long-term soil warming alters fine root dynamics and morphology, and their ectomycorrhizal fungal community in a temperate forest soil. *Global Change Biology, 28*(10), 3441-3458.

Kwatcho Kengdo, S., Ahrens, B., Tian, Y., Heinzle, J., Wanek, W., Schindlbacher, A., & Borken, W. (2023). Increase in carbon input by enhanced fine root turnover in a long-term warmed forest soil. *Science of the Total Environment, 855*, 158800.

Liu, X., & Locasale, J. W. (2017). Metabolomics: A Primer. *Trends in biochemical sciences, 42*(4), 274-284.

Maxwell, T. L., Canarini, A., Bogdanovic, I., Böckle, T., Martin, V., Noll, L., . . . Wanek, W. (2022). Contrasting drivers of belowground nitrogen cycling in a montane grassland exposed to a multifactorial global change experiment with elevated $CO_2$, warming, and drought. *Global Change Biology*, 28(7), 2425-2441.

Meyer, R. C., Steinfath, M., Lisec, J., Becher, M., Witucka-Wall, H., Torjek, O., . . . Altmann, T. (2007). The metabolic signature related to high plant growth rate in Arabidopsis thaliana. *Proceedings of the National Academy of Sciences, 104*(11), 4759-4764.

Pan, Y., Birdsey, R. A., Fang, J., Houghton, R., Kauppi, P. E., Kurz, W. A., . . . Hayes, D. (2011). A large and persistent carbon sink in the world's forests. *Science, 333*(6045), 988-993.

Peñuelas, J., Sardans, J., Estiarte, M., Ogaya, R., Carnicer, J., Coll, M., . . . Jump, A. S. (2013). Evidence of current impact of climate change on life: a walk from genes to the biosphere. *Global Change Biology*, 19(8), 2303-2338.

Petrík, P., Scapucci, L., Petek-Petrik, A., Bosela, M., Huang, W., Kurjak, D., & Ræbild, A. (2024). Winter warming response of gas-exchange and growth of Abies alba and Picea abies seedlings. *Trees*, 38(1), 151-167.

Proctor, M.C. (2000). The bryophyte paradox: tolerance of desiccation, evasion of drought. *Plant Ecology* 151, 41–49.

Prinsloo, G., & Nogemane, N. (2018). The effects of season and water availability on chemical composition, secondary metabolites and biological activity in plants. *Phytochemistry Reviews*, 17(4), 889-902.

Prieto P., Peñuelas J., Llusià J., Asensio D., Estiarte M. (2009) Effects of long-term experimental night-time warming and drought on photosynthesis, Fv/Fm and stomatal conductance in the dominant species of a Mediterranean shrubland. *Acta Physiol Plant* 31:729-739.

R Core Team. (2019) R: A language and environment for statistical computing. Vienna, Austria: R Foundation for Statistical Computing. Retrieved from https://www.R-project.org/.

Reich, P. B., Tjoelker, M. G., Pregitzer, K. S., Wright, I. J., Oleksyn, J., & Machado, J. L. (2008). Scaling of respiration to nitrogen in leaves, stems and roots of higher land plants. *Ecology letters, 11*(8), 793-801.

Rivas-Ubach, A., Sardans, J., Perez-Trujillo, M., Estiarte, M., & Penuelas, J. (2012). Strong relationship between elemental stoichiometry and metabolome in plants. *Proceedings of the National Academy of Sciences, 109*(11), 4181-4186.

Rodrigues, A. M., Jorge, T., Osorio, S., Pott, D. M., Lidon, F. C., DaMatta, F. M., . . . Antonio, C. (2021). Primary Metabolite Profile Changes in Coffea spp. Promoted by Single and Combined Exposure to Drought and Elevated $CO_2$ Concentration. *Metabolites, 11*(7), 427.

Salas, E., Gorfer, M., Bandian, D., Wang, B., Kaiser, C., & Wanek, W. (2023) A rapid and sensitive assay to quantify amino sugars, neutral sugars and uronic acid necromass biomarkers using pre-column derivatization, ultra-high-performance liquid chromatography and high-resolution mass spectrometry. *Soil Biology and Biochemistry* 177: 108927.

Sardans, J., Gargallo-Garriga, A., Urban, O., Klem, K., Walker, T. W. N., Holub, P., . . . Penuelas, J. (2020). Ecometabolomics for a Better Understanding of Plant Responses and Acclimation to Abiotic Factors Linked to Global Change. *Metabolites, 10*(6), 239.

Schindlbacher, A., Schnecker, J., Takriti, M., Borken, W., & Wanek, W. (2015). Microbial physiology and soil $CO_2$ efflux after 9 years of soil warming in a temperate forest - no indications for thermal adaptations. *Global Change Biology*, 21(11), 4265-4277.

Schindlbacher, A., Wunderlich, S., Borken, W., Kitzler, B., Zechmeister-Boltenstern, S., & Jandl, R. (2012). Soil respiration under climate change: prolonged summer drought offsets soil warming effects. *Global Change Biology, 18*(7), 2270-2279.

Schindlbacher, A., Zechmeister-boltenstern, S., & Jandl, R. (2009). Carbon losses due to soil warming: do autotrophic and heterotrophic soil respiration respond equally? *Global Change Biology, 15*(4), 901-913.

Simon, J., & Adamczyk, B. (2019). Editorial: Plant Secondary Compounds in Forest Ecosystems Under Global Change: From Defense to Carbon Sequestration. *Frontiers in Plant Science, 10*(831), 831.

Suseela, V., Tharayil, N., Xing, B., & Dukes, J. S. (2015). Warming and drought differentially influence the production and resorption of elemental and metabolic nitrogen pools in Quercus rubra. *Global Change Biology, 21*(11), 4177-4195.

Sytiuk, A., Hamard, S., Cereghino, R., Dorrepaal, E., Geissel, H., Kuttim, M., . . . Jassey, V. E. J. (2023). Linkages between Sphagnum metabolites and peatland $CO_2$ uptake are sensitive to seasonality in warming trends. *New phytologist*, 237(4), 1164-1178.

Tian, Y., Schindlbacher, A., Malo, C. U., Shi, C. P., Heinzle, J., Kengdo, S. K., . . . Wanek, W. (2023a). Long-term warming of a forest soil reduces microbial biomass and its carbon and nitrogen use efficiencies. *Soil Biology and Biochemistry*, 184, 109109.

Tian, Y., Shi, C., Malo, C. U., Kwatcho Kengdo, S., Heinzle, J., Inselsbacher, E., . . . Wanek, W. (2023b). Long-term soil warming decreases microbial phosphorus utilization by increasing abiotic phosphorus sorption and phosphorus losses. *Nature Communications*, 14(1), 864.

Trovato, M., Funck, D., Forlani, G., Okumoto, S., & Amir, R. (2021). Editorial: Amino Acids in Plants: Regulation and Functions in Development and Stress Defense. *Frontiers in Plant Science, 12*(2287), 772810.

Wang, L., Ma, K. B., Lu, Z. G., Ren, S. X., Jiang, H. R., Cui, J. W., . . . Jin, B. (2020). Differential physiological, transcriptomic and metabolomic responses of Arabidopsis leaves under prolonged warming and heat shock. *BMC Plant Biology, 20*(1), 86.

Wang, W., Chen, F., Wang, Y., Wang, L., Fu, H., Zheng, F., & Beecher, L. (2018). Optimization of reactions between reducing sugars and 1-phenyl-3-methyl-5-pyrazolone (PMP) by response surface methodology. *Food Chemistry 254*, 158-164.

Yang, Q., Zhao, D., & Liu, Q. (2020). Connections Between Amino Acid Metabolisms in Plants: Lysine as an Example. *Frontiers in Plant Science, 11*, 928.

Yang, Q. Q., Zhao, D. S., Zhang, C. Q., Wu, H. Y., Li, Q. F., Gu, M. H., . . . Liu, Q. Q. (2018). A Connection between Lysine and Serotonin Metabolism in Rice Endosperm. *Plant Physiology, 176*(3), 1965-1980.

Yi, C., Hendrey, G., Niu, S., McDowell, N., & Allen, C. D. (2022). Tree mortality in a warming world: causes, patterns, and implications. *Environmental Research Letters, 17*(3), 030201.

Yoneyama, T., & Suzuki, A. (2020). Light-Independent Nitrogen Assimilation in Plant Leaves: Nitrate Incorporation into Glutamine, Glutamate, Aspartate, and Asparagine Traced by 15N. *Plants, 9*(10), 1303.

Zhou, P., Zhao, F., Chen, M. J., Ye, N. X., Lin, Q., Ouyang, L. Q., . . . Wang, Y. (2019). Determination of 21 free amino acids in 5 types of tea by ultra-high performance liquid chromatography coupled with tandem mass spectrometry (UHPLC-MS/MS) using a modified 6-aminoquinolyl-N-hydroxysuccinimidyl carbamate (AQC) method. *Journal of Food Composition and Analysis, 81*, 46-54.

Zulfiqar, F., Ashraf, M., & Siddique, K. H. M. (2022). Role of Glycine Betaine in the Thermotolerance of Plants. *Agronomy-Basel, 12*(2), 276.

**Table 1** Results of the PERMANOVA of the fixed effects of soil warming and sampling date during two years of root collections on the concentration of primary metabolites in the fine roots of adult Norway spruce trees

| | PERMANOVA tests | | | | PERMDISP tests | |
|---|---|---|---|---|---|---|
| Source | *df* | $R^2$ | *Pseudo F* | *P* | *Pseudo F* | *P* |
| Warming | 1 | 0.017 | 5.799 | **0.002** | 0.583 | 0.451 |
| Season | 2 | 0.170 | 29.831 | **0.001** | 0.918 | **0.001** |
| Year | 1 | 0.254 | 88.784 | **0.001** | 1.483 | 0.240 |
| Warming×Season | 2 | 0.013 | 2.247 | **0.033** | | |
| Warming×Year | 1 | 0.004 | 1.486 | 0.187 | | |
| Season×Year | 2 | 0.157 | 27.550 | **0.001** | | |
| Warming×Season×Year | 2 | 0.008 | 1.395 | 0.183 | | |
| Residual | 132 | 0.377 | | | | |
| Total | 143 | 1.000 | | | | |

All statistical analyses were tested against $\alpha$=0.05, and statistically significant results are marked in bold. The permutation tests were performed Adonis on the basis of Bray-Curtis distance.

**Table 2** Kyoto Encyclopedia of Genes and Genomes (KEGG) pathway analysis of altered metabolites in fine roots of adult Norway spruce in response to soil warming in a temperate montane forest

| Metabolic pathway | Total compounds | Hits | Raw p | -log(p) | Holm adjust | FDR | Impact |
|---|---|---|---|---|---|---|---|
| Amino sugar and nucleotide sugar metabolism | 50 | 3 | 0.0000 | 6.4271 | 0.0000 | 0.0000 | 0 |
| Pentose phosphate pathway | 19 | 2 | 0.0002 | 3.6448 | 0.0097 | 0.0044 | 0 |
| Lysine degradation | 18 | 1 | 0.0003 | 3.4600 | 0.0146 | 0.0044 | 0 |
| [a]Starch and sucrose metabolism | 22 | 1 | 0.0004 | 3.3940 | 0.0165 | 0.0044 | 0.0889 |
| Lysine biosynthesis | 9 | 2 | 0.0012 | 2.9220 | 0.0479 | 0.0097 | 0 |
| [a]Galactose metabolism | 27 | 2 | 0.0013 | 2.8804 | 0.0514 | 0.0097 | 0.1225 |
| [a]Glycine, serine and threonine metabolism | 33 | 4 | 0.0129 | 1.8899 | 0.4896 | 0.0782 | 0.3322 |
| [a]Arginine and proline metabolism | 34 | 4 | 0.0145 | 1.8400 | 0.5349 | 0.0782 | 0.2524 |
| [a]Arginine biosynthesis | 18 | 5 | 0.0186 | 1.7311 | 0.6687 | 0.0782 | 0.1699 |
| [a]Pyruvate metabolism | 22 | 3 | 0.0199 | 1.7006 | 0.6973 | 0.0782 | 0.0846 |
| Thiamine metabolism | 22 | 1 | 0.0201 | 1.6963 | 0.6973 | 0.0782 | 0 |
| [a]Carbon fixation in photosynthetic organisms | 21 | 2 | 0.0213 | 1.6709 | 0.7041 | 0.0782 | 0.0647 |
| Aminoacyl-tRNA biosynthesis | 46 | 15 | 0.0266 | 1.5756 | 0.8503 | 0.0816 | 0 |
| [a]Tryptophan metabolism | 28 | 1 | 0.0278 | 1.5558 | 0.8622 | 0.0816 | 0.1204 |
| Indole alkaloid biosynthesis | 4 | 1 | 0.0278 | 1.5558 | 0.8622 | 0.0816 | 0 |
| [a]Glutathione metabolism | 26 | 2 | 0.0368 | 1.4343 | 1 | 0.1012 | 0.1216 |
| [a]Glycolysis / Gluconeogenesis | 26 | 3 | 0.0434 | 1.3629 | 1 | 0.1122 | 0.0019 |
| Citrate cycle (TCA cycle) | 20 | 5 | 0.0591 | 1.2285 | 1 | 0.1432 | 0.3160 |
| Alanine, aspartate and glutamate metabolism | 22 | 8 | 0.0618 | 1.2088 | 1 | 0.1432 | 0.8202 |
| Glyoxylate and dicarboxylate metabolism | 29 | 10 | 0.1053 | 0.9775 | 1 | 0.2317 | 0.2136 |
| Butanoate metabolism | 17 | 3 | 0.1647 | 0.7833 | 1 | 0.3451 | 0.1364 |
| Phenylalanine, tyrosine and tryptophan biosynthesis | 22 | 3 | 0.1842 | 0.7348 | 1 | 0.3641 | 0.0215 |
| Cyanoamino acid metabolism | 29 | 4 | 0.1903 | 0.7205 | 1 | 0.3641 | 0 |
| Porphyrin and chlorophyll metabolism | 48 | 1 | 0.2030 | 0.6924 | 1 | 0.3723 | 0 |
| Tyrosine metabolism | 16 | 2 | 0.2132 | 0.6712 | 1 | 0.3753 | 0.2162 |
| Valine, leucine and isoleucine biosynthesis | 22 | 4 | 0.2243 | 0.6492 | 1 | 0.3796 | 0 |
| Glucosinolate biosynthesis | 65 | 5 | 0.3136 | 0.5037 | 1 | 0.5053 | 0 |
| Propanoate metabolism | 20 | 1 | 0.3216 | 0.4927 | 1 | 0.5053 | 0 |
| Fructose and mannose metabolism | 20 | 1 | 0.3594 | 0.4444 | 1 | 0.5244 | 0 |
| Monobactam biosynthesis | 8 | 1 | 0.3814 | 0.4187 | 1 | 0.5244 | 0 |
| Cysteine and methionine metabolism | 46 | 1 | 0.3814 | 0.4187 | 1 | 0.5244 | 0 |
| Nicotinate and nicotinamide metabolism | 13 | 1 | 0.3814 | 0.4187 | 1 | 0.5244 | 0 |
| Nitrogen metabolism | 12 | 3 | 0.4374 | 0.3591 | 1 | 0.5832 | 0 |
| beta-Alanine metabolism | 18 | 2 | 0.6004 | 0.2216 | 1 | 0.7695 | 0.2540 |
| Sulfur metabolism | 15 | 2 | 0.6121 | 0.2132 | 1 | 0.7695 | 0.0939 |
| Pantothenate and CoA biosynthesis | 23 | 2 | 0.6819 | 0.1663 | 1 | 0.8334 | 0.0842 |
| Purine metabolism | 63 | 1 | 0.7862 | 0.1045 | 1 | 0.9350 | 0 |
| Valine, leucine and isoleucine degradation | 37 | 3 | 0.8397 | 0.0759 | 1 | 0.9406 | 0 |
| Pyrimidine metabolism | 38 | 2 | 0.8487 | 0.0713 | 1 | 0.9406 | 0 |
| Isoquinoline alkaloid biosynthesis | 6 | 1 | 0.9272 | 0.0328 | 1 | 0.9406 | 0.5000 |
| Ubiquinone and other terpenoid-quinone biosynthesis | 38 | 1 | 0.9272 | 0.0328 | 1 | 0.9406 | 0 |
| Phenylalanine metabolism | 11 | 1 | 0.9406 | 0.0266 | 1 | 0.9406 | 0.4706 |

| | | | | | | | |
|---|---|---|---|---|---|---|---|
| Phenylpropanoid biosynthesis | 46 | 1 | 0.9406 | 0.0266 | 1 | 0.9406 | 0 |
| Tropane, piperidine and pyridine alkaloid biosynthesis | 8 | 1 | 0.9406 | 0.0266 | 1 | 0.9406 | 0 |

[a] indicates those metabolic pathways being significantly impacted by soil warming in roots.

**Figure 1** Absolute concentrations (a) and relative proportions (b) of major groups of primary metabolites in fine roots of adult Norway spruce as affected by ca. 14 years of experimental soil warming in a temperate montane forest. Values in (b) are the relative percentages of each group. Error bars represent standard errors of the means (n=6). Asterisks represent significant differences ($p$<0.05) between the control and warming treatments in total primary metabolite concentration. The capital letters on the 'average' bars to the right represent significant differences (p<0.05) between the control and warming treatment within the same group of compounds, e.g. sugars.

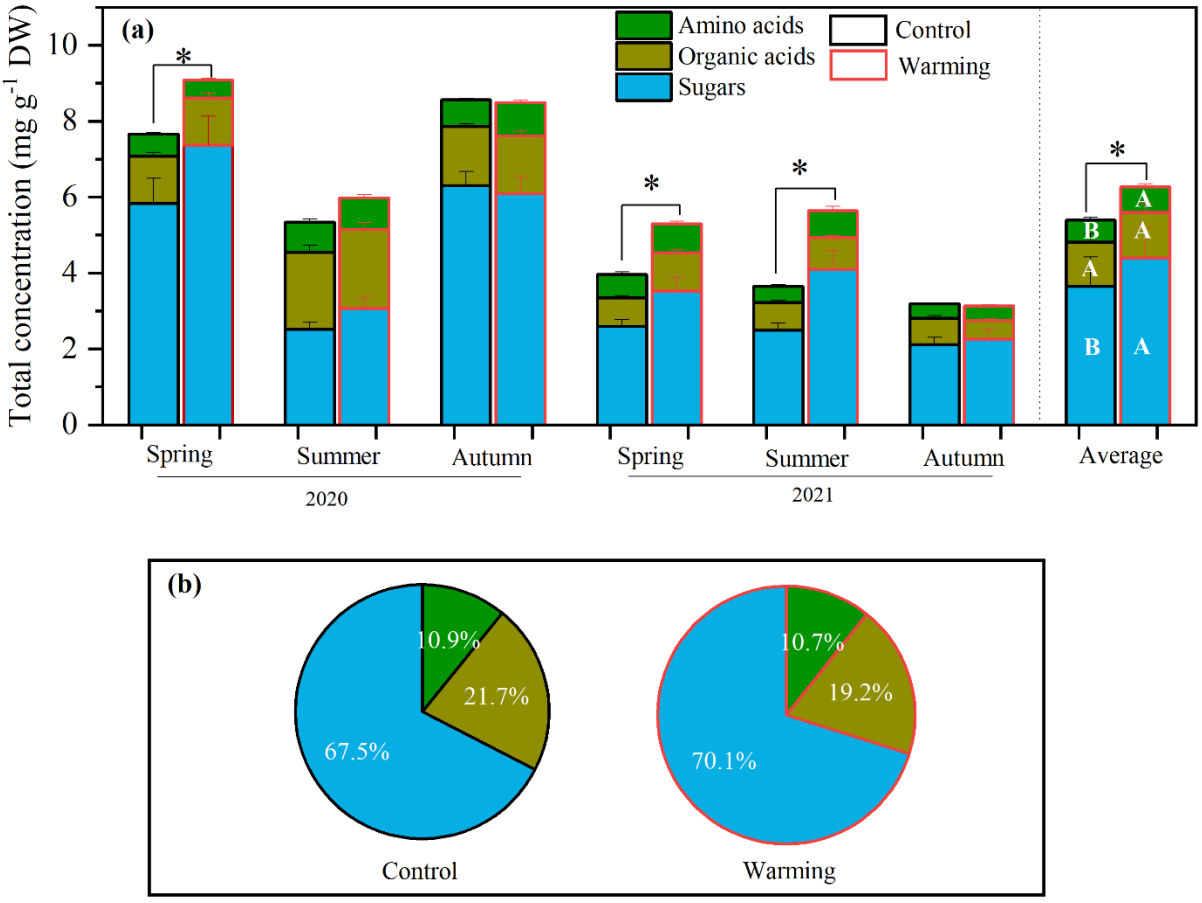

**Figure 2** Boxplot illustrating the average concentrations of specific amino acids (a, b), organic acids (c), and sugars (d) in the fine roots of adult Norway spruce in a temperate montane forest, following approximately 14 years of experimental surface soil warming in an alpine forest, across all six sampling dates (n=6). The box ends represent the 25th and 75th quantiles. The line across the middle of the box is the median value. Asterisks represent significant differences ($p$<0.05) between the control and warming treatments in single compounds.

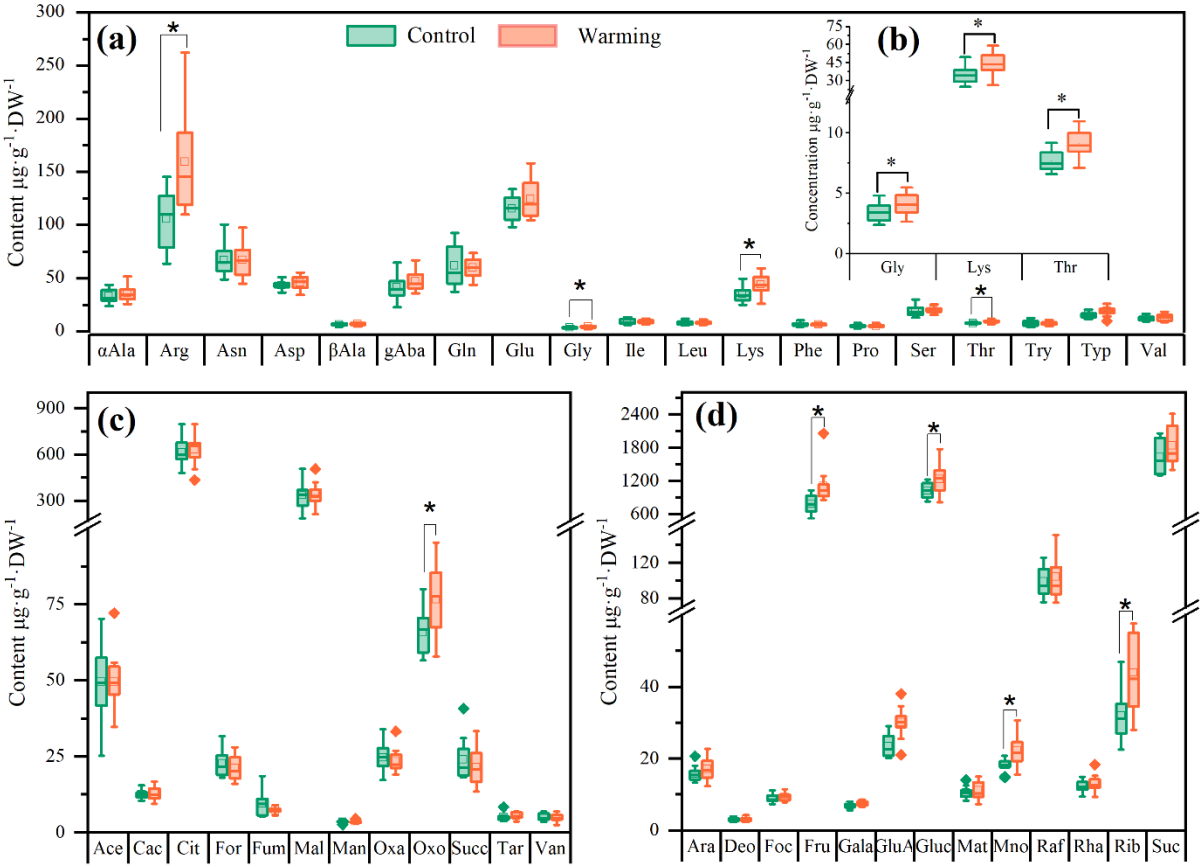

**Figure 3** Non-metric multidimensional scaling (NMDS) (a) plot detailing the influence of warming and sampling dates (combined sampling date and year) on primary metabolite profiles of the fine roots of adult Norway spruce under 14 years soil warming in a temperate montane forest, and (b) spearman's rank correlation matrix of the root metabolites and NMDS scores. The scale of correlation coefficients ranges from -1 (blue) to 1 (red), with a median of 0 (white). Significance levels are denoted as follows: ***P < 0.001; **P < 0.01; *P < 0.05. RSA: Root surface area; SRL: Specific root length; SRA: specific root area; RTD: Root tissue density.

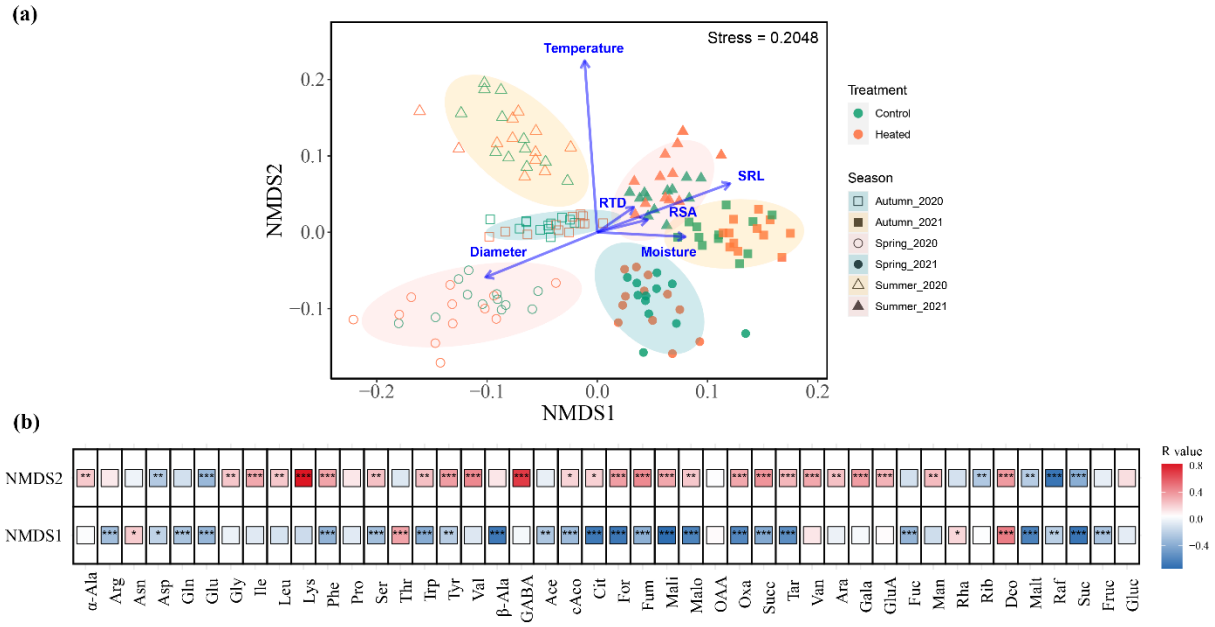

**Figure 4** Linear relationships between primary metabolite NMDS scores and the soil environment (soil temperature and soil moisture) or root morphological traits (root diameter and specific root length), depicted for NMDS1 (a-d) and NMDS2 (e) scores in control and warmed plots.

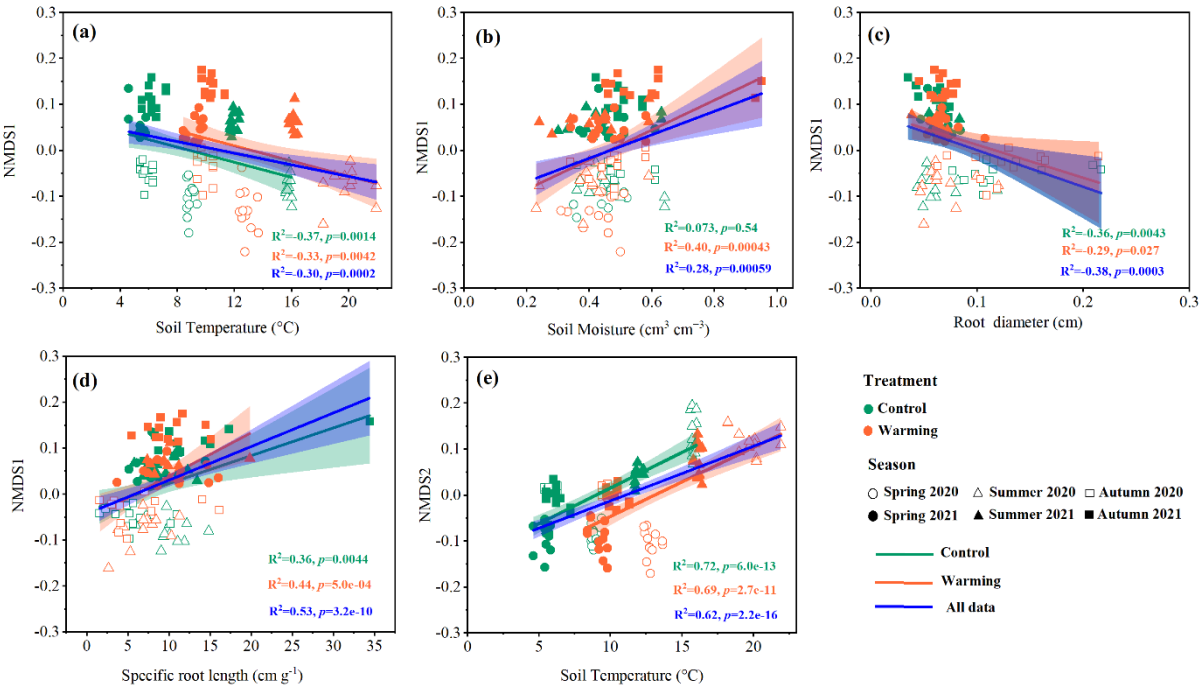

**Figure 5** Graphical representation of pathway analysis showing soil warming induced changes in different metabolic pathways in fine roots of adult Norway spruce in a temperate montane forest. The results from the pathway analysis are explained in detail in Table 2. The metabolome view shows all matched pathways according to p values from pathway enrichment analysis (-log10(p)) and pathway impact (effect size) values from topology analysis. The colors yellow to red represent metabolites with different levels of significance, red represents more significant, and yellow represents less significant. The numbers corresponding to different points denote the respective metabolic pathways being significantly impacted in warmed roots.

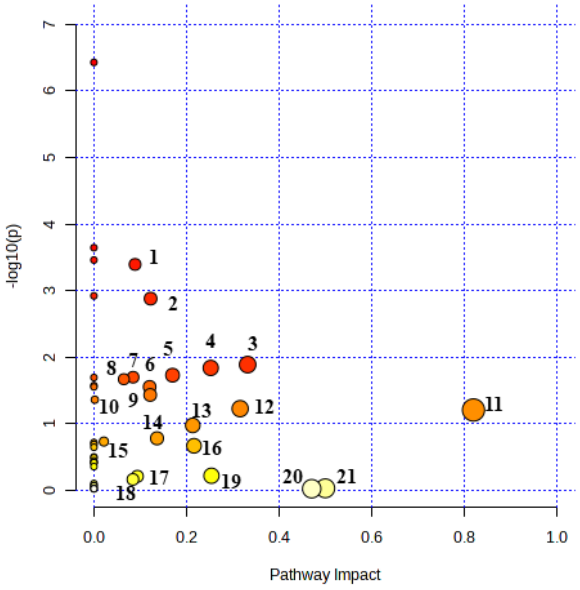


1. Starch and sucrose metabolism
2. Galactose metabolism
3. Glycine, serine and threonine metabolism
4. Arginine and proline metabolism
5. Arginine biosynthesis
6. Tryptophan metabolism
7. Pyruvate metabolism
8. Carbon fixation in photosynthetic organisms
9. Glutathione metabolism
10. Glycolysis / Gluconeogenesis
11. Alanine, aspartate and glutamate metabolism
12. Citrate cycle (TCA cycle)
13. Glyoxylate and dicarboxylate metabolism
14. Butanoate metabolism
15. Phenylalanine, tyrosine and tryptophan biosynthesis
16. Tyrosine metabolism
17. Sulfur metabolism
18. Pantothenate and CoA biosynthesis
19. beta-Alanine metabolism
20. Phenylalanine metabolism
21. Isoquinoline alkaloid biosynthesis

**Supplementary Material**

Article title: **Long-term soil warming changes the profile of primary metabolites in fine roots of Norway Spruce in a temperate montane forest**

Authors: Xiaofei Liu[1,2,3], Jakob Heinzle[4], Ye Tian[1], Erika Salas[1], Steve Kwatcho-Kengdo[5], Werner Borken[5], Andreas Schindlbacher[4], Wolfgang Wanek[1]

**Table S1** Relative retention times and mass to charge (m/z) ratios of organic acids, amino acids, and sugars analyzed in tree (spruce) roots from control and warmed plots.

**Table S2** Linear mixed-effects models testing the effects of warming, season, year and their interactions on the contents of amino acids, organic acids, and sugars of tree (spruce) roots. The numbers in the columns are F- and P-values generated by linear mixed-effects model testing ($P < 0.05$). All statistical tests were two-sided and p values were corrected for multiple comparison using the Benjamini-Hochberg procedure.

**Table S3** Linear mixed-effects models testing the effects of warming, season, year and their interactions on soil moisture, soil temperature, and root morphology. The numbers in the columns are F- and P-values generated by linear mixed-effects model testing ($P < 0.05$). All statistical tests were two-sided and p values were corrected for multiple comparison using the Benjamini-Hochberg procedure.

**Table S4** Soil temperature, soil moisture, and root morphological parameters in control and warmed plots across years and treatments. All statistical tests were two-sided and p values were corrected for multiple comparison using the Benjamini-Hochberg procedure.

**Table S1** Relative retention times and mass to charge (m/z) ratios of organic acids, amino acids, and sugars analyzed in tree (spruce) roots from control and warmed plots.

| No. | Groups | Metabolites | Abbreviation | Retention Time (min) | Quantifier ion | |
|---|---|---|---|---|---|---|
| | | | | | m/z | Type |
| 1 | Amino acids | α-Alanine | αAla | 6.539 | 260.1035 | [M+H] + |
| 2 | | Arginine | Arg | 3.193 | 345.16751 | [M+H] + |
| 3 | | Asparagine | Asn | 2.594 | 303.1093 | [M+H] + |
| 4 | | Aspartic | Asp | 5.531 | 304.0933 | [M+H] + |
| 5 | | Glutamine | Gln | 4.736 | 317.1249 | [M+H] + |
| 6 | | Glutamic | Glu | 5.938 | 318.1089 | [M+H] + |
| 7 | | Glycine | Gly | 5.058 | 246.0878 | [M+H] + |
| 8 | | Isoleucine | Ile | 10.021 | 302.1504 | [M+H] + |
| 9 | | Leucine | Leu | 10.180 | 302.1504 | [M+H] + |
| 10 | | Lysine | Lys | 7.842 | 317.1613 | [M+H] + |
| 11 | | Phenylalanine | Phe | 10.320 | 336.1348 | [M+H] + |
| 12 | | Proline | Pro | 7.054 | 286.1191 | [M+H] + |
| 13 | | Serine | Ser | 4.520 | 276.0984 | [M+H] + |
| 14 | | Threonine | Thr | 6.217 | 290.1140 | [M+H] + |
| 15 | | Tryptophan | Trp | 10.427 | 375.1457 | [M+H] + |
| 16 | | Tyrosine | Tyr | 8.226 | 352.1297 | [M+H] + |
| 17 | | Valine | Val | 8.697 | 288.1348 | [M+H] + |
| 18 | | β-Alanine | βAla | 6.038 | 260.1035 | [M+H] + |
| 19 | | γ-amino butyric | GABA | 6.619 | 274.1191 | [M+H] + |
| 20 | Organic acids | Acetic acid | Ace | 6.31 | 59.0124 | [M-H]- |
| 21 | | Cis-Aconitic acid | cAco | 14.20 | 173.0084 | [M-H]- |
| 22 | | Citric acid | Cit | 13.15 | 191.0192 | [M-H]- |
| 23 | | Formic acid | For | NA | NA | NA |
| 24 | | Fumaric acid | Fum | 10.87 | 115.0023 | [M-H]- |
| 25 | | Malic acid | Mali | 9.53 | 133.0133 | [M-H]- |
| 26 | | Malonic acid | Malo | 9.83 | 103.0024 | [M-H]- |
| 27 | | Oxaloacetate acid | OAA | 9.41 | 131.0339 | [M-H]- |
| 28 | | Oxalic acid | Oxa | 10.78 | 88.9867 | [M-H]- |
| 29 | | Succinic acid | Succ | 9.54 | 117.0182 | [M-H]- |
| 30 | | Tartaric acid | Tar | 9.80 | 149.0086 | [M-H]- |
| 31 | | Vanillic acid | Van | 13.65 | 167.0351 | [M-H]- |
| 32 | Sugars | Arabinose | Ara | 7.93 | 481.2082 | [M+H]+ |
| 33 | | Galacturonic acid | Gala | 7.12 | 525.1982 | [M+H]+ |
| 34 | | Glucosamine | GluA | 6.72 | 510.2347 | [M+H]+ |
| 35 | | Fucose | Fuc | 7.25 | 495.2238 | [M+H]+ |
| 36 | | Mannose | Man | 6.11 | 511.2188 | [M+H]+ |
| 37 | | Rhamnose | Rha | 6.83 | 495.2238 | [M+H]+ |
| 38 | | Ribose | Rib | 6.67 | 481.2082 | [M+H]+ |
| 39 | | Deoxyribose | Deo | 8.75 | 465.2133 | [M+H]+ |
| 40 | | Maltose | Malt | 7.20 | 673.2716 | [M+H]+ |
| 41 | | Glucose | Gluc | 7.55 | 511.2188 | [M+H]+ |

| No. | Groups | Metabolites | Abbreviation | Retention Time (min) | Quantifier ion | |
|---|---|---|---|---|---|---|
| | | | | | m/z | Type |
| 42 | | Raffinose | Raf | NA | NA | NA |
| 43 | | Sucrose | Suc | NA | NA | NA |
| 44 | | Fructose | Fruc | NA | NA | NA |

AQC: 6-aminoquinolyl-N-hydroxysuccinimidyl carbamate; PMP: 1-phenyl-3-methyl-5-pyrazolone. NA denotes that analyses were conducted using the Dionex ICS-5000 ion chromatography system followed by conductivity detection.

**Table S2** Linear mixed-effects models testing the effects of warming, season, year and their interactions on the contents of amino acids, organic acids, and sugars of tree (spruce) roots. The numbers in the columns are F- and P-values generated by linear mixed-effects model testing ($P < 0.05$). All statistical tests were two-sided and p values were corrected for multiple comparison using the Benjamini-Hochberg procedure.

| Parameter | Treatment | | | | Season | | | | Year | | | | Treatment:Season | | | | Treatment:Year | | | | Season:Year | | | | Treatment:Season:Year | | | |
|---|---|---|---|---|---|---|---|---|---|---|---|---|---|---|---|---|---|---|---|---|---|---|---|---|---|---|---|---|
| | N DF | D DF | F | P | N DF | D DF | F | P | N DF | D DF | F | P | N DF | D DF | F | P | N DF | D DF | F | P | N DF | D DF | F | P | N DF | D DF | F | P |
| αAla | 1 | 138 | 1.172 | 0.281 | 2 | 138 | 4.836 | 0.009 | 1 | 138 | 1.333 | 0.250 | 2 | 138 | 0.907 | 0.406 | 1 | 138 | 0.498 | 0.482 | 2 | 138 | 6.883 | **0.001** | 2 | 138 | 0.284 | 0.753 |
| Arg | 1 | 144 | 12.544 | **0.001** | 2 | 144 | 6.690 | **0.002** | 1 | 144 | 0.585 | 0.446 | 2 | 144 | 2.246 | 0.110 | 1 | 144 | 4.248 | **0.041** | 2 | 144 | 6.607 | **0.002** | 2 | 144 | 6.401 | **0.002** |
| Asn | 1 | 144 | 0.002 | 0.965 | 2 | 144 | 1.062 | 0.349 | 1 | 144 | 3.072 | 0.082 | 2 | 144 | 0.926 | 0.398 | 1 | 144 | 0.774 | 0.381 | 2 | 144 | 28.339 | **0.000** | 2 | 144 | 4.332 | **0.015** |
| Asp | 1 | 144 | 0.950 | 0.331 | 2 | 144 | 98.557 | **0.000** | 1 | 144 | 101.063 | **0.000** | 2 | 144 | 1.416 | 0.246 | 1 | 144 | 6.094 | **0.015** | 2 | 144 | 64.058 | **0.000** | 2 | 144 | 10.980 | **0.000** |
| Gln | 1 | 138 | 0.077 | 0.782 | 2 | 138 | 19.091 | **0.000** | 1 | 138 | 0.264 | 0.608 | 2 | 138 | 1.711 | 0.184 | 1 | 138 | 0.055 | 0.814 | 2 | 138 | 16.216 | **0.000** | 2 | 138 | 0.628 | 0.535 |
| Glu | 1 | 144 | 1.778 | 0.184 | 2 | 144 | 34.926 | **0.000** | 1 | 144 | 43.559 | **0.000** | 2 | 144 | 1.058 | 0.350 | 1 | 144 | 3.026 | 0.084 | 2 | 144 | 73.291 | **0.000** | 2 | 144 | 2.636 | 0.075 |
| Gly | 1 | 138 | 6.005 | **0.016** | 2 | 138 | 5.185 | **0.007** | 1 | 138 | 13.321 | **0.000** | 2 | 138 | 2.290 | 0.105 | 1 | 138 | 1.623 | 0.205 | 2 | 138 | 25.206 | **0.000** | 2 | 138 | 3.224 | **0.043** |
| Ile | 1 | 144 | 0.001 | 0.976 | 2 | 144 | 6.001 | **0.003** | 1 | 144 | 12.030 | **0.001** | 2 | 144 | 0.008 | 0.992 | 1 | 144 | 1.202 | 0.275 | 2 | 144 | 22.178 | **0.000** | 2 | 144 | 0.195 | 0.823 |
| Leu | 1 | 144 | 0.100 | 0.752 | 2 | 144 | 4.279 | **0.016** | 1 | 144 | 18.637 | **0.000** | 2 | 144 | 0.259 | 0.772 | 1 | 144 | 1.381 | 0.242 | 2 | 144 | 36.993 | **0.000** | 2 | 144 | 0.638 | 0.530 |
| Lys | 1 | 72 | 6.861 | **0.011** | 1 | 72 | 11.056 | **0.001** | 1 | 72 | 7.717 | **0.007** | 1 | 72 | 0.034 | 0.854 | 1 | 72 | 0.223 | 0.638 | NA | NA | NA | NA | NA | NA | NA | NA |
| Phe | 1 | 138 | 0.006 | 0.941 | 2 | 138 | 11.606 | **0.000** | 1 | 138 | 55.818 | **0.000** | 2 | 138 | 0.038 | 0.963 | 1 | 138 | 0.710 | 0.401 | 2 | 138 | 16.214 | **0.000** | 2 | 138 | 0.288 | 0.751 |
| Pro | 1 | 144 | 0.130 | 0.719 | 2 | 144 | 1.979 | 0.142 | 1 | 144 | 0.624 | 0.431 | 2 | 144 | 0.479 | 0.620 | 1 | 144 | 1.979 | 0.162 | 2 | 144 | 13.499 | **0.000** | 2 | 144 | 3.712 | **0.027** |
| Ser | 1 | 138 | 0.465 | 0.496 | 2 | 138 | 4.614 | **0.011** | 1 | 138 | 37.302 | **0.000** | 2 | 138 | 0.490 | 0.613 | 1 | 138 | 0.971 | 0.326 | 2 | 138 | 21.062 | **0.000** | 2 | 138 | 2.780 | 0.065 |
| Thr | 1 | 144 | 5.694 | **0.018** | 2 | 144 | 1.872 | 0.157 | 1 | 144 | 15.995 | **0.000** | 2 | 144 | 0.770 | 0.465 | 1 | 144 | 0.627 | 0.430 | 2 | 144 | 2.755 | 0.067 | 2 | 144 | 4.788 | **0.010** |
| Trp | 1 | 144 | 5.268 | **0.023** | 2 | 144 | 30.285 | **0.000** | 1 | 144 | 36.806 | **0.000** | 2 | 144 | 0.278 | 0.758 | 1 | 144 | 1.751 | 0.188 | 2 | 144 | 30.755 | **0.000** | 2 | 144 | 2.551 | 0.082 |
| Tyr | 1 | 138 | 0.009 | 0.925 | 2 | 138 | 14.487 | **0.000** | 1 | 138 | 6.051 | **0.015** | 2 | 138 | 0.339 | 0.713 | 1 | 138 | 4.268 | **0.041** | 2 | 138 | 10.103 | **0.000** | 2 | 138 | 1.231 | 0.295 |
| Val | 1 | 138 | 0.496 | 0.482 | 2 | 138 | 23.173 | **0.000** | 1 | 138 | 39.479 | **0.000** | 2 | 138 | 1.139 | 0.323 | 1 | 138 | 0.032 | 0.858 | 2 | 138 | 18.130 | **0.000** | 2 | 138 | 1.794 | 0.170 |
| βAla | 1 | 120 | 0.610 | 0.436 | 2 | 120 | 35.340 | **0.000** | 1 | 120 | 298.363 | **0.000** | 2 | 120 | 0.342 | 0.711 | 1 | 120 | 0.001 | 0.978 | 1 | 120 | 38.546 | **0.000** | 1 | 120 | 0.198 | 0.657 |
| GABA | 1 | 138 | 2.646 | 0.106 | 2 | 138 | 110.124 | **0.000** | 1 | 138 | 103.497 | **0.000** | 2 | 138 | 0.704 | 0.496 | 1 | 138 | 3.924 | **0.050** | 2 | 138 | 107.240 | **0.000** | 2 | 138 | 0.913 | 0.404 |
| Aaa | 1 | 144 | 2.164 | 0.143 | 2 | 144 | 28.054 | **0.000** | 1 | 144 | 39.048 | **0.000** | 2 | 144 | 0.252 | 0.777 | 1 | 144 | 3.080 | 0.081 | 2 | 144 | 23.715 | **0.000** | 2 | 144 | 1.978 | 0.142 |
| Taa | 1 | 144 | 5.918 | **0.016** | 2 | 144 | 3.366 | **0.037** | 1 | 144 | 22.428 | **0.000** | 2 | 144 | 1.191 | 0.307 | 1 | 144 | 2.872 | 0.092 | 2 | 144 | 24.101 | **0.000** | 2 | 144 | 3.958 | **0.021** |
| Ace | 1 | 138 | 0.000 | 0.991 | 2 | 138 | 42.557 | **0.000** | 1 | 138 | 0.254 | 0.615 | 2 | 138 | 0.339 | 0.713 | 1 | 138 | 0.070 | 0.792 | 2 | 138 | 133.861 | **0.000** | 2 | 138 | 0.149 | 0.862 |
| cAco | 1 | 144 | 0.068 | 0.794 | 2 | 144 | 2.591 | 0.078 | 1 | 144 | 49.594 | **0.000** | 2 | 144 | 1.237 | 0.293 | 1 | 144 | 6.531 | 0.012 | 2 | 144 | 83.099 | **0.000** | 2 | 144 | 2.859 | 0.061 |
| Cit | 1 | 144 | 0.314 | 0.576 | 2 | 144 | 5.992 | **0.003** | 1 | 144 | 105.025 | **0.000** | 2 | 144 | 1.263 | 0.286 | 1 | 144 | 2.068 | 0.153 | 2 | 144 | 6.694 | **0.002** | 2 | 144 | 2.684 | 0.072 |
| For | 1 | 138 | 1.022 | 0.314 | 2 | 138 | 12.173 | **0.000** | 1 | 138 | 172.968 | **0.000** | 2 | 138 | 1.300 | 0.276 | 1 | 138 | 0.008 | 0.930 | 2 | 138 | 4.771 | **0.010** | 2 | 138 | 2.553 | 0.082 |
| Fum | 1 | 138 | 3.488 | 0.064 | 2 | 138 | 25.036 | **0.000** | 1 | 138 | 37.505 | **0.000** | 2 | 138 | 1.557 | 0.214 | 1 | 138 | 6.895 | **0.010** | 2 | 138 | 20.381 | **0.000** | 2 | 138 | 2.986 | 0.054 |
| Mali | 1 | 138 | 0.048 | 0.827 | 2 | 138 | 13.847 | **0.000** | 1 | 138 | 142.504 | **0.000** | 2 | 138 | 0.810 | 0.447 | 1 | 138 | 0.646 | 0.423 | 2 | 138 | 8.141 | **0.000** | 2 | 138 | 0.038 | 0.963 |
| Malo | 1 | 138 | 0.227 | 0.634 | 2 | 138 | 141.504 | **0.000** | 1 | 138 | 323.837 | **0.000** | 2 | 138 | 0.172 | 0.842 | 1 | 138 | 0.024 | 0.877 | 2 | 138 | 140.731 | **0.000** | 2 | 138 | 0.064 | 0.938 |
| OAA | 1 | 140 | 7.761 | **0.006** | 2 | 140 | 2.152 | 0.120 | 1 | 4 | 0.078 | 0.794 | 2 | 140 | 0.714 | 0.492 | 1 | 140 | 5.790 | **0.017** | 2 | 140 | 15.631 | **0.000** | 2 | 140 | 1.616 | 0.202 |
| Oxa | 1 | 144 | 0.294 | 0.588 | 2 | 144 | 6.384 | **0.002** | 1 | 144 | 102.426 | **0.000** | 2 | 144 | 0.072 | 0.931 | 1 | 144 | 1.277 | 0.260 | 2 | 144 | 3.058 | **0.050** | 2 | 144 | 0.440 | 0.645 |
| Succ | 1 | 138 | 1.001 | 0.319 | 2 | 138 | 21.117 | **0.000** | 1 | 138 | 56.815 | **0.000** | 2 | 138 | 0.570 | 0.567 | 1 | 138 | 0.049 | 0.825 | 2 | 138 | 34.941 | **0.000** | 2 | 138 | 0.793 | 0.455 |
| Tar | 1 | 140 | 2.103 | 0.149 | 2 | 140 | 99.409 | **0.000** | 1 | 4 | 158.067 | **0.000** | 2 | 140 | 3.003 | 0.053 | 1 | 140 | 1.175 | 0.280 | 2 | 140 | 162.923 | **0.000** | 2 | 140 | 0.113 | 0.894 |
| Van | 1 | 138 | 0.271 | 0.604 | 2 | 138 | 21.526 | **0.000** | 1 | 138 | 1.519 | 0.220 | 2 | 138 | 1.882 | 0.156 | 1 | 138 | 1.238 | 0.268 | 2 | 138 | 53.183 | **0.000** | 2 | 138 | 1.112 | 0.332 |

| | | | | | | | | | | | | | | | | | | | | | | | | | | | |
|---|---|---|---|---|---|---|---|---|---|---|---|---|---|---|---|---|---|---|---|---|---|---|---|---|---|---|---|
| TOA | 1 | 144 | 0.309 | 0.579 | 2 | 144 | 17.027 | **0.000** | 1 | 144 | 226.519 | **0.000** | 2 | 144 | 1.693 | 0.188 | 1 | 144 | 0.150 | 0.699 | 2 | 144 | 21.640 | **0.000** | 2 | 144 | 1.214 | 0.300 |
| Ara | 1 | 137 | 1.782 | 0.184 | 2 | 137 | 154.312 | **0.000** | 1 | 1 | 49.822 | 0.080 | 2 | 137 | 0.015 | 0.985 | 1 | 137 | 0.016 | 0.898 | 2 | 137 | 50.447 | **0.000** | 2 | 137 | 2.785 | 0.065 |
| Gala | 1 | 140 | 6.035 | **0.015** | 2 | 140 | 79.870 | **0.000** | 1 | 4 | 13.009 | **0.023** | 2 | 140 | 0.405 | 0.668 | 1 | 140 | 0.040 | 0.842 | 2 | 140 | 63.021 | **0.000** | 2 | 140 | 0.614 | 0.542 |
| GluA | 1 | 107 | 20.254 | **0.000** | 2 | 107 | 50.480 | **0.000** | 1 | 4 | 78.972 | **0.001** | 2 | 107 | 2.081 | 0.130 | 1 | 107 | 12.417 | **0.001** | 1 | 107 | 12.753 | **0.001** | 1 | 107 | 2.668 | 0.105 |
| Fuc | 1 | 140 | 0.904 | 0.343 | 2 | 140 | 10.446 | **0.000** | 1 | 4 | 3.180 | 0.149 | 2 | 140 | 2.987 | 0.054 | 1 | 140 | 1.341 | 0.249 | 2 | 140 | 17.032 | **0.000** | 2 | 140 | 1.991 | 0.140 |
| Man | 1 | 136 | 16.141 | **0.000** | 2 | 136 | 18.632 | **0.000** | 1 | 3 | 10.666 | 0.053 | 2 | 136 | 0.239 | 0.788 | 1 | 136 | 0.037 | 0.848 | 2 | 136 | 11.144 | **0.000** | 2 | 136 | 0.319 | 0.727 |
| Rha | 1 | 138 | 1.496 | 0.223 | 2 | 138 | 0.983 | 0.377 | 1 | 138 | 7.677 | **0.006** | 2 | 138 | 0.391 | 0.677 | 1 | 138 | 5.098 | **0.026** | 2 | 138 | 13.653 | **0.000** | 2 | 138 | 1.998 | 0.140 |
| Rib | 1 | 138 | 18.158 | **0.000** | 2 | 138 | 7.233 | **0.001** | 1 | 138 | 8.503 | **0.004** | 2 | 138 | 0.612 | 0.543 | 1 | 138 | 0.397 | 0.530 | 2 | 138 | 23.685 | **0.000** | 2 | 138 | 0.869 | 0.422 |
| Deo | 1 | 120 | 2.116 | 0.148 | 2 | 123 | 0.235 | 0.791 | 1 | 124 | 0.131 | 0.718 | 2 | 119 | 0.442 | 0.644 | 1 | 120 | 0.498 | 0.482 | 2 | 123 | 47.334 | **0.000** | 2 | 119 | 0.449 | 0.639 |
| Malt | 1 | 136 | 0.766 | 0.383 | 2 | 136 | 65.905 | **0.000** | 1 | 3 | 95.625 | **0.003** | 2 | 136 | 0.291 | 0.748 | 1 | 136 | 0.155 | 0.694 | 2 | 136 | 42.941 | **0.000** | 2 | 136 | 1.987 | 0.141 |
| Raf | 1 | 114 | 0.312 | 0.578 | 2 | 114 | 19.747 | **0.000** | 1 | 114 | 133.086 | **0.000** | 2 | 114 | 4.146 | **0.018** | 1 | 114 | 1.404 | 0.238 | 1 | 114 | 79.758 | **0.000** | 1 | 114 | 0.202 | 0.654 |
| Suc | 1 | 138 | 2.525 | 0.114 | 2 | 138 | 70.798 | **0.000** | 1 | 138 | 172.102 | **0.000** | 2 | 138 | 2.232 | 0.111 | 1 | 138 | 0.082 | 0.775 | 2 | 138 | 47.312 | **0.000** | 2 | 138 | 0.187 | 0.830 |
| Fruc | 1 | 138 | 14.132 | **0.000** | 2 | 138 | 0.616 | 0.542 | 1 | 138 | 16.160 | **0.000** | 2 | 138 | 2.738 | 0.068 | 1 | 138 | 0.511 | 0.476 | 2 | 138 | 18.931 | **0.000** | 2 | 138 | 2.711 | 0.070 |
| Gluc | 1 | 138 | 7.831 | **0.006** | 2 | 138 | 35.022 | **0.000** | 1 | 138 | 11.523 | **0.001** | 2 | 138 | 1.105 | 0.334 | 1 | 138 | 2.081 | 0.151 | 2 | 138 | 17.244 | **0.000** | 2 | 138 | 1.504 | 0.226 |
| TS | 1 | 138 | 12.080 | **0.001** | 2 | 138 | 23.063 | **0.000** | 1 | 138 | 115.765 | **0.000** | 2 | 138 | 3.368 | **0.037** | 1 | 138 | 0.371 | 0.543 | 2 | 138 | 43.299 | **0.000** | 2 | 138 | 1.237 | 0.293 |
| TPM | 1 | 138 | 12.882 | **0.000** | 2 | 138 | 10.333 | **0.000** | 1 | 138 | 191.881 | **0.000** | 2 | 138 | 3.773 | **0.025** | 1 | 138 | 0.775 | 0.380 | 2 | 138 | 27.056 | **0.000** | 2 | 138 | 0.923 | 0.400 |

**Note:** TAA: Total Amino Acids; TS: Total Sugars; TOA: Total Organic Acids; TPM: Total Primary Metabolites. All statistical tests were two-sided and p values were corrected for multiple comparison using the Benjamini-Hochberg procedure. N DF: numerator degrees of freedom, D DF: denominator degrees of freedom.

**Table S3** Linear mixed-effects models testing the effects of warming, season, year and their interactions on soil moisture, soil temperature, and root morphology. The numbers in the columns are F- and P-values generated by linear mixed-effects model testing ($P < 0.05$). All statistical tests were two-sided and p values were corrected for multiple comparison using the Benjamini-Hochberg procedure.

| Parameter | Treatment | | | | Season | | | | Year | | | | Treatment:Season | | | | Treatment:Year | | | | Season:Year | | | | Treatment:Season:Year | | | |
|---|---|---|---|---|---|---|---|---|---|---|---|---|---|---|---|---|---|---|---|---|---|---|---|---|---|---|---|---|
| | N DF | D DF | F | P | N DF | D DF | F | P | N DF | D DF | F | P | N DF | D DF | F | P | N DF | D DF | F | P | N DF | D DF | F | P | N DF | D DF | F | P |
| SRL | 1 | 114 | 0.207 | 0.650 | 2 | 114 | 2.492 | 0.087 | 1 | 114 | 26.533 | **0.000** | 2 | 114 | 1.816 | 0.167 | 1 | 114 | 0.001 | 0.977 | 1 | 114 | 8.242 | **0.005** | 1 | 114 | 8.748 | **0.004** |
| SRA | 1 | 114 | 0.389 | 0.534 | 2 | 114 | 0.699 | 0.499 | 1 | 114 | 0.455 | 0.501 | 2 | 114 | 0.530 | 0.590 | 1 | 114 | 0.065 | 0.799 | 1 | 114 | 0.207 | 0.650 | 1 | 114 | 3.327 | 0.071 |
| RTD | 1 | 120 | 1.148 | 0.286 | 2 | 120 | 13.970 | **0.000** | 1 | 120 | 3.617 | 0.060 | 2 | 120 | 1.992 | 0.141 | 1 | 120 | 0.019 | 0.890 | 1 | 120 | 15.464 | **0.000** | 1 | 120 | 0.005 | 0.942 |
| Diameter | 1 | 114 | 0.192 | 0.662 | 2 | 114 | 22.629 | **0.000** | 1 | 114 | 50.832 | **0.000** | 2 | 114 | 0.031 | 0.970 | 1 | 114 | 0.007 | 0.933 | 1 | 114 | 45.077 | **0.000** | 1 | 114 | 1.178 | 0.280 |
| Temp | 1 | 138 | 2717 | **0.000** | 2 | 138 | 4079 | **0.000** | 1 | 138 | 902 | **0.000** | 2 | 138 | 1.161 | 0.316 | 1 | 138 | 0.034 | 0.854 | 2 | 138 | 316.667 | **0.000** | 2 | 138 | 0.376 | 0.687 |
| Moisture | 1 | 138 | 0.001 | 0.976 | 2 | 138 | 28.103 | **0.000** | 1 | 138 | 11.838 | **0.001** | 2 | 138 | 8.246 | **0.000** | 1 | 138 | 8.748 | **0.004** | 2 | 138 | 5.731 | **0.004** | 2 | 138 | 2.606 | 0.077 |

**Note:** SRL: Specific root length; SRA: specific root area; RTD: Root tissue density. All statistical tests were two-sided and p values were corrected for multiple comparison using the Benjamini-Hochberg procedure. N DF: numerator degrees of freedom, D DF: denominator degrees of freedom.

**Table S4** Soil temperature, soil moisture, and root morphological parameters in control and warmed plots across years and treatments. All statistical tests were two-sided and p values were corrected for multiple comparison using the Benjamini-Hochberg procedure.

| Parameter | Average | | 2020 | | 2021 | |
|---|---|---|---|---|---|---|
| | **Control** | **Warming** | **Control** | **Warming** | **Control** | **Warming** |
| SRL ($cm\ g^{-1}$) | 9.27±0.59 | 8.79±0.48 | 7.79±0.69 | 6.68±0.73 | 10.26±0.84 | 10.2±0.53 |
| SRA ($cm^2\ g^{-1}$) | 2.06±0.1 | 1.98±0.08 | 2.06±0.16 | 1.89±0.18 | 2.06±0.13 | 2.03±0.07 |
| RTD ($g\ cm^{-3}$) | 0.32±0.02 | 0.30±0.01 | 0.27±0.03 | 0.28±0.03 | 0.35±0.02 | 0.32±0.01 |
| Diameter (cm) | 0.08±0.01 | 0.08±0.01 | 0.10±0.01 | 0.10±0.01 | 0.06±0.01 | 0.07±0.01 |
| Temperature (°C) | 9.02±0.45 | 13.04±0.46 | 10.19±0.7 | 14.19±0.72 | 7.86±0.49 | 11.89±0.52 |
| Moisture (Vol. %) | 0.47±0.01 | 0.47±0.01 | 0.46±0.01 | 0.44±0.01 | 0.47±0.01 | 0.50±0.02 |

SRL: Specific root length; SRA: specific root area; RTD: Root tissue density.

**Figure.S1** Monthly(a) and annual (b) air temperatures and precipitation for 2020-2021 versus 2000-2019.

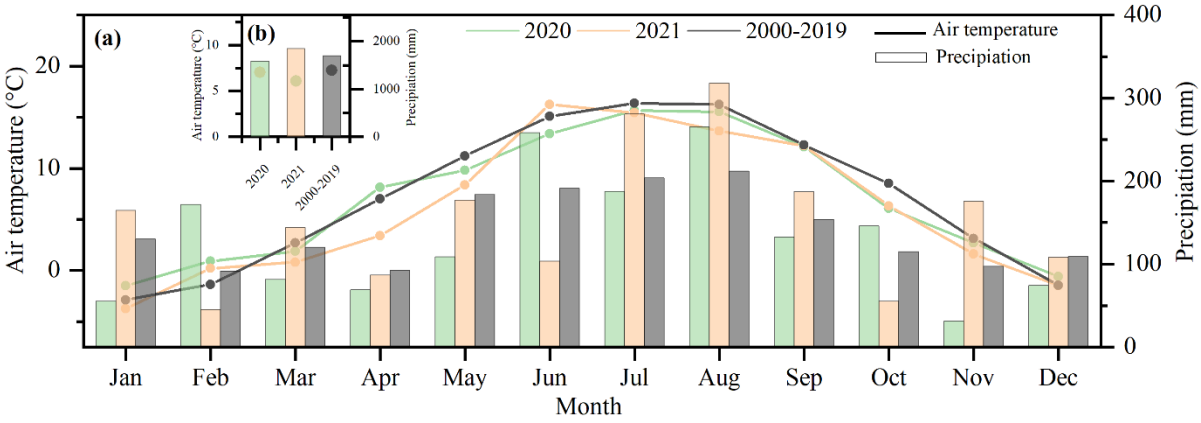

# Chapter III

# The quantity and biochemical composition of root exudates is not affected by long-term soil warming in a temperate forest

# The quantity and biochemical composition of root exudates is not affected by long-term soil warming in a temperate forest

Xiaofei Liu[1,2,3], Jakob Heinzle[4], Ye Tian[1], Erika Salas[1], Steve Kwatcho-Kengdo[5], Werner Borken[5], Andreas Schindlbacher[4], Wolfgang Wanek[1]

[1]Division of Terrestrial Ecosystem Research, Department of Microbiology and Ecosystem Science, Center of Microbiology and Environmental Systems Science, University of Vienna, Djerassiplatz 1, 1030 Vienna, Austria;

[2]Doctoral School in Microbiology and Environmental Science, University of Vienna, Djerassiplatz 1, A-1030 Vienna, Austria;

[3]Key Laboratory of Humid Subtropical Eco-geographical Process of Ministry of Education, School of Geographical Sciences, Fujian Normal University, Fuzhou 350117, China;

[4]Department of Forest Ecology and Soils, Federal Research and Training Centre for Forests, Natural Hazards and Landscape-BFW, Seckendorff-Gudent Weg 8, 1131 Vienna, Austria;

[5]Department of Soil Ecology, Bayreuth Center of Ecology and Environmental Research (BAYCEER), University of Bayreuth, Dr.-Hans-Frisch-Straße 1-3, 95448, Bayreuth, Germany

**Abstract**

Primary metabolites in root exudates are crucial for plant growth and interactions within the rhizosphere, with their release being sensitive to climate warming. However, the specific effects of long-term soil warming on the exudation of these metabolites are yet not fully understood. In this study, we examined how soil warming impacts the rates and profiles of primary metabolites in root exudates in a temperate forest soil warming experiment (Achenkirch, >14 years, +4 °C) in Austria. We also explored how strongly root exudate rates are controlled by root tissue metabolism and metabolite patterns. We showed that the rates and profiles of primary metabolites in root exudates showed no response to long-term soil warming, while sampling date (season and year) showed significant effects. Seasonal changes in exudate primary metabolite profiles could be partly predicted by differences in soil temperature, root diameter, and specific root length. Our findings reveal that root tissues and root exudates showed largely overlapping primary metabolite profiles, and that these metabolites exhibited a strong positive correlation between root tissue and root exudate levels. This implies that primary metabolite exudation rates were largely driven by concentration differences between fine root tissues and soil solution. Our results demonstrate that the metabolic response of woody plants to long-term warming is highly conservative. This study highlights the complex nature of root exudation processes in response to environmental change and underscores the importance of in-depth metabolomic research in forest ecology to comprehend the broader impacts of climate change on tree root metabolism.

**Key words:** primary metabolites, root exudates, root tissue, long term soil warming, temperate forest.

## Introduction

Plants allocate 20-40% of recent photosynthetic carbon (C) to the soil through root exudates (Pausch and Kuzyakov, 2018; Brunn et al., 2022). Root exudates contain a complex array of primary and secondary metabolites, such as amino acids, organic acids, sugars, flavonoids, and terpenoids (Badri and Vivanco, 2009; Williams and de Vries, 2020). These compounds are not only a C source for microbial growth and proliferation, stimulating microbial decomposition of soil organic matter (Pausch and Kuzyakov, 2018; Panchal et al., 2022), but are also considered to serve as plant defensive compounds, as physical and chemical signals, and to control interactions with other organisms (Badri and Vivanco, 2009; Hong et al., 2022; Panchal et al., 2022). The rates and profiles of root exudates varies depending on many factors, such as plant species (Proctor and He, 2017), root morphology (Williams et al., 2022), abiotic factors (i.e., temperature and moisture) (Berini et al., 2018; Williams and de Vries, 2020), and biotic factors (i.e., insect infestation or mycorrhizal colonization) (Meier et al., 2020; Lv et al., 2023). Among these factors, temperature is of utmost concern because global air temperatures rise continuously and rising temperatures being accompanied by other stresses like soil moisture deficits (Berini et al., 2018; Reich et al., 2018). For instance, warming adversely affects plant photosynthesis by reducing soil moisture (Reich et al., 2018), which may in turn modify plant metabolite levels (Berini et al., 2018). These metabolic changes not only directly impact the biochemical interactions between plants and soil microbes but may also lead to unforeseen outcomes, reducing the plants' beneficial role in mitigating climate change, specifically through reduced fixation and storage of atmospheric C in plant biomass and transfer into soils (Badri and Vivanco, 2009; Panchal et al., 2022). Therefore, gaining a deeper understanding of how primary metabolite profiles of root exudates respond to warming is crucial for shedding light on plant-soil-microbe adaptations to climate change.

Over recent decades, studies have more extensively documented the impact of warming on root exudation rates, though the findings have been inconsistent (Yin et al., 2013; Xiong et al., 2020; Wang et al., 2021; Leuschner et al., 2022; Heinzle et al., 2023). Some research indicates enhanced root exudation rates across ecosystems with increased temperature, caused by experimental soil warming or along an altitudinal transect (Yin et al., 2013;

Leuschner et al., 2022). However, other studies found that warming led to a decline in root exudation, attributed to decreased fine root activity at temperatures above optimal levels and diminished soil moisture, as observed in Chinese fir seedlings in subtropical forests (Xiong et al., 2020). Interestingly, temperate forests subjected to long-term warming showed no significant changes in root exudation rates (Heinzle et al., 2023). These controversial results may be attributed to the differences in soil N availability, plant species, plant age, and experimental duration (Yin et al., 2013; Xiong et al., 2020; Wang et al., 2021; Heinzle et al., 2023). However, most of this research has focused on bulk root C exudation rates (Yin et al., 2013; Brunn et al., 2022), while the primary metabolite profiles of root exudates have rarely been qualitatively and absolutely quantitatively studied (Sandnes et al., 2005; Gargallo-Garriga et al., 2018; Wilson et al., 2021). This may be explained by the following reasons: firstly, the analysis of primary metabolite profiles and their absolute quantification in root exudates has been hampered by their concentration, being too low to be detected by common methods. For instance, concentrations of organic acids in root exudates (in the low μM range; Sandnes et al., 2005) are approximately 1000-fold lower than they are in root tissue (in the mM range in root cytoplasm and vacuoles, Ryan et al., 2001). On the other hand, many primary metabolites may require time-consuming chemical derivatization methods for quantitative measurement, such as amino acids, sugar nucleotides and oligosaccharides (Wang et al., 2018; Zhou et al., 2019). While the few compound-specific root exudate studies have mostly been performed on grasses, herbs, and crops (Carvalhais et al., 2010; Gargallo-Garriga et al., 2015; Gargallo-Garriga et al., 2018; Tiziani et al., 2022), little is known about primary metabolites in root exudates of woody species. Furthermore, most of these studies relied on hydroponic incubations or pot experiments in the lab or greenhouse (Escandon et al., 2018). Such controlled settings might not truly capture how plant primary metabolite profiles of root exudates respond to warming under natural conditions. Notably, no field warming experiments in forests (especially long-term experiments >10 years) have yet targeted the effects of warming on primary metabolite profiles in root exudates, highlighting a significant knowledge gap in this field.

Previous studies have revealed that root morphological traits, such as specific root length, root tissue density, and root diameter are viable predictors of root exudate profiles and

of root exudation rates (Williams et al., 2022; Rathore et al., 2023). Earlier studies demonstrated that root morphology and physiology are significantly affected by warming (Jiang et al., 2022a; Kwatcho Kengdo et al., 2022). For instance, in a long-term soil warming experiment in a temperate forest warming significantly increased specific root length, specific root area, and root tip density (Kwatcho Kengdo et al., 2022). In addition, warming can directly or indirectly influence soil nutrient availability, such as the bioavailability of nitrogen (N) or phosphorus (P) (Bai et al., 2013; Tian et al., 2023b), which may in turn alter the rates and profiles of root exudates (Tawaraya et al., 2018; Jiang et al., 2022b). For example, under P deficiency, of the exudation of γ-aminobutyric acid and of carbohydrates was stimulated in maize plants (Carvalhais et al., 2010). However, still few studies considered the within-root variability of the exudation processes, and no studies explored how the primary metabolite profile of root exudation is affected by root morphology under warming. It is crucial to study these variations, as they will provide a deeper understanding of how root exudates influence plant-soil interactions in a warming environment.

Although the role of C supply to roots in mediating the rates of C release via root exudates has been acknowledged (Farrar and Jones, 2000; Dilkes et al., 2004; Brunn et al., 2022), there's a gap in understanding how the concentration and dynamics of primary metabolites in root tissues relate to the flux rates of root exudates, and this particularly in the context of climate warming. Though the specific underlying transporters are yet to be characterized the exudation of primary metabolites in fine roots is likely mediated by relatively specific efflux carriers, which enable the passive efflux of primary metabolites along the inside-outside pointing concentration gradient in a regulated way (through up- and down-regulation of the gene expression of those carriers (Canarini et al., 2019). The carriers thereby confer a high level of regulation and of specificity to the root exudation process, as metabolites lacking carrier systems will not turn up in the root exudates in substantial quantities, given that cellular bio-membranes are largely impermeable to hydrophilic polar metabolites.

Primary metabolites have multiple functions in root tissues, contributing to osmotic regulation, enhancing drought and freezing tolerance, and serving as metabolic substrates and storage products (Nagele et al., 2022; Long and Adams, 2023). Conversely, primary

metabolites in root exudates are primarily recognized as essential C and N sources for rhizosphere soil microbial communities (Badri and Vivanco, 2009; Canarini et al., 2019). For example, different microbial groups may preferentially utilize specific compounds in root exudates, root exudates thereby influencing microbial community assembly and soil organic C decomposition (Zhalnina et al., 2018). Moreover, organic acids in root exudates play a crucial role in mobilizing P from mineral bound P pools in P-deficient soils (Badri and Vivanco, 2009; Tawaraya et al., 2018; Jiang et al., 2022b), while in plants they are involved in energy production and serve as precursors for amino acid biosynthesis (Lopez-Bucio et al., 2000). The intricate relationships between primary metabolites in root tissues and those in root exudates, particularly under changing climate conditions, remain an underexplored topic and present an important field for further scientific investigation (Canarini et al., 2019).

Metabolomic techniques are considered a powerful tool to investigate the response of plants to environmental change at the metabolite level (Sardans et al., 2020; Carrera et al., 2021; Escolà Casas and Matamoros, 2021), yet such techniques have been applied only to a few warming studies (Gargallo-Garriga et al., 2015; Berini et al., 2018; Escandon et al., 2018). For example, warming lead to distinct changes in secondary metabolite profiles in several temperate tree species in the United States (Berini et al., 2018). These few metabolomics studies provided some insight in how plant metabolite profiles change with warming, but they were performed with untargeted method, which provides only qualitative but not quantitative information (Gargallo-Garriga et al., 2015; Escandon et al., 2018; Gargallo-Garriga et al., 2018; Williams et al., 2022). Targeted analysis can provide reliable identification and accurate quantification of those specific compounds, which are commercially available as standards (Carrera et al., 2021). Thus, it is important to apply metabolomics techniques to improve our knowledge and understanding of the possible changes in primary metabolites in root exudates under future warming, due to their important role in plant-soil-microbe functioning (Preece et al., 2018; Panchal et al., 2022).

Here, utilizing the infrastructure of the Achenkirch soil warming experiment, we investigated how prolonged soil warming (>10 years) influences the quantity and composition of primary metabolites in tree root exudates. We hypothesized that (1) soil warming increases the rates of primary metabolites in root exudates due to higher root

activity and root growth rates. We particularly expected roots to increase the exudation of organic acids in warmed soils, to increase the mobilization of inorganic P, given the strong signs of (increased) soil P limitation in warmed soils (Tian et al., 2023b). We also expected (2) that variations in root exudation can be predicted by related differences in root morphology between plots, treatments, and seasons. Finally, we hypothesized that (3) differences in the metabolomes of root tissues and root exudates indicate the specificity of the root exudation processes, driven by the absence/presence of specific carrier systems for the efflux of metabolites into the rhizosphere. At the same time, given that carrier-driven efflux of primary metabolites in exudates is passive and largely follows concentration differences between the root simplest and the external medium we hypothesized that those metabolites that occur in root tissues and in exudates show a positive relationship between exudation rates and root tissue contents, highlighting intricate metabolic relationships between tissue metabolite dynamics and root exudation as potentially influenced by prolonged soil warming.

## Materials and Methods

### Study location and experimental design

This study was conducted in a temperate forest located in the Northern Limestone Alps of Achenkirch, Austria (47°34′50″ N, 11° 38′ 21″ E) at an elevation of 910 m a.s.l. This 140-year-old forest primarily consists of spruce trees (*Picea abies*, approximately 80%), interspersed with European beech (*Fagus sylvatica*, about 15%) and a minority of white fir (*Abies alba*, around 5%). The soils are characterized by patches of Chromic Cambisols, varying between 30-60 cm in depth, and shallower Rendzic Leptosols, measuring between 10-30 cm in depth. Dolomite bedrock underpins the forest, and the prevailing humus form is Mull. Due to significant carbonate presence, the soil has a nearly neutral pH. The site receives an average annual rainfall of 1563 mm and has an average annual air temperature of 6.8 °C (both from 1988 to 2017). Annual wet N deposition is approximately 15 kg $ha^{-1}$.

The soil warming facility was laid out in a paired block design consisting of twelve plots, each measuring 2 m × 2 m. These plots were grouped into six blocks, with three blocks established in 2004 and the remaining three in 2007, resulting in a total of six pairs. Each pair of plots within a block was subjected to one of two treatments: ambient temperature serving as the control, and soil warming by 4 °C above ambient. To achieve the warming effect, soil warming cables (Etherma, Salzburg, Austria) were installed at a depth of 3 cm, spaced 7.5 cm apart, in the warming plots. Similarly, dummy cables were inserted in the control plots to replicate the physical disturbance caused by the installation of active cables. During the snow-free period, which typically spans from April to November, the soil temperature in the warmed plots was maintained at a consistent 4 °C above that of the control plots. During winter the soil warming was stalled to omit unintended effects by snow melt. Soil temperature was recorded accurately at half-hourly intervals at 5 cm and 15 cm soil depth in all control and warmed plots.

### Root exudate and root tissue collection

Root exudates were collected during May, August, and October 2020, as well as in April, July, and October 2021 using a dedicated cuvette system designed for *in-situ* root exudate collection (Phillips et al., 2008), as modified and described in Heinzle et al. (2023). Briefly,

in each subplot two terminal fine root branches (5-10 cm long, consisting of first to third order fine roots < 2mm diameter) were identified and traced in the top 10 cm of soil, and cleaned by detaching soil particles, by rinsing with ultrapure (Milli Q) water and treatment with 0.5 mM $CaCl_2$ for an hour. Then the live (attached) root branches were placed in 30 mL glass syringes equipped with a three-way Luer lock and filled with acid-washed glass beads (1 mm diameter). After sealing (glass cotton) the syringes with Parafilm, they were flushed twice with 30 mL of 0.5 mM $CaCl_2$, filled with 15 mL $CaCl_2$ and positioned in the topsoil at ~5 cm depth between two heating or dummy cables. Each one control syringe without roots was also prepared similarly for each subplot. After a day's incubation in situ, the exudates in the $CaCl_2$ solution were extracted using suction, followed by flushing the cuvette systems two times with $CaCl_2$ solution via the Luer-lock using a sterile syringe. The sample solution and the flushing solutions were then combined, passed through Chromafil CA-20/25-sterile cellulose acetate filters (0.20 µm pore size), and stored at -20 °C. Roots were cut at the location where they entered the syringe and carefully rinsed from glass beads, after the exudate sampling was completed. The root segments were cooled at +4 °C until they were scanned for root morphological traits (Heinzle et al., 2023) and subsequent freeze-drying for root metabolite analysis (Liu et al., 2024, in press).

**Root morphological trait analyses**

The root segments were scanned for root morphological traits including root length, surface area, and volume using WinRHIZO 2004b (Regents Instruments Inc., Quebec, Canada). After scanning, the roots were freeze-dried to establish dry mass, and exudation rates of primary metabolites were computed based on single metabolite concentrations accumulated in syringe solutions over incubation time, factoring in root dry mass, root length, and/or root surface area. Metrics like specific root length (SRL), specific root area (SRA), and root tissue density (RTD) were derived from the ratio of root dry mass to its length, area, and volume.

**Metabolite extraction from root tissue**

For metabolite extraction from freeze-dried root tissues, samples were pulverized in a ball mill and 20-40 mg of fine powder (<10 µm) was subjected to extraction in 2 ml vials using

1.5 ml of methanol/chloroform/MQ mixture (12:3:5 v/v/v) at 70 °C for 30 min with intermittent vortexing. Cooled samples were centrifuged at 10,000 g for 5 min, and 800 µl supernatant was pipetted into a new vial. Phase separation was achieved by adding 800 µl MQ and 250 µl chloroform and mixing thoroughly, followed by centrifugation to partition chloroform and aqueous phases. The aqueous phase was further purified by transferring 1.2 ml into a new vial, adding 500 µl chloroform, mixing, and centrifuging to separate phases. The final aqueous phase (1.0 ml) was vacuum-dried (Speed Vac, Savant, Thermo Fisher) and redissolved in 1.0 ml MQ water for metabolite analysis.

**Root exudate and root tissue metabolite analysis**

**Amino acids**

Amino acids were analyzed using an Ultimate 3000 UPLC (Thermo Fisher Scientific Dionex., Sunnyvale, CA, USA) after derivatization with AQC reagent (AccQ-Tag Ultra Derivatization Kit, Waters Corp., Milford, U.S.A). The UPLC system was coupled to a Q Exactive Orbitrap mass spectrometer with an ESI source run in the positive ion mode (Thermo Fisher Scientific Inc., USA). For the derivatization process, 10 µl sample was added to 70 µl borate buffer in a 1.5 ml polypropylene tube, followed by 20 µL AQC reagent. The mixture was vortexed and heated for 10 min at 55 °C. Once derivatized, the samples underwent chromatographic analysis on a 2.1 × 100 mm, 1.7 µm C18 reverse-phase column (AccQ-TagTM ULTRA, Waters, USA) that was maintained at 55 °C, and the injection volume was 1 µL. The eluents utilized were 0.1% formic acid in Milli Q water (A) and 100% acetonitrile (B), with a flow rate of 0.4 ml $min^{-1}$, following a binary gradient program: 0-0.5 min, 0.1% B; 0.5-2.5 min, 0.1%-5.0% B; 2.5-8 min, 5.0%-20% B; 8-8.25 min, 20% B; 8.25-11 min, 20%-10% B; 11-11.2 min, 10%-0.1% B; 11.2-15 min, 0.1% B. Analysis conditions of the Orbitrap mass spectrometer are listed below: spray voltage at 3 kV, capillary temperature at 320 °C, resolution at 70,000, and mass scan range of 50-750 m/z.

**Organic acids**

Organic acids underwent direct analysis (no pre-column derivatization) on a Dionex ICS-5000 ion chromatography system (Thermo Fisher Scientific Dionex., Sunnyvale, CA, USA)

coupled to a Q Exactive Orbitrap mass spectrometer (Thermo Fisher Scientific Inc., USA). Using a Dionex IonPac AS11-HC analytical column (2 × 250 mm) paired with an AS11-HC Guard Column (2 × 250 mm), the samples were separated at a flow rate of 0.3 ml/min and a column temperature of 30 °C. Samples (10 µl injection volume) were separated according to the following gradient: 0-0.2 min, 1 mM KOH; 0.2-17 min, 1-85 mM; 17-20 min, 85 mM KOH; 20-21 min, 85-1 mM KOH), and 21-30 min, 1 mM KOH. The gradient was produced online using a EGM4 eluent generator. During analysis, the Orbitrap was operated in negative ESI mode with parameters set to: spray voltage of 3 kV, capillary temperature of 320 °C, resolution of 70,000, and a mass scan range between 50-750 m/z. Due to its mass being below the Orbitrap's detection limit (< 50 m/z), formic acid (monoisotopic mass 44.99765 g/mol) was exclusively quantified using conductivity detection by ICS-5000 and the Chromeleon 7.2 software. In contrast, the remaining organic acids were quantified using the mass spectrometric signals with Freestyle 1.7 software by Thermo Scientific.

**Sugars**

Sugars were analyzed via pre-column derivatization with 1-phenyl-3-methyl-5-pyrazolone (PMP, Sigma-Aldrich) using the Ultimate 3000 UPLC system coupled to a Q Exactive Orbitrap mass spectrometer (Thermo Scientific) (Salas et al., 2023). Fresh 0.5 M PMP solution in methanol was prepared daily and 100 µl aliquots of samples or standards were mixed with the 100 µl PMP solution and 200 µl ammonia (25-30% ammonium hydroxide solution, Sigma-Aldrich). The mixture was then vortexed briefly and subjected to a 20-minutes reaction at 70 °C in a water bath. After cooling, it was neutralized with 200 µl 100% formic acid and subsequently filtered to be ready for LC-MS analysis. The chromatographic separation was conducted on a 2.1 × 100 mm AccQ-TagTM ULTRA column (Waters, USA). The mobile phases used for the sugar separation were 20 mM ammonium acetate in water (solvent A) and acetonitrile (solvent B). The gradient was as follows: 0-0.5 min, 13% B; 0.5-2 min, 13%-16% B; 2-15 min,16%-21% B; 15-16 min, 21%-60% B; 16-17 min, 60%-90% B; 17-20 min, 90%-13% B; 20-25 min, 13% B. The total analysis time was 25 min per injection, with a constant flow rate of 0.3 ml $min^{-1}$. An injection volume of 2 µL and a column temperature of 35 °C were used. For analysis, the Orbitrap mass spectrometer was set to

positive ESI mode, with further parameters being 3.5 kV spray voltage, 300 °C capillary temperature, and 50-1000 m/z mass scan range.

Fructose, sucrose, and raffinose do not respond well to PMP derivatization due being non-reducing sugars, having a less reactive keto group, or their unique molecular structure causing steric hindrance. To tackle this, we utilized the Dionex ICS-5000 ion chromatography system (Dionex, Thermo Scientific) for direct sugar separation using a CarboPac PA20 analytical column (4 × 250 mm i.d.), paired with a CarboPac PA20 guard column (4 × 50 mm i.d.). For sugar detection, we used pulsed amperometric detection with a gold electrode and a palladium hydrogen (PdH) reference electrode. The elution was performed at a flow rate of 0.3 ml $min^{-1}$, with a column temperature of 30 °C, an injection volume of 10 µl, and a KOH gradient as follows: 0-15 min, 20 mM KOH; 15-20 min, 20 mM to 100 mM KOH; 20-25 min, 100 mM KOH; 25-30 min, 100 to 20 mM KOH.

**Statistical analysis**

The statistical analyses were performed using R software 4.2.3 version. Logarithmic or square root transformations were applied to metabolite concentration data to ensure homoscedasticity and normality when necessary. Linear mixed-effects models using the "lme4" package were run to assess the effects of sampling time and warming treatment, considering warming and season as fixed factors and block and warming duration as random factors.

To determine differences in primary metabolite profiles in root exudates between control and warming treatments, we employed PERMANOVA (through the ADONIS procedure) based on the Bray-Curtis distance. Differences in metabolite profiles were visualized using non-metric multidimensional scaling (NMDS), and Spearman correlations revealed compound associations to NMDS1 and NMDS2 axis scores. These analyses leveraged the "vegan" and "corrplot" R packages. We used the scores of the first two components (NMDS1 and NMDS2) as the summarized root exudate composition proxies for subsequent analyses. Using the “envfit” function with 999 permutations, sampling time and treatment were fitted as centroids, and soil moisture, temperature, root diameter, root surface area, specific root length (SRL), root tissue density (RTD), and specific root area (SRA) were fitted as vectors

onto the NMDS ordination plot to examine how root exudate composition was related to these variables. Venn diagrams were constructed using the "VennDiagram" package to visualize shared and unique metabolites between root tissue and root exudates. Principal component analysis (PCA) was performed to investigate the metabolite profiles of root tissues versus root exudates. Additionally, regressions were run to relate the natural logarithms of the average metabolite values in root exudates to those in root tissues within each metabolite group (amino acids, organic acids, and sugars).

Finally, utilizing the "LEAPS" package in R, we conducted regression subset selection to identify the subset of predictor variables that best explains the response variable (root exudate composition) in a regression model. We applied an all-subset regression based on a branch-and-bound algorithm to ascertain the optimal model elucidating root exudate composition, as gauged by the maximum $R^2$ value. After this model selection, we rigorously assessed the influence of distinct predictors on root exudation patterns, ensuring the absence of confounding effects from other incorporated variables. Our chosen predictors encompassed both abiotic factors, such as soil moisture and temperature, and biotic properties such as root morphological attributes, namely specific root length, root tissue density, specific root area, and diameter.

## Results

### Warming effects on the quantity and composition of root exudates

In the control treatment, amino acids, organic acids, and sugars constituted 7.7%, 47.2%, and 45.1% of the primary metabolites in root exudates per fine root biomass, respectively. These proportions remained consistent in the warming treatment (Figure 1d). Similarly, based on root surface area (Figure 1e) and root length (Figure 1f), there were no discernible differences between the control and warming plots. The linear mixed effects models showed that warming had no significant effect on the root exudation rates of primary metabolite groups (i.e., total organic acids, TOA; total amino acids, TAA; total sugars, TS; and total primary metabolites, TPM) based on fine root biomass (Figure 1a, Table S1), root surface area (Figure 1b, Table S1), and root length (Figure 1c, Table S1), but season had significant effects (Table S1). The exudation rates of TPM and TS per fine root biomass were lowest in spring 2021 and peaked in summer 2021 (Figure 1a). Exudation of TAA was lowest in summer 2020 and reached the highest values in autumn 2021, while TOA exudation was lowest in summer 2021 and highest in autumn 2020. Notably, compared to totals i.e. group-wise rates, root exudation rates of single compounds, such as glycine, proline, fumaric acid, and ribose, were increased in warmed plots (Figure S1a, b, c).

Non-parametric dissimilarity analyses following PERMANOVA (Adonis) (Table 1) revealed significant differences in primary metabolite profiles of root exudates across sampling dates ($F$=56.563, $P$=0.001), but not between warmed and control treatments ($F$=1.231, $P$=0.277, Table 1). NMDS analysis corroborated these findings (Figure 2a, Stress=0.0802). NMDS 1 delineated metabolite distinctions between 2021 and 2022, while NMDS 2 highlighted the differentiation of metabolite profiles between summer, autumn, and spring seasons (Figure. 2a). Most metabolites, and most notably amino acids and organic acids, were negatively correlated with NMDS1, whereas sugars showed a positive association. Conversely, on NMDS2, amino acids exhibited a positive correlation, while both organic acids and sugars were negatively associated (Figure 2b).

### Drivers of variation in root exudate composition

The envfit analysis on of the NMDS plot revealed significant correlations between root exudate composition and soil temperature ($R^2$ = 0.583, P = 0.001), root diameter ($R^2$ = 0.204, P = 0.001), root surface area ($R^2$ = 0.412, P = 0.001), and specific root length (SRL) ($R^2$ = 0.151, P = 0.001) (Figure. 2a). Using NMDS1 scores as response variables, the best model selection pinpointed four predictors accounting for 47% variation, with root surface area being significant and SRL and root diameter being marginally significant. For NMDS2, three predictors explained 59% variation, with both soil temperature and root diameter being significant and SRL being marginally significant (Table 2). These results were consistent with linear regression analysis (Figure S2).

**Comparison of metabolite profiles in root tissues and root exudates**

We quantified 34 primary metabolites in the root exudates, comprising 12 amino acids, 11 organic acids, and 11 sugars, across five sampling dates in both warmed and control treatments. More metabolites were found in root tissues than in root exudates, with counts of 44 metabolites in root tissues and 34 in root exudates, respectively (Figure 3a). All metabolites detected in root exudates were also present in root tissues, except for maleic acid. Conversely, 11 unique compounds were identified exclusively in root tissues. Principal component analysis (PCA) distinctly segregated the metabolite profiles of root tissues and root exudates, whether considering only shared compounds (Figure 3b) or the entire metabolite profiles (Figure 3c). Amino acids and organic acids were the primary contributors to the separation along PC1, while sugars (specifically arabinose) and organic acids (such as acetic acid) drove the distinction along PC2, for both shared and all metabolite profiles. When metabolites were categorized by compound group, all groups showed differences between root tissues and root exudates (Figure S3). Significant positive correlations were identified between metabolite levels in root tissues and root exudates for all compounds (Figure 4a), and for organic acids (Figure 4c) and sugars (Figure 4d), with amino acids displaying only a marginal positive correlation (Figure 4b). However, when considering different treatments, the positive correlations for all compounds and sugars persisted, whereas organic acids and amino acids showed no significant correlation between tissue and exudate levels (Figure S4).

## Discussion

### Response of primary metabolites in root exudates to soil warming

Extensive research has documented the rates of root exudation in response to warming (Yin et al., 2013; Xiong et al., 2020; Wang et al., 2021; Leuschner et al., 2022; Heinzle et al., 2023). However, the response of primary metabolites (such as amino acids, organic acids, and sugars) in root exudates to warming conditions has remained little understood.

In contrast to our initial hypothesis, which proposed that warming would increase primary metabolites in root exudates due to decreased soil nutrient availability (i.e., P) (Tian et al., 2023b), our results indicate no upregulation of root exudation rates of primary metabolites, particularly of organic acids, between control and warmed samples. This absence of root exudate response was independent of these bases for its calculation, relating exudation to fine root biomass, root surface area, or root length (Figure 1). This indicates that plants and microbes showed differential warming responses in terms of what macronutrient constrains their function. Here plant roots were less constrained by P than microbes were (no change in fine root P content (Kwatcho Kengdo et al., 2022). This lack of constraint did not trigger a strong P limitation response in higher plants, which would have manifested as elevated organic acid exudation in warmed, P-limited roots. In contrast, though plant roots can also produce extracellular phosphatases, the bulk increase in soil phosphatases in warmed soil (Tian et al., 2023a) was likely originating from soil microbes, as a response to strong microbial P limitation which showed up in P-deficiency related declines in microbial growth in warmed soils, decreased microbial P immobilization and lower microbial biomass P. Differential nutrient constraints of plants and microbes in the same ecosystem have been proposed for high latitude systems and beyond (Čapek et al., 2018), with far-reaching biogeochemical implications for global change effects, including warming responses of vegetation and soil microbes. In fertilizer experiments in the Arctic for examples vegetation was shown to be N-limited while microbial processes seemed to be constrained by P (Čapek et al., 2018).

However, we not only found no response in root exudation of organic acids, but also none for all other classes of root primary metabolites. This clearly contrasts the expectation in our first hypothesis that faster root growth and root respiration in warmed plots (Kwatcho

Kengdo et al., 2022; Kengdo et al., 2023) will be paralleled by generally higher rates of root metabolism and higher primary metabolite contents (Liu et al., 2024, in press), and that these higher root metabolite contents will trigger higher rates of root exudation of primary metabolites. The lack of significant finding suggests a parallelism in the response of both, the exudation rates of primary metabolites (this study) and the overall root C exudation rates (measured as exudation of dissolved organic C, which includes low- and high-molecular weight organic C compounds) to warming (Heinzle et al., 2023), which were both insignificant. This lack of warming response may be explained by concomitant and inverse effects of soil warming on soil moisture dynamics, soil nutrient availability, and root morphology.

Soil moisture plays a pivotal role in modulating primary metabolite profiles and root exudates rates. For instance, plant net C allocation belowground and into root exudates tended to increase under drought (Brunn et al., 2022), which would likely be accompanied by increased root exudation of primary metabolites. In another study plant root exudates were dominated by secondary metabolites under drought, and shifted to primary metabolites during drought recovery (Gargallo-Garriga et al., 2018). Soil warming is generally expected to reduce soil moisture levels, possibly leading to drier conditions, while our findings showed no significant change between control and warming treatments (Heinzle et al., 2023). This stability in soil moisture might partially explain why the root exudation rates of primary metabolites were unaffected by warming. It is noteworthy, however, that while the overall exudation rates of primary metabolites remained unchanged, specific compounds such as proline and glycine showed increased exudation rates (Figure S1). These findings suggest that plants may employ nuanced strategies to adapt their exudate profiles in response to climatic warming.

Soil nutrient availability is another key factor influencing the rates and the profiles of root exudates. Numerous studies have shown that plants can promote the accessibility of soil mineral nutrients, specifically by secreting organic acids to solubilize P (Lambers. et al., 2006; Canarini et al., 2019), by releasing biological nitrification inhibitors to optimize the utilization of N (Subbarao et al., 2007), or by generally upregulating the exudation of primary metabolites to trigger a rhizosphere priming effects to mobilize soil N (Dijkstra et al., 2013).

Our recent research at the same site revealed that prolonged soil warming led to a reduction in soil N and P content (Tian et al., 2023a; Tian et al., 2023b). This was expected to result in an increase in primary metabolites in root exudates. However, our findings suggest that root exudates might not be as responsive to variations in soil nutrient availability as previously believed. The consistent levels of primary metabolites in root exudates, despite the potential nutrient depletion, imply that factors other than nutrient availability may play a significant role in controlling the root exudation process. Alternatively, plants might adjust their physiological traits to adapt to the changing soil nutrient dynamics. In the Achenkirch experiment plant root systems adjusted N and P uptake to a level that root N and P contents were not altered or did not decrease. This indicates that plants largely circumvented any P limitation, and were highly competitive in the acquisition of this resource while microbes showed strong signs of P limitation. This plant adjustment hypothesis is supported by our earlier study indicating that soil warming lead to an increase in root biomass, root production, and turnover (Kwatcho Kengdo et al., 2022; Kengdo et al., 2023), indicating that one major warming response of higher plants was to increase belowground C allocation to relieve belowground resource constraints. These changes could secondarily increase root surface area and the total flux of primary metabolites from root exudates to soil on ground surface area basis (though not per root biomass), thereby further helping to mitigate the limitations imposed by soil nutrient scarcity.

Root morphology, including specific root length, root diameter, and root tissue density, is known to significantly impact the quantity and chemical composition of root exudates (Williams et al., 2022; Rathore et al., 2023). It has been suggested that variations in root diameter, root tissue density, and root N content substantially explained the differences in exudate metabolome profiles, with a notable negative correlation between root exudation rate and root tissue density (Williams et al., 2022). In our study, however, specific root length, specific fine root area, and root tissue density of the sampled roots did not exhibit significant differences between treatments (Heinzle et al., 2023). This may partially explain why the exudation rates of primary metabolites showed no difference between the control and warming treatments.

**Seasonal variation patterns of primary metabolites in root exudates**

Seasonal dynamics of root C exudation rates have been documented in previous studies (Xiong et al., 2020; Heinzle et al., 2023; Gao et al., 2024). Surprisingly, much less research has been directed towards understanding the seasonal dynamics of root exudate composition, particularly of primary metabolites (Xiong et al., 2023). It has been shown that root exudation rates show strong seasonal plasticity, typically exhibiting higher rates in spring and autumn (Jakoby et al., 2020; Heinzle et al., 2023; Zhao et al., 2023; Gao et al., 2024). However, our results do not support this result, as we showed that the exudation rates of primary metabolites were relatively low in spring and tended to increase in summer and autumn (Figure 1). These findings highlight that root C exudation and primary metabolite exudation are not congruent and that the seasonal patterns of primary metabolites and of total C in root exudates can be asynchronous. This is attributed to the lower contribution of primary metabolites to root exudate C in spring (approximately 12% in both treatments, data not shown) compared to summer and autumn (around 40% in both treatments, data not shown), as observed in our study. This suggests that during certain seasons there is a greater allocation of C in root exudates to other compounds than the primary metabolites analyzed here, such as lipids and secondary metabolites. For example, in a subtropical aged Chinese fir plantation a higher proportion of lipids and salicylic acid metabolites were present in winter as part of prominent defense strategies, whereas in summer, more carbohydrates were exuded by roots priming the biogeochemical activity of the soil microbes (Chen et al., 2023).

Asynchrony of exudation rates of primary metabolites and of total C in root exudates further suggests that the profiles of primary metabolites in root exudates also changes with season (interannually) and year (interannually). This speculation was confirmed by non-parametric dissimilarity analyses and NMDS (Figure 2 and Table 1). Both, the linear regression and the prediction models showed that the compositional changes of root exudates with season were well predicted by soil temperature (Figure 2), and those between years by changes in root diameter and specific root length ($R^2$=0.59, $p<0.001$, Table 2). This aligns with the findings of Proctor and He (2017) and Rathore et al. (2023) who demonstrated that root traits (such as specific root length and root diameter) are strong predictors of changes in the root exudate metabolites profiles. Root diameter and specific root length reflect the

belowground resource requirements of plants, implying that the plant's growth strategy across seasons and years might be an important factor influencing the composition of root exudates. Root diameter (and inversely specific root length) is also strongly affected by mycorrhizal colonization. In ectomycorrhizal trees fungal colonization causes shorter and thicker fine root tips with lower specific root length (Sun et al., 2010), and the ectomycorrhizal fungal sheath development alters root exudate patterns (see also, Lv et al., 2023). On the other hand, soil temperature was a strong interannual predictor of root exudate composition (Figure 2 and Table 2). This relationship may be due to the close relationship between plant photosynthesis and the release of root exudates. For example, the quantity of exudates produced is strongly influenced by solar radiation received the day before sample collection (Tixier et al., 2023). Moreover, photoperiod and air temperature are strongly linked during the plant growth season, further strengthening the above relationship, and plant phenology and with this likely exudate composition changes dramatically with season, from spring through summer to autumn.

**Selectivity and drivers of the root exudation process**

Root exudates are released from the root tips, either actively or passively (Canarini et al., 2019), but the relationship between the composition of primary metabolites in root tissues and in root exudates is poorly known (Canarini et al., 2016; Weinhold et al., 2021). Most primary metabolites are thought to be released from the root cytoplasm into the soil environment through specific transporter proteins, by facilitated passive diffusion. This process does not require energy investment and is driven by the concentration difference between the intracellular and the extracellular compartments and this is directed outwards (Canarini et al., 2019). The nature of the root exudation process therefore is passive (driven by the outward concentration gradient), but likely selective. This selectivity would be triggered by the expression and activity of the respective transporter systems allowing only the efflux of specific metabolites catalyzed by the complement of specific efflux carrier proteins (Canarini et al., 2019; Sharma et al., 2023). Our results show that root tissue and root exudate metabolites showed a high overlap in the number and type of compounds that we were able to quantify (Figure 3a), yet their relative compositions were markedly different.

This is evident in both the shared and the overall compounds found in root exudates and root tissues (Figure 3b, c), supporting our third hypothesis. This result is in line with a previous study on rice plants (*Oryza sativa* cv. Haenuki) which showed that ~70% of metabolites in the root tissue were detected in the root exudates of N- or P-treated plants (Tawaraya et al., 2018) and in the tree species *Cinnamomum camphora* (L.) J. Presl. (camphor, Lauraceae) in a biodiversity experiment in the subtropical region of China (Weinhold et al., 2021). This notable difference in the relative composition can be (i) attributed to the metabolic processes within the root tissue which are primarily geared towards growth and survival, driving nutrient absorption, water uptake, and storage (Long and Adams, 2023). Conversely, (ii) root exudates are specialized for external interactions with the soil environment, including communication with microorganisms, nutrient acquisition, and defense against pathogens (Badri and Vivanco, 2009; Canarini et al., 2019). For example, soluble sugars (e.g., glucose and sucrose) are used as a fuel for respiratory metabolism and for C skeletons to build other organic molecules (Long and Adams, 2023), while they function as important C sources for microbial growth in root exudates to prime microbial activity (Haichar et al., 2014). Similarly, citric acid in exudates plays an important role in enhancing the recruitment of beneficial bacteria (Jiao et al., 2022) and increasing the availability of soil P (Carvalhais et al., 2010), whereas an increase in citric acid within plant tissues has been correlated with enhanced plant growth, as observed in *Medicago sativa* L under heavy metals and petroleum hydrocarbons contaminated soil (Agnello et al., 2016). This is further supported by principal component analysis (PCA), where the most significant compounds determining PC axis 1 and thereby the separation of the metabolite composition of root exudates and root tissues include organic acids (acetic acid, citric acid, oxaloacetic acid) and amino acids (phenylalanine, tyrosine) (Figure 3b, c).

In our study, we further explored whether high concentrations of specific primary metabolites trigger high rates of the passive exudation process of the same compounds. The correlations between primary metabolite contents in root tissues and root exudates were strong and positive across sugars and organic acids, but not for amino acids (Figure 4). These positive correlations indicate that high intracellular concentrations (here in bulk fine root tissue) drive high exudation rates of these compounds and align with those found in the study

by Canarini et al. (2016) though we observed weaker correlations. This difference could be attributed to their specific sampling and extraction of root tips, which represent the primary sites for the release of root exudates (Canarini et al., 2019). Furthermore, the weaker correlation observed between concentrations of amino acids in root tissues and root exudates, compared to that of organic acids and sugars (Figure 4), may be attributed to the fact that many amino acids can be actively reabsorbed by plant roots from the root exudates or from the soil solution (Phillips et al., 2006). For instance, Phillips et al. (2006) reported that the amino acid uptake capacity of roots in *Lolium multiflorum* Lam., *Medicago truncatula* L., and *Zea mays* L. exceeded their efflux rate by 94-374%.

The "push" and "pull" hypotheses have been fundamental in clarifying the relationship of concentrations between root tissues and root exudates (Farrar and Jones, 2000; Farrar et al., 2003; Dilkes et al., 2004; Karst et al., 2017; Jakoby et al., 2020; Leuschner et al., 2022). The "push" hypothesis suggests a direct transfer mechanism of increased photosynthate C allocated to roots leading to higher root exudation (Dilkes et al., 2004; Karst et al., 2017). However, this hypothesis is in contrast with our previous studies at the same site, which highlighted that long term soil warming increased C allocation to root growth (i.e., fine root production and turnover doubled) (Kwatcho Kengdo et al., 2022; Kengdo et al., 2023) but did not affect root C exudation rates (Heinzle et al., 2023). This may be explained by the fact that root exudates can be rapidly adjusted to respond to transient environmental stresses, whereas modifications of root morphological and architectural traits typically occur over a longer period. In contrast, the "pull" hypothesis argues that root exudation is influenced by external biotic or abiotic factors, such as by ectomycorrhizal fungal colonization (Meier et al., 2013), which attracts and “pulls” photosynthate C via exudates into the rhizosphere. Based on the "pull" hypothesis and previous results demonstrating that long term soil warming triggered an emerging soil P limitation at this site (Tian et al., 2023b), we expected that root exudation of organic acids will be increased to mobilize P bound abiotically but our results did not support this hypothesis. Overall, the relationship of primary metabolite concentration in root tissues and root exudates was more complex than what the "push" and "pull" hypotheses can explain. Notably, another study indicated that the changes in concentration of metabolites in root tissue and root exudates are not related under N-deficient or P-deficient conditions (Tawaraya

et al., 2018). This lack of correlation might be attributed to active re-uptake systems operating at the cellular or tissue level, which could alter metabolite distribution in response to nutrient stress. On the other hand, this might also be amplified by the weak relation between bulk fine root tissue metabolite contents and their contents at the sites of exudate release, the root tips and the fine root rhizodermis.

## Conclusion

Understanding the role of primary metabolites in root exudates within the context of global change is crucial for accurately interpreting their impact on forest ecosystems. Here we show that root exudation of primary metabolites in terms of the quantity and relative composition did not respond to long term soil warming, while changes in soil microclimate, root morphology and plant phenology with season and year showed considerable effects. We also found a strong positive correlation between individual metabolites in root tissues and root exudates, despite their differing profiles (Figure 5), indicating that tree root exudation was selective but mediated by facilitated passive diffusion. Our results challenge the initial hypothesis that soil warming increases root exudation of primary metabolites, suggesting that root exudate responses to environmental change are highly nuanced and may involve complex physiological and morphological adjustments. Further investigations into root exudate composition, including primary and secondary metabolites, and their environmental responses will assist in more clearly understanding their functional roles. This includes their connection to the rhizosphere microbial communities, their relevance in plants with specific growth strategies, and their significance in plant adaptation and survival under climate warming.

## Conflict of interest

The authors have no conflicts of interest to declare.

## Funding

This study was funded by the Austrian Science Fund (FWF; project I 3745) and China Scholarship Council (CSC) Grant (202008350128).

**Acknowledgements**

We sincerely thank Christian Holtermann for his invaluable contributions to maintaining the soil warming system in the field site, Ludwig Seidl for technical support on metabolite analysis.

**Author contributions**

WW, AS, and WB designed the study. XF, JH, YT, SKK, WW, AS, and WB implemented the field experiment. XF, ES, and WW conducted the lab experiment. XF performed data analysis and wrote the manuscript, with the contributions of all co-authors.

## References


Agnello, A.C., Huguenot, D., van Hullebusch, E.D., Esposito, G., 2016. Citric acid- and Tween® 80-assisted phytoremediation of a co-contaminated soil: alfalfa (Medicago sativa L.) performance and remediation potential. Environmental Science and Pollution Research 23, 9215-9226.

Badri, D.V., Vivanco, J.M., 2009. Regulation and function of root exudates. Plant Cell Environment 32, 666-681.

Bai, E., Li, S., Xu, W., Li, W., Dai, W., Jiang, P., 2013. A meta-analysis of experimental warming effects on terrestrial nitrogen pools and dynamics. New phytologist 199, 441-451.

Berini, J.L., Brockman, S.A., Hegeman, A.D., Reich, P.B., Muthukrishnan, R., Montgomery, R.A., Forester, J.D., 2018. Combinations of Abiotic Factors Differentially Alter Production of Plant Secondary Metabolites in Five Woody Plant Species in the Boreal-Temperate Transition Zone. Frontiers in Plant Science 9, 1257.

Brunn, M., Hafner, B.D., Zwetsloot, M.J., Weikl, F., Pritsch, K., Hikino, K., Ruehr, N.K., Sayer, E.J., Bauerle, T.L., 2022. Carbon allocation to root exudates is maintained in mature temperate tree species under drought. New phytologist 235, 965-977.

Canarini, A., Kaiser, C., Merchant, A., Richter, A., Wanek, W., 2019. Root Exudation of Primary Metabolites: Mechanisms and Their Roles in Plant Responses to Environmental Stimuli. Frontires in Plant Science 10, 157.

Canarini, A., Merchant, A., Dijkstra, F.A., 2016. Drought effects on Helianthus annuus and Glycine max metabolites: from phloem to root exudates. Rhizosphere 2, 85-97.

Čapek, P., Manzoni, S., Kaštovská, E., Wild, B., Diáková, K., Bárta, J., Schnecker, J., Biasi, C., Martikainen, P.J., Alves, R.J.E., Guggenberger, G., Gentsch, N., Hugelius, G., Palmtag, J., Mikutta, R., Shibistova, O., Urich, T., Schleper, C., Richter, A., Šantrůčková, H., 2018. A plant–microbe interaction framework explaining nutrient effects on primary production. Nature Ecology & Evolution 2, 1588-1596.

Carrera, F.P., Noceda, C., Maridueña-Zavala, M.G., Cevallos-Cevallos, J.M., 2021. Metabolomics, a Powerful Tool for Understanding Plant Abiotic Stress. Agronomy-Basel 11, 824.

Carvalhais, L.C., Dennis, P.G., Fedoseyenko, D., Hajirezaei, M.R., Borriss, R., von Wirén, N., 2010. Root exudation of sugars, amino acids, and organic acids by maize as affected by nitrogen, phosphorus, potassium, and iron deficiency. Journal of Plant Nutrition and Soil Science 174, 3-11.

Chen, M., Yao, X.D., Cheng, H.Z., Fan, A.L., Lin, R.R., Wang, X.H., Yang, Y.S., Chen, G.S., 2023. Changes in Chinese fir plantations root exudation strategies seasonally and as tree age. Forest Ecology and Management 545, 121239.

Dijkstra, F.A., Carrillo, Y., Pendall, E., Morgan, J.A., 2013. Rhizosphere priming: a nutrient perspective. Frontiers in microbiology 4.

Dilkes, N.B., Jones, D.L., Farrar, J., 2004. Temporal dynamics of carbon partitioning and rhizodeposition in wheat. Plant Physiology 134, 706-715.

Escandon, M., Meijon, M., Valledor, L., Pascual, J., Pinto, G., Canal, M.J., 2018. Metabolome Integrated Analysis of High-Temperature Response in Pinus radiata. Frontiers in Plant Science 9, 485.

Escolà Casas, M., Matamoros, V., 2021. Analytical challenges and solutions for performing metabolomic analysis of root exudates. Trends in Environmental Analytical Chemistry 31, e00130.

Farrar, J., Hawes, M., Jones, D., Lindow, S., 2003. How roots control the flux of carbon to the rhizosphere. Ecology 84, 827-837.

Farrar, J.F., Jones, D.L., 2000. The control of carbon acquisition by roots. New phytologist 147, 43-53.

Gao, Y., Wang, H., Yang, F., Dai, X., Meng, S., Hu, M., Kou, L., Fu, X., 2024. Relationships between root exudation and root morphological and architectural traits vary with growing season. Tree physiology 44.

Gargallo-Garriga, A., Preece, C., Sardans, J., Oravec, M., Urban, O., Penuelas, J., 2018. Root exudate metabolomes change under drought and show limited capacity for recovery. Scientific reports 8, 12696.

Gargallo-Garriga, A., Sardans, J., Perez-Trujillo, M., Oravec, M., Urban, O., Jentsch, A., Kreyling, J., Beierkuhnlein, C., Parella, T., Penuelas, J., 2015. Warming differentially influences the effects of drought on stoichiometry and metabolomics in shoots and roots. New phytologist 207, 591-603.

Haichar, F.E., Santaella, C., Heulin, T., Achouak, W., 2014. Root exudates mediated interactions belowground. Soil Biology and Biochemistry 77, 69-80.

Heinzle, J., Liu, X.F., Tian, Y., Kengdo, S.K., Heinze, B., Nirschi, A., Borken, W., Inselsbacher, E., Wanek, W., Schindlbacher, A., 2023. Increase in fine root biomass enhances root exudation by long-term soil warming in a temperate forest. Frontiers in Forests and Global Change 6.

Hong, Y., Zhou, Q., Hao, Y., Huang, A.C., 2022. Crafting the plant root metabolome for improved microbe-assisted stress resilience. New phytologist 234, 1945-1950.

Jakoby, G., Rog, I., Megidish, S., Klein, T., 2020. Enhanced root exudation of mature broadleaf and conifer trees in a Mediterranean forest during the dry season. Tree physiology 40, 1595-1605.

Jiang, Q., Jia, L.Q., Wang, X.H., Chen, W.Y., Xiong, D.C., Chen, S.D., Liu, X.F., Yang, Z.J., Yao, X.D., Chen, T.T., Fan, A.L., Chen, G.S., Yang, Y.S., 2022a. Soil warming alters fine root lifespan, phenology, and architecture in a Cunninghamia lanceolata plantation. Agricultural and Forest Meteorology 327, 109201.

Jiang, Z., Thakur, M.P., Liu, R.Q., Zhou, G.Y., Zhou, L.Y., Fu, Y.L., Zhang, P.P., He, Y.H., Shao, J.J., Gao, J., Li, N., Wang, X.X., Jia, S.X., Chen, Y., Zhang, C.X., Zhou, X.H., 2022b. Soil P availability and mycorrhizal type determine root exudation in sub-tropical forests. Soil Biology and Biochemistry 171, 108722.

Jiao, H., Xu, W., Hu, Y., Tian, R., Wang, Z., 2022. Citric Acid in Rice Root Exudates Enhanced the Colonization and Plant Growth-Promoting Ability of Bacillus altitudinis LZP02. Microbiology Spectrum 10, e0100222.

Karst, J., Gaster, J., Wiley, E., Landhausser, S.M., 2017. Stress differentially causes roots of tree seedlings to exude carbon. Tree physiology 37, 154-164.

Kengdo, S.K., Ahrens, B., Tian, Y., Heinzle, J., Wanek, W., Schindlbacher, A., Borken, W., 2023. Increase in carbon input by enhanced fine root turnover in a long-term warmed forest soil. Science of the total environment 855, 158800.

Kwatcho Kengdo, S., Persoh, D., Schindlbacher, A., Heinzle, J., Tian, Y., Wanek, W., Borken, W., 2022. Long-term soil warming alters fine root dynamics and morphology, and their ectomycorrhizal fungal community in a temperate forest soil. Global Change Biology 28, 3441-3458.

Lambers., H., Shane, M.W., Cramer, M.D., Pearse, S.J., Veneklaas, E.J., 2006. Root Structure and Functioning for Efficient Acquisition of Phosphorus: Matching Morphological and Physiological Traits. Annals of botany 98, 693-713.

Leuschner, C., Tückmantel, T., Meier, I.C., 2022. Temperature effects on root exudation in mature beech (Fagus sylvatica L.) forests along an elevational gradient. Plant and Soil 481, 147-163.

Long, R.W., Adams, H.D., 2023. The osmotic balancing act: When sugars matter for more than metabolism in woody plants. Global Change Biology 29, 1684-1687.

Lopez-Bucio, J., Nieto-Jacobo, M.F., Ramirez-Rodriguez, V.V., Herrera-Estrella, L., 2000. Organic acid metabolism in plants: from adaptive physiology to transgenic varieties for cultivation in extreme soils. Plant Science 160, 1-13.

Lv, C., Wang, C., Li, Y., Zhou, Z., 2023. Coordination among root exudation C, mycorrhizal colonization, and functional traits and their responses to drought in five temperate tree species. Forest Ecology and Management 546, 121316.

Meier, I.C., Avis, P.G., Phillips, R.P., 2013. Fungal communities influence root exudation rates in pine seedlings. FEMS Microbiology Ecology 83, 585-595.

Meier, I.C., Tuckmantel, T., Heitkotter, J., Muller, K., Preusser, S., Wrobel, T.J., Kandeler, E., Marschner, B., Leuschner, C., 2020. Root exudation of mature beech forests across a nutrient availability gradient: the role of root morphology and fungal activity. New phytologist 226, 583-594.

Nagele, T., Gibon, Y., Le Hir, R., 2022. Plant sugar metabolism, transport and signalling in challenging environments. Physiologia plantarum 174, e13768.

Panchal, P., Preece, C., Penuelas, J., Giri, J., 2022. Soil carbon sequestration by root exudates. Trends Plant Science 27, 749-757.

Pausch, J., Kuzyakov, Y., 2018. Carbon input by roots into the soil: Quantification of rhizodeposition from root to ecosystem scale. Global Change Biology 24, 1-12.

Phillips, D.A., Fox, T.C., Six, J., 2006. Root exudation (net efflux of amino acids) may increase rhizodeposition under elevated $CO_2$. Global Change Biology 12, 561-567.

Phillips, R.P., Erlitz, Y., Bier, R., Bernhardt, E.S., 2008. New approach for capturing soluble root exudates in forest soils. Functional Ecology 22, 990-999.

Preece, C., Farre-Armengol, G., Llusia, J., Penuelas, J., 2018. Thirsty tree roots exude more carbon. Tree physiology 38, 690-695.

Proctor, C., He, Y.H., 2017. Quantifying root extracts and exudates of sedge and shrub in relation to root morphology. Soil Biol Biochem 114, 168-180.

Rathore, N., Hanzelkova, V., Dostalek, T., Semerad, J., Schnablova, R., Cajthaml, T., Munzbergova, Z., 2023. Species phylogeny, ecology, and root traits as predictors of root exudate composition. New phytologist 239, 1212-1224.

Reich, P.B., Sendall, K.M., Stefanski, A., Rich, R.L., Hobbie, S.E., Montgomery, R.A., 2018. Effects of climate warming on photosynthesis in boreal tree species depend on soil moisture. Nature 562, 263-267.

Ryan, P., Delhaize, E., Jones, D., 2001. Function and Mechanism of Organic Anion Exudation from Plant Roots. Annual Review of Plant Physiology and Plant Molecular Biology 52, 527-560.

Salas, E., Gorfer, M., Bandian, D., Wang, B., Kaiser, C., Wanek, W., 2023. A rapid and sensitive assay to quantify amino sugars, neutral sugars and uronic acid necromass biomarkers using pre-column derivatization, ultra-high-performance liquid chromatography and high-resolution mass spectrometry. Soil Biology and Biochemistry 177, 108927.

Sandnes, A., Eldhuset, T.D., Wollebæk, G., 2005. Organic acids in root exudates and soil solution of Norway spruce and silver birch. Soil Biology and Biochemistry 37, 259-269.

Sardans, J., Gargallo-Garriga, A., Urban, O., Klem, K., Walker, T.W.N., Holub, P., Janssens, I.A., Penuelas, J., 2020. Ecometabolomics for a Better Understanding of Plant Responses and Acclimation to Abiotic Factors Linked to Global Change. Metabolites 10, 239.

Sharma, I., Kashyap, S., Agarwala, N., 2023. Biotic stress-induced changes in root exudation confer plant stress tolerance by altering rhizospheric microbial community. Frontiers in Plant Science 14.

Subbarao, G.V., Rondon, M., Ito, O., Ishikawa, T., Rao, I.M., Nakahara, K., Lascano, C., Berry, W.L., 2007. Biological nitrification inhibition (BNI)-is it a widespread phenomenon? Plant and Soil 294, 5-18.

Sun, Y., Gu, J.-C., Zhuang, H.-F., Wang, Z.-Q., 2010. Effects of ectomycorrhizal colonization and nitrogen fertilization on morphology of root tips in a Larix gmelinii plantation in northeastern China. Ecological Research 25, 295-302.

Tawaraya, K., Horie, R., Wagatsuma, T., Saito, K., Oikawa, A., 2018. Metabolite profiling of shoot extract, root extract, and root exudate of rice under nitrogen and phosphorus deficiency. Soil Science and Plant Nutrition 64, 312-322.

Tian, Y., Schindlbacher, A., Malo, C.U., Shi, C.P., Heinzle, J., Kengdo, S.K., Inselsbacher, E., Borken, W., Wanek, W., 2023a. Long-term warming of a forest soil reduces microbial biomass and its carbon and nitrogen use efficiencies. Soil Biology and Biochemistry 184, 109109.

Tian, Y., Shi, C., Malo, C.U., Kwatcho Kengdo, S., Heinzle, J., Inselsbacher, E., Ottner, F., Borken, W., Michel, K., Schindlbacher, A., Wanek, W., 2023b. Long-term soil warming decreases microbial phosphorus utilization by increasing abiotic phosphorus sorption and phosphorus losses. Nature Communications 14, 864.

Tixier, A., Forest, M., Prudent, M., Durey, V., Zwieniecki, M., Barnard, R.L., 2023. Root exudation of carbon and nitrogen compounds varies over the day-night cycle in pea: The role of diurnal changes in internal pools. Plant Cell Environment 46, 962-974.

Tiziani, R., Miras-Moreno, B., Malacrinò, A., Vescio, R., Lucini, L., Mimmo, T., Cesco, S., Sorgonà, A., 2022. Drought, heat, and their combination impact the root exudation patterns and rhizosphere microbiome in maize roots. Environmental and Experimental Botany 203, 105071.

Wang, Q.T., Chen, L.Y., Xu, H., Ren, K.X., Xu, Z.G., Tang, Y., Xiao, J., 2021. The effects of warming on root exudation and associated soil N transformation depend on soil nutrient availability. Rhizosphere 17, 100263.

Wang, W., Chen, F., Wang, Y., Wang, L., Fu, H., Zheng, F., Beecher, L., 2018. Optimization of reactions between reducing sugars and 1-phenyl-3-methyl-5-pyrazolone (PMP) by response surface methodology. Food Chemistry 254, 158-164.

Weinhold, A., Döll, S., Liu, M., Schedl, A., Pöschl, Y., Xu, X., Neumann, S., van Dam, N.M., 2021. Tree species richness differentially affects the chemical composition of leaves, roots and root exudates in four subtropical tree species. Journal of Ecology 110, 97-116.

Williams, A., de Vries, F.T., 2020. Plant root exudation under drought: implications for ecosystem functioning. New phytologist 225, 1899-1905.

Williams, A., Langridge, H., Straathof, A.L., Muhamadali, H., Hollywood, K.A., Goodacre, R., de Vries, F.T., 2022. Root functional traits explain root exudation rate and composition across a range of grassland species. Journal of Ecology 110, 21-33.

Wilson, R.M., Tfaily, M.M., Kolton, M., Johnston, E.R., Petro, C., Zalman, C.A., Hanson, P.J., Heyman, H.M., Kyle, J.E., Hoyt, D.W., Eder, E.K., Purvine, S.O., Kolka, R.K., Sebestyen, S.D., Griffiths, N.A., Schadt, C.W., Keller, J.K., Bridgham, S.D., Chanton, J.P., Kostka, J.E., 2021. Soil metabolome response to whole-ecosystem warming at the Spruce and Peatland Responses under Changing Environments experiment. Proceedings of the National Academy of Sciences 118, e2004192118.

Xiong, D.C., Huang, J.X., Lin, T.C., Liu, X.F., Xu, C., Chen, S.D., Yang, Z.J., Chen, G.S., Yang, Y.S., 2023. Warming Increased Metabolite Composition and Pathways in Root Exudates of Chinese Fir Saplings in Subtropical China. Journal of Soil Science and Plant Nutrition 23, 2545-2565.

Xiong, D.C., Huang, J.X., Yang, Z.J., Cai, Y.Y., Lin, T.C., Liu, X.F., Xu, C., Chen, S.D., Chen, G.S., Xie, J.S., Li, Y.Q., Yang, Y.S., 2020. The effects of warming and nitrogen addition on fine root exudation rates in a young Chinese-fir stand. Forest Ecology and Management 458, 117793.

Yin, H., Li, Y., Xiao, J., Xu, Z., Cheng, X., Liu, Q., 2013. Enhanced root exudation stimulates soil nitrogen transformations in a subalpine coniferous forest under experimental warming. Global Change Biology 19, 2158-2167.

Zhalnina, K., Louie, K.B., Hao, Z., Mansoori, N., da Rocha, U.N., Shi, S., Cho, H., Karaoz, U., Loque, D., Bowen, B.P., Firestone, M.K., Northen, T.R., Brodie, E.L., 2018. Dynamic root exudate chemistry and microbial substrate preferences drive patterns in rhizosphere microbial community assembly. Nature Microbiology 3, 470-480.

Zhao, J.H., Ye, Y.Q., Sun, X.D., Shi, L.Y., Chen, X.L., Guan, Q.W., 2023. Root exudation patterns of Chinese fir after thinning relating to root characteristics and soil conditions. Forest Ecology and Management 541, 121068.

Zhou, P., Zhao, F., Chen, M.J., Ye, N.X., Lin, Q., Ouyang, L.Q., Cai, X.M., Meng, P., Gong, X.D., Wang, Y., 2019. Determination of 21 free amino acids in 5 types of tea by ultra-high performance liquid chromatography coupled with tandem mass spectrometry (UHPLC-MS/MS) using a modified 6-aminoquinolyl-hydroxysuccinimidyl carbamate (AQC) method. Journal of Food Composition and Analysis 81, 46-54.

**Table 1** Significance tests of the influences of warming and sampling date on root exudate profiles

| | PERMANOVA tests | | | |
|---|---|---|---|---|
| Source | *df* | $R^2$ | *Pseudo F* | *P* |
| Warming | 1 | 0.003 | 1.231 | 0.277 |
| Sampling date | 4 | 0.659 | 56.563 | **0.001** |
| Warming×Sampling date | 4 | 0.017 | 1.469 | 0.110 |
| Residual | 110 | 0.321 | | |
| Total | 119 | 1.000 | | |

All statistical analyses were tested against α=0.05, and statistically significant results are highlighted in bold. PERMANOVA tests were performed (Adonis) on the basis of Bray–Curtis distances.

**Table 2** Best predictors for explaining variation of root exudate composition

| Predictors | NMDS1. Scores | NMDS2. Scores |
|---|---|---|
| Adjusted $R^2$ | 0.25 | 0.59 |
| *p* | 4.533e-07 | < 2.2e-16 |
| Soil moisture | | |
| Soil temperature | √ | √** |
| Root diameter | √*** | √* |
| SRL | √* | √° |
| SRA | √* | |
| RTD | √* | |

Tick marks indicate predictors selected in the best model. The effect of selected predictors on exudate composition was tested in R program using linear models (function *lm*). Significance levels: °0.1; *0.05; **0.01. RTD, root tissue density; SRL, specific root length; SRA, specific root area.

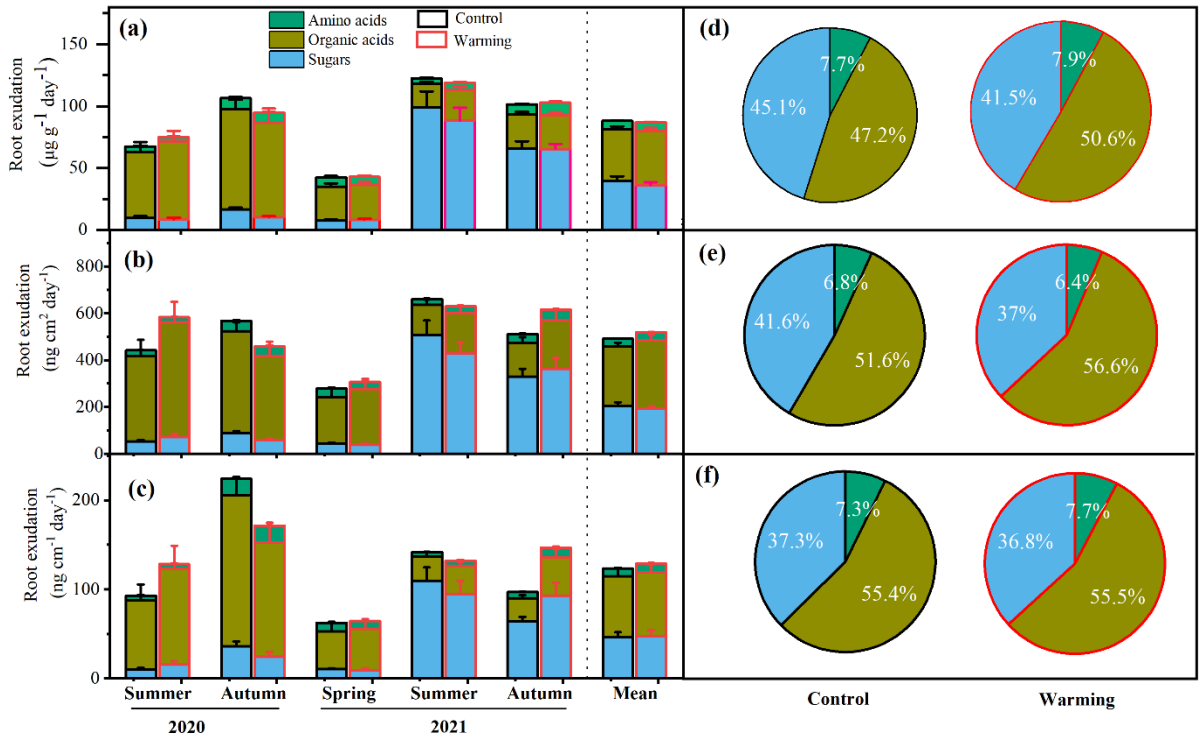


**Figure 1** Effect of warming and season on composition fine root exudation rates base on the specific fine root biomass (a), root surface area (b), and root length (c), and the proportion (d, e, f) of root exudates by major groups of primary metabolites. Values in brackets are the relative percentage of each group. Error bars represent standard errors of the means (n=6).

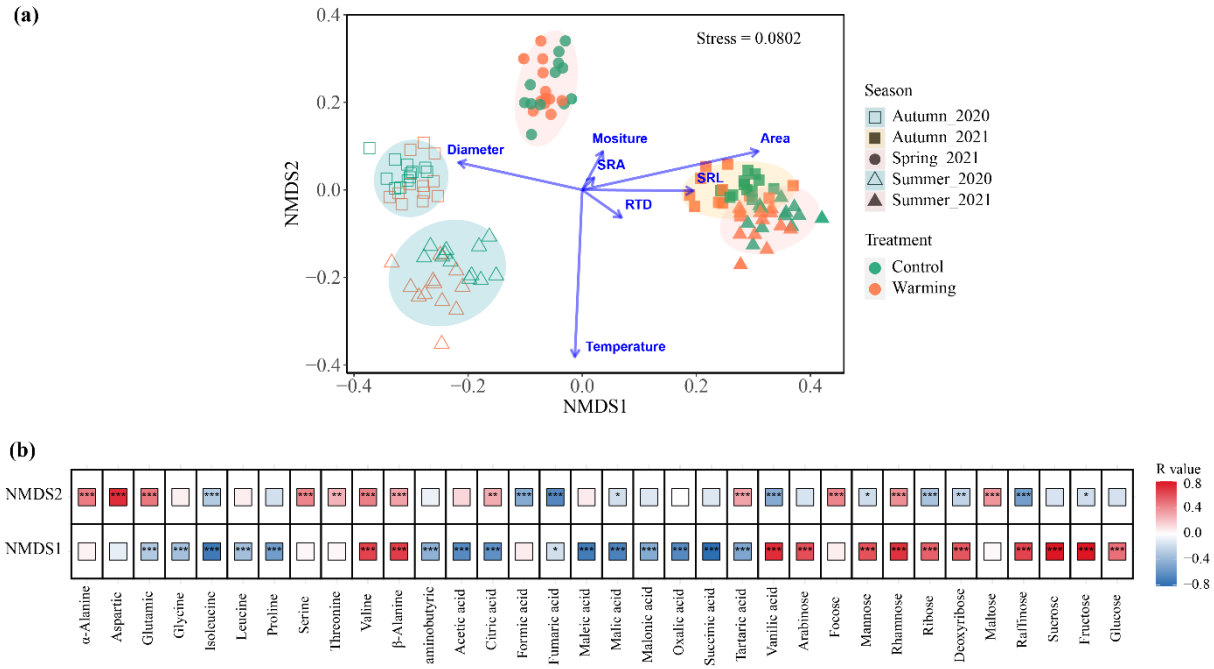


**Figure 2** Non-metric multidimensional scaling (NMDS) (a) plots detailing the influence of warming and season on primary metabolites profiles of root exudates and spearman's rank correlation matrix of the root exudates metabolites compounds and NMDS scores (b). The direction and length of the vectors of environment factors or root morphology trait are computed by Bray-Curtis distances the "envfit()" function in the vegan package. The scale from -1 (blue) to 1 (red) with a median of 0 (white). Significance levels are indicated relative to NA: ***P < 0.001; **P < 0.01; *P < 0.05. RSA: Root surface area; SRL: Specific root length; SRA: specific root area; RTD: Root tissue density.

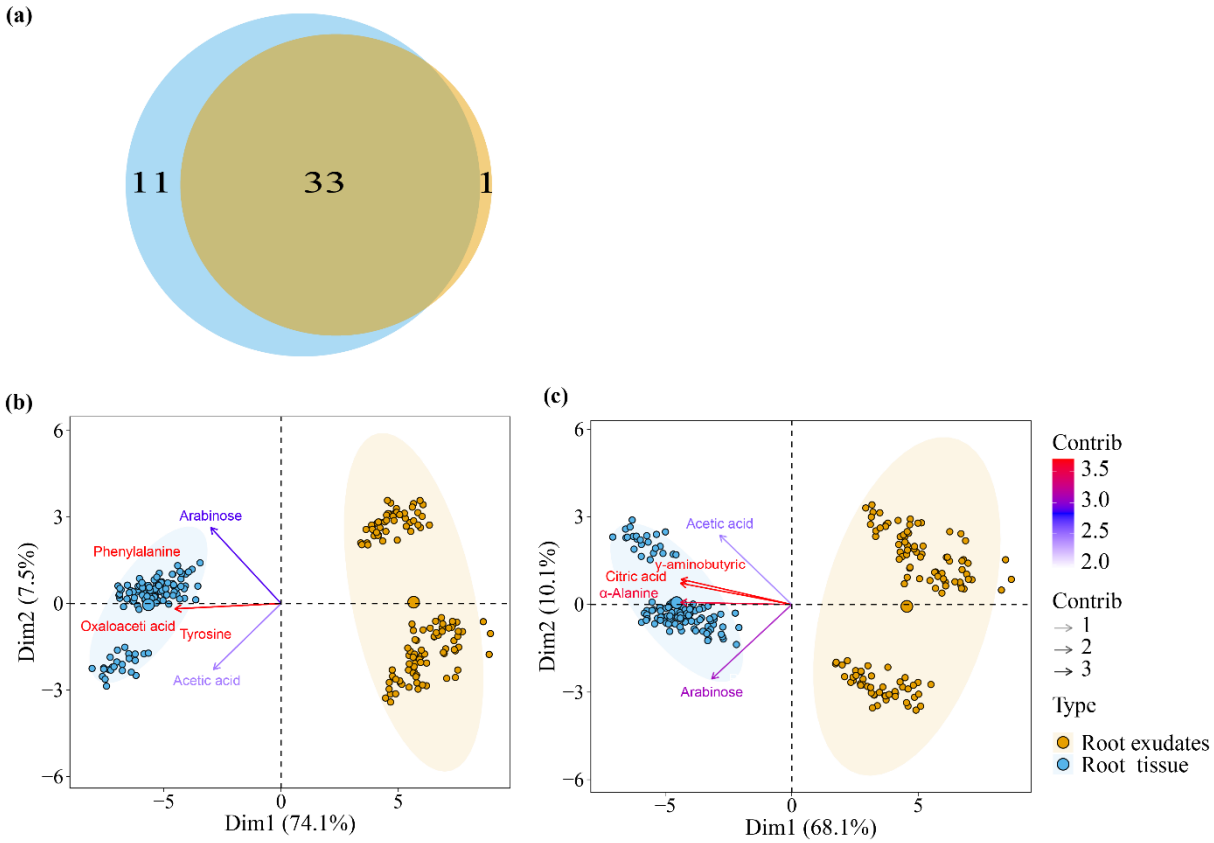


**Figure 3** Venn diagram for primary metabolites showing shared and unique metabolites numbers identified in both root tissue and root exudates (a) and biplot of the first two significant components of the PCA for the investigated metabolites for the root tissue (blue) and root exudates (yellow) by the common compounds (b) and all compounds (c).

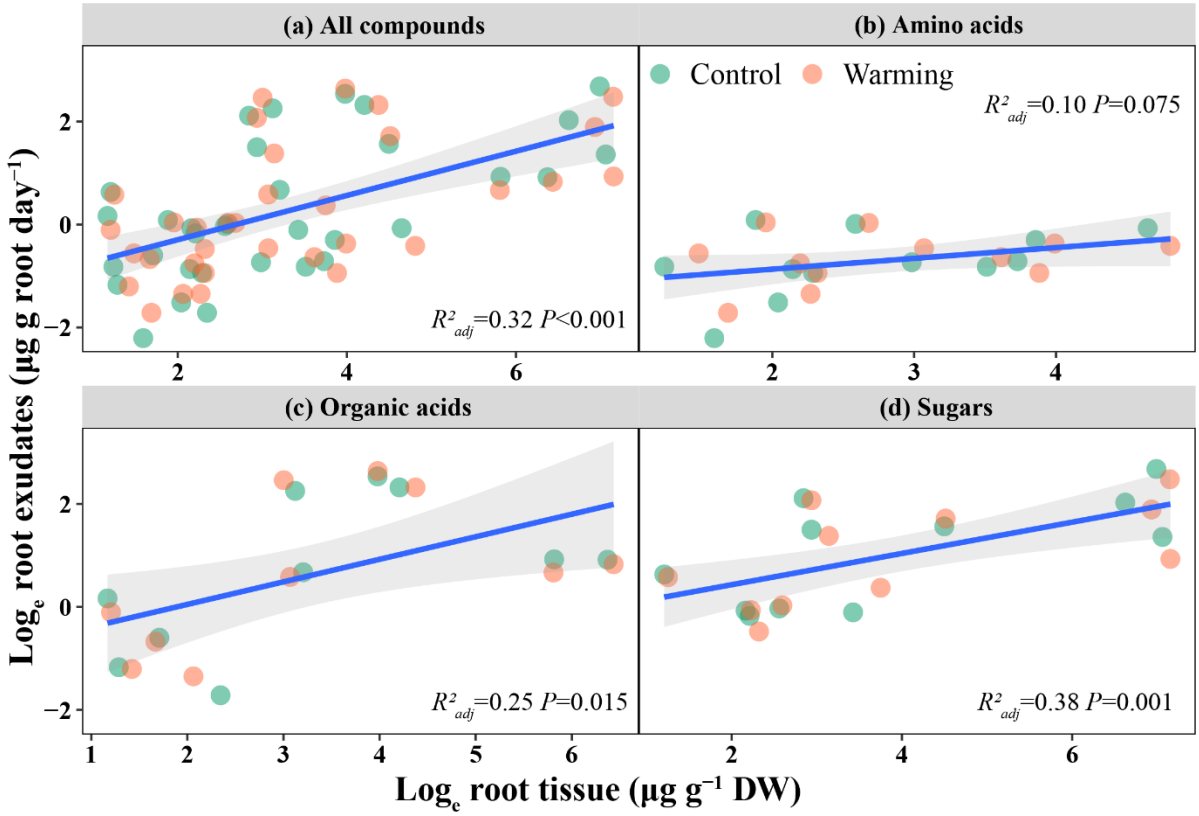


**Figure. 4.** Relationship between root biomass metabolite concentration with root exudate metabolite concentrations. Values are expressed as natural logarithm of root biomass concentrations (grams per dry matter) and root exudates rates (gram per gram of dry root in per day). Each point represents the average value of each investigated metabolite. $R^2$ and equation are reported when relationships were significant.

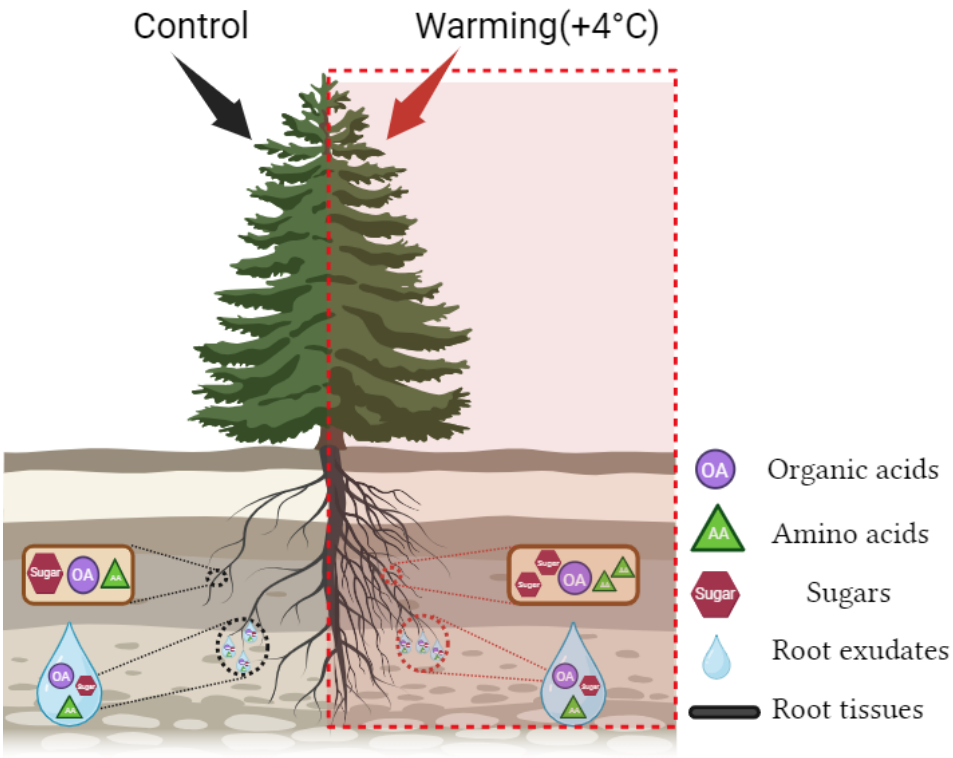


Figure 5 A simplified schematic figure summarizing the effects of warming-induced changes the primary metabolites in root exudation and root tissues.

## Supplement material

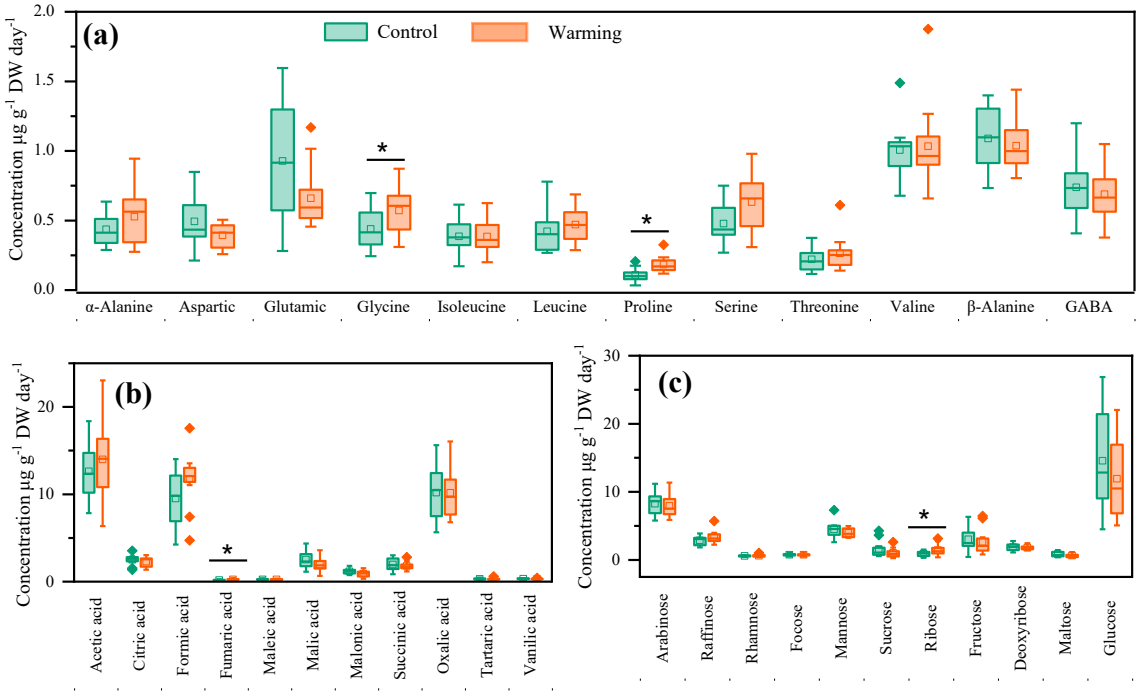


**Figure S1** Boxplots of concentrations of amino acids (a), organic acids (b), and sugars (c) in root tissues averaged across all five sampling times. The ends of the boxes are the 25th and 75th quantiles. The lines across the middle of the boxes are the median values. Asterisks represent significant differences ($p$<0.05) between the control and warming treatments in single compounds.

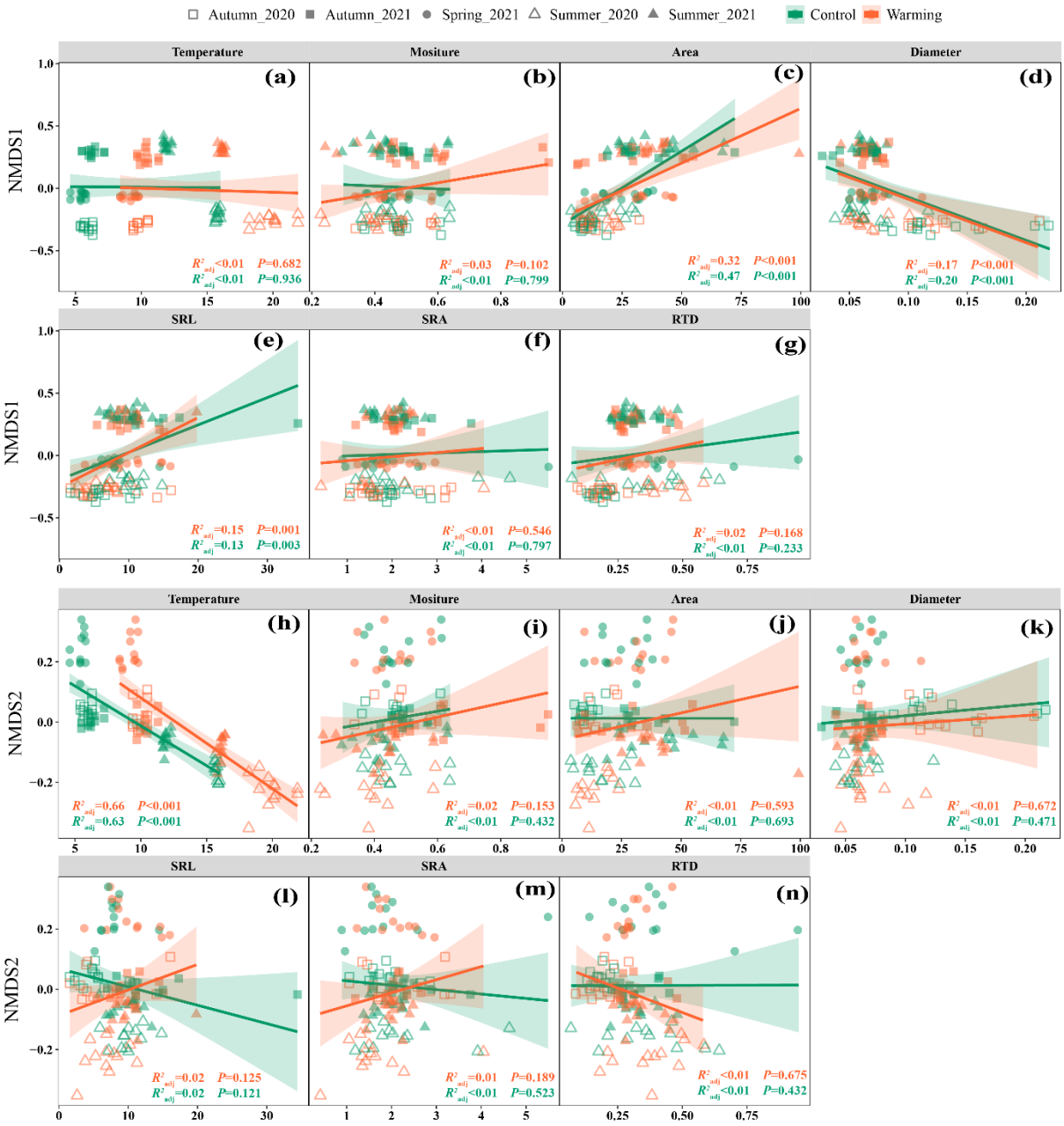


**Figure S2** Linear relationships between the soil environment (soil temperature and soil moisture), root morphological traits and the profiles of primary metabolites in root exudates, expressed as NMDS1 (a-h) and NMDS2 (i-p) scores from NMDS analysis in control and warmed plots. Aera: Root surface area; SRL: Specific root length; SRA: Specific root area; RTD: Root tissue density.

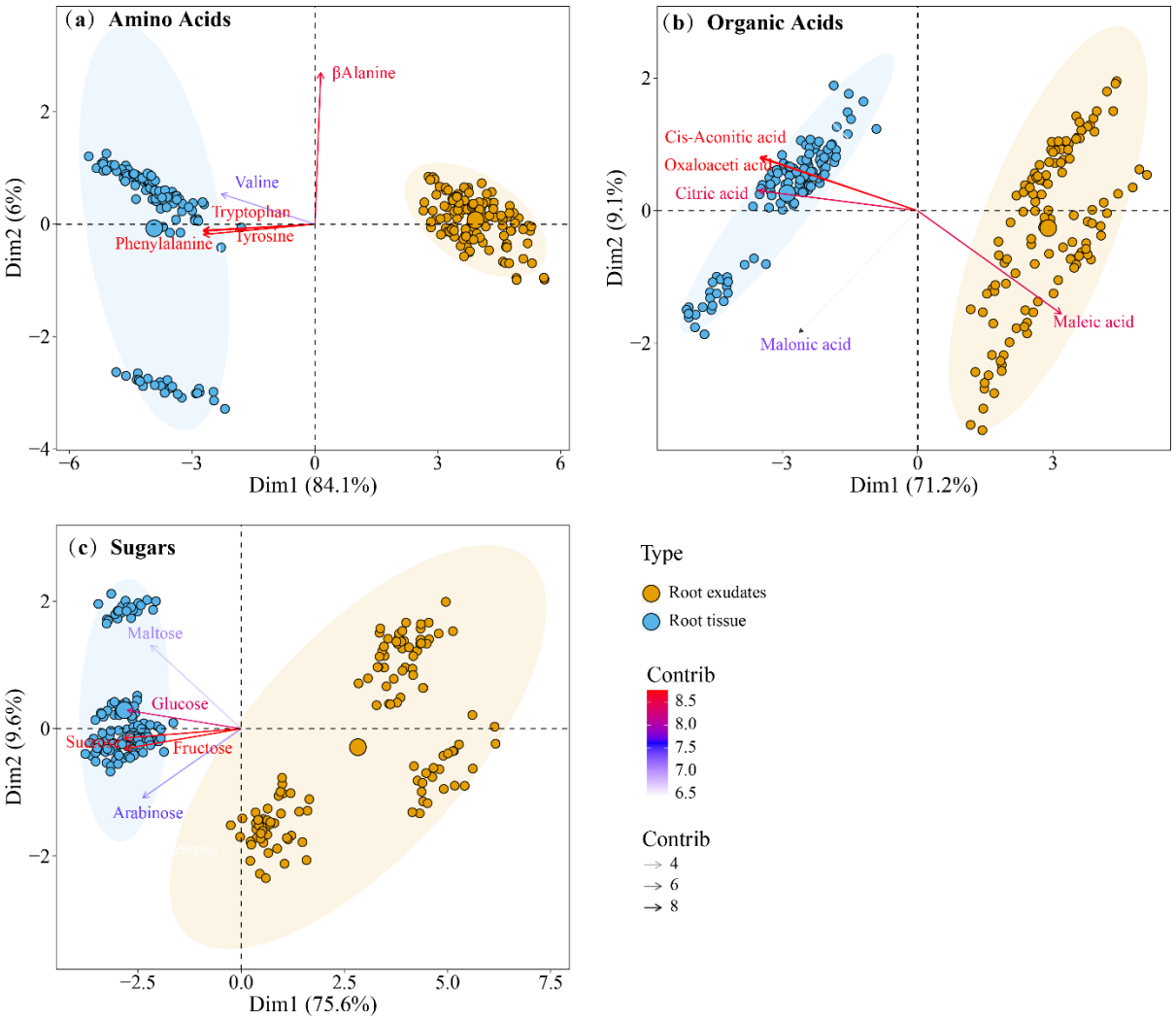


**Figure S3** Biplot of the first two significant components of principal component analysis (PCA) for the investigated metabolites for root tissues (blue) and root exudates (yellow), plotted for amino acids (a), organic acids (b), and sugars (c).

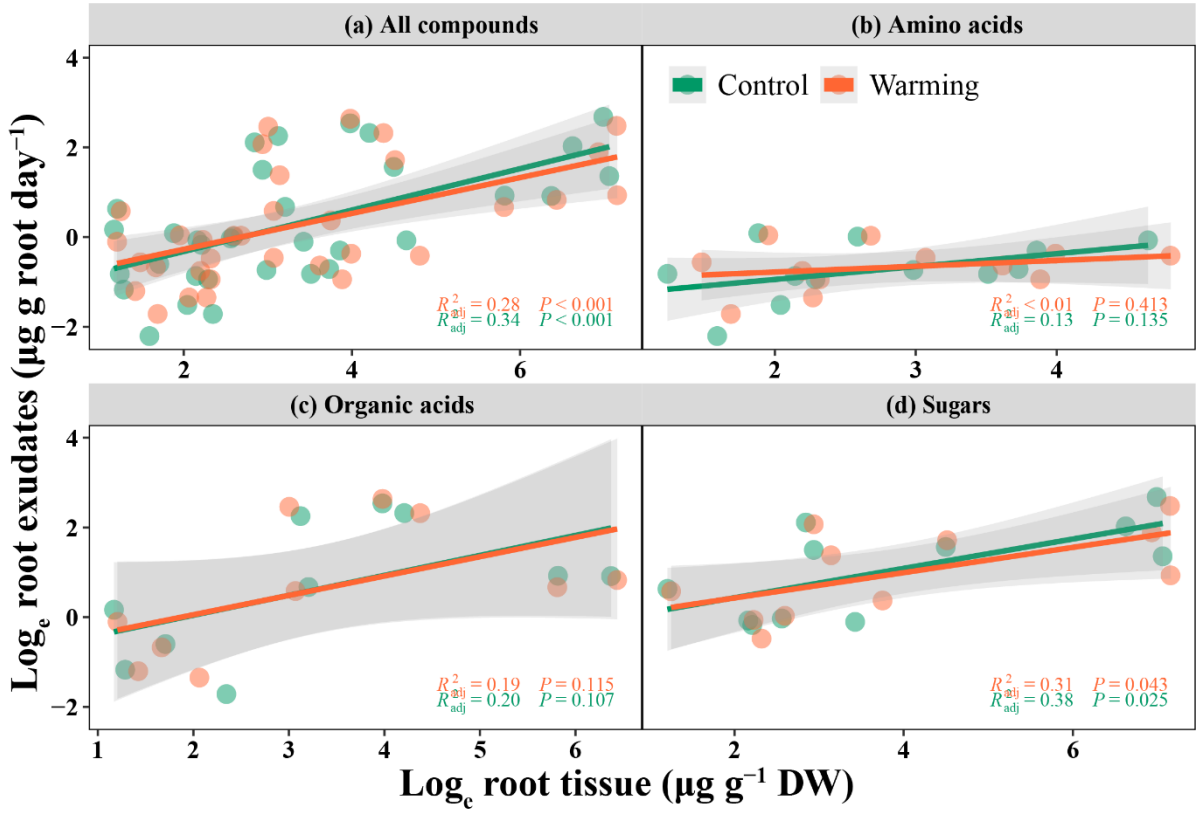


**Figure. S4.** Relationship between root biomass metabolite concentration with root exudate metabolite concentrations in warming and control treatment. Values are expressed as natural logarithm of root biomass concentrations (grams per dry matter) and root exudates rates (gram per gram of dry root in per day). Each point represents the average value of each investigated metabolite.

**Table S1** Linear mixed-effects models testing the effects of warming, season, and their interactions on total amino acids (TAA), organic acids (TOA), sugars (TS), and total primary metabolites (TPM) in root exudates based on fine root biomass, root surface area, and root length. The numbers in the columns are F- and P-values generated by linear mixed-effects model testing ($P < 0.05$).

| | | Treatment | | Sampling | | Treatment* Sampling | |
|---|---|---|---|---|---|---|---|
| unit | Parameter | F | P | F | P | F | P |
| ug $g^{-1}$ $day^{-1}$ | TAA | 0.004 | 0.952 | 32.451 | **0.000** | 0.269 | 0.765 |
| | TOA | 0.360 | 0.549 | 6.675 | **0.002** | 0.702 | 0.497 |
| | TS | 0.427 | 0.515 | 16.411 | **0.000** | 0.081 | 0.923 |
| | TPM | 0.005 | 0.943 | 37.076 | **0.000** | 0.270 | 0.764 |
| ng $cm^{-2}$ $day^{-1}$ | TAA | 0.357 | 0.551 | 30.284 | **0.000** | 0.937 | 0.395 |
| | TOA | 1.598 | 0.209 | 0.752 | 0.473 | 0.744 | 0.477 |
| | TS | 0.578 | 0.448 | 20.422 | **0.000** | 0.310 | 0.734 |
| | TPM | 0.276 | 0.600 | 18.449 | **0.000** | 0.689 | 0.504 |
| ng $cm^{-1}$ $day^{-1}$ | TAA | 0.473 | 0.493 | 38.078 | **0.000** | 0.564 | 0.570 |
| | TOA | 0.579 | 0.448 | 3.817 | **0.025** | 0.326 | 0.723 |
| | TS | 0.263 | 0.609 | 22.366 | **0.000** | 0.286 | 0.752 |
| | TPM | 0.083 | 0.774 | 20.765 | **0.000** | 0.227 | 0.797 |

TAA, total amino acids; TOA, total organic acids; TS, total sugars; TPM, total primary metabolites.

**Table S2** Linear mixed-effects models testing the effects of warming, season, and their interactions on the concentrations of single compounds in root exudates. The numbers in the columns are F- and P-values generated by linear mixed-effects model testing ($P < 0.05$).

| Parameter | Treatment | | Sampling | | Treatment* Sampling | |
|---|---|---|---|---|---|---|
| | *F* | *P* | *F* | *P* | *F* | *P* |
| α-Alanine | 0.0001 | 0.9915 | 19.1994 | **0.0000** | 1.5019 | 0.2269 |
| Aspartic | 1.7365 | 0.1902 | 43.8976 | **0.0000** | 0.1939 | 0.8240 |
| Glutamic | 0.8255 | 0.3654 | 33.0512 | **0.0000** | 0.0258 | 0.9745 |
| Glycine | 5.6538 | **0.0191** | 1.5928 | 0.2078 | 3.1170 | 0.0481 |
| Isoleucine | 1.6314 | 0.2040 | 16.8793 | **0.0000** | 0.1324 | 0.8761 |
| Leucine | 0.2824 | 0.5961 | 7.9587 | **0.0006** | 1.2170 | 0.2997 |
| Proline | 10.1991 | **0.0018** | 3.8107 | **0.0250** | 2.6198 | 0.0772 |
| Serine | 1.1070 | 0.2948 | 10.2008 | **0.0001** | 1.2577 | 0.2880 |
| Threonine | 0.5501 | 0.4598 | 6.8939 | **0.0015** | 0.7047 | 0.4964 |
| Valine | 0.0274 | 0.8687 | 10.5263 | **0.0001** | 0.1128 | 0.8935 |
| β-Alanine | 0.0917 | 0.7626 | 7.2341 | **0.0011** | 0.1786 | 0.8367 |
| aminobutyric | 0.0217 | 0.8830 | 28.0500 | **0.0000** | 0.4392 | 0.6456 |
| Acetic acid | 0.0895 | 0.7653 | 6.5125 | **0.0021** | 0.0071 | 0.9929 |
| Citric acid | 0.0105 | 0.9184 | 20.9823 | **0.0000** | 0.2522 | 0.7775 |
| Formic acid | 1.1817 | 0.2793 | 12.9911 | **0.0000** | 1.0257 | 0.3618 |
| Fumaric acid | 3.1805 | 0.0770 | 78.4336 | **0.0000** | 0.7105 | 0.4935 |
| Maleic acid | 0.0169 | 0.8966 | 5.7624 | **0.0041** | 0.8231 | 0.4416 |
| Malic acid | 0.0066 | 0.9354 | 26.8892 | **0.0000** | 0.1400 | 0.8695 |
| Malonic acid | 2.6422 | 0.1067 | 8.1916 | **0.0005** | 0.0448 | 0.9562 |
| Oxalic acid | 0.2923 | 0.5898 | 17.5536 | **0.0000** | 0.3406 | 0.7121 |
| Succinic acid | 0.0029 | 0.9573 | 1.8323 | 0.1645 | 0.1930 | 0.8247 |
| Tartaric acid | 0.2195 | 0.6402 | 43.1289 | **0.0000** | 0.3276 | 0.7213 |
| Vanilic acid | 0.0539 | 0.8169 | 34.3897 | **0.0000** | 0.0280 | 0.9724 |
| Arabinose | 0.4802 | 0.4897 | 20.2040 | **0.0000** | 0.1393 | 0.8701 |
| Focose | 0.0009 | 0.9765 | 39.8679 | **0.0000** | 0.0034 | 0.9966 |
| Mannose | 0.5816 | 0.4472 | 26.3632 | **0.0000** | 0.0143 | 0.9858 |
| Rhamnose | 0.0001 | 0.9908 | 12.3874 | **0.0000** | 0.0012 | 0.9988 |
| Ribose | 0.7125 | 0.4004 | 19.5845 | **0.0000** | 0.4553 | 0.6354 |
| Deoxyribose | 0.1231 | 0.7263 | 29.8782 | **0.0000** | 0.0279 | 0.9725 |
| Maltose | 0.6639 | 0.4169 | 7.4084 | **0.0009** | 1.5291 | 0.2211 |
| Raffinose | 0.0037 | 0.9516 | 65.7705 | **0.0000** | 0.0064 | 0.9936 |
| Sucrose | 0.0898 | 0.7649 | 11.9024 | **0.0000** | 0.0909 | 0.9132 |
| Fructose | 0.0202 | 0.8872 | 11.8127 | **0.0000** | 0.0951 | 0.9094 |
| Glucose | 0.6642 | 0.4167 | 11.6251 | **0.0000** | 0.0827 | 0.9207 |

# Chapter IV

# Long-term soil warming decreases soil microbial necromass carbon by adversely affecting its production and decomposition

# Long-term soil warming decreases soil microbial necromass carbon by adversely affecting its production and decomposition

Xiaofei Liu[1,2,3], Jakob Heinzle[4], Ye Tian[1], Erika Salas[1], Steve Kwatcho-Kengdo[5], Werner Borken[5], Andreas Schindlbacher[4], Wolfgang Wanek[1]

[1]Division of Terrestrial Ecosystem Research, Department of Microbiology and Ecosystem Science, Center of Microbiology and Environmental Systems Science, University of Vienna, Djerassiplatz 1, 1030 Vienna, Austria;

[2]Doctoral School in Microbiology and Environmental Science, University of Vienna, Djerassiplatz 1, A-1030 Vienna, Austria;

[3]Key Laboratory of Humid Subtropical Eco-geographical Process of Ministry of Education, School of Geographical Sciences, Fujian Normal University, Fuzhou 350117, China;

[4]Department of Forest Ecology and Soils, Federal Research and Training Centre for Forests, Natural Hazards and Landscape-BFW, Seckendorff-Gudent Weg 8, 1131 Vienna, Austria;

[5]Department of Soil Ecology, Bayreuth Center of Ecology and Environmental Research (BAYCEER), University of Bayreuth, Dr.-Hans-Frisch-Straße 1-3, 95448, Bayreuth, Germany

**Abstract**

Microbial necromass carbon (MNC) accounts for a large fraction of soil organic carbon (SOC) in terrestrial ecosystems. Yet our understanding of the fate of this large carbon pool under long-term warming is uncertain. Here we show that 14 years of soil warming (+4 °C) in a temperate forest resulted in a reduction of MNC by 11% (0-10 cm) and 33% (10-20 cm). Warming caused a decrease in the content of MNC due to a decline in microbial biomass carbon and reduced microbial carbon use efficiency. This reduction was primarily caused by warming-induced limitations in available soil phosphorus, which, in turn, constrained the production of microbial biomass. Conversely, warming increased the activity of soil extracellular enzymes, specifically N-acetylglucosaminidase and leucine-aminopeptidase, which accelerated the decomposition of MNC. These findings collectively demonstrate that decoupling of MNC formation and decomposition underlie the observed MNC loss under climate warming, which could affect SOC content in temperate forest ecosystems more widespread.

**Key words:** Long- term soil warming, microbial necromass carbon, microbial biomass carbon, microbial carbon use efficiency, soil phosphorus, enzymes activity, temperate forest

## Introduction

Soil microbial necromass carbon (MNC) plays a crucial role as a precursor in the formation and stabilization of soil organic carbon (SOC), constituting over half of the SOC (Buckeridge et al., 2022a; Liang & Amelung, 2019; Whalen et al., 2022). Despite its potential ecological significance, the effects of global warming on MNC and its subsequent fate in the soil has remained inadequately explored (Buckeridge, et al., 2022a; Cao et al., 2023). Empirical and theoretical evidence has demonstrated that global warming can directly or indirectly trigger changes in soil nutrient availability (such as nitrogen (N) and phosphorus (P) content) (Bai et al., 2013; Tian, et al., 2023b), soil extracellular enzyme activity (Chen et al., 2018), microbial physiological traits, and the composition and function of soil microbial communities (Donhauser et al., 2021; Melillo et al., 2017). These changes, in turn, can significantly impact the accumulation of MNC in soils (Buckeridge et al., 2022a; Kästner et al., 2021; Whalen et al., 2022). Hence, comprehending the dynamics of MNC in a warming world is critical to improve our mechanistic understanding of SOC cycling in a warmer world.

Soil MNC refers to the organic carbon (C) fraction in soils that derives from the remains of dead microbial cells, including cell walls, excreted compounds, and remnants of microbial cells and fragments (Buckeridge et al., 2022a; Liang et al., 2019; Whalen et al., 2022). The fate and dynamics of MNC is determined by the balance between MNC formation and decomposition and their interaction with MNC (de)stabilization (Buckeridge et al., 2022b; Liang et al., 2019). MNC formation is controlled by microbial physiological traits including microbial C use efficiency (CUE, the proportion of microbial C taken up that is allocated to the synthesis of new biomass), microbial growth rate, as well as microbial turnover rate (Buckeridge et al., 2022a; Kästner et al., 2021). Multiple studies support that microorganisms with higher CUE and microbial turnover rate are more favorable for the accumulation of MNC (Buckeridge et al., 2022a; Kästner et al., 2021), but they may also promote MNC decomposition through priming effects (Craig et al., 2022). These studies therefore indicated that the relationship between microbial physiological traits and MNC is more complex. Moreover, these microbial physiological traits are affected by warming, as shown in lab and field settings (Purcell et al., 2022; Walker et al., 2018; Zhang, et al., 2022). For example, microbial CUE may decrease due to increased microbial maintenance costs under elevated

temperatures (Zhang et al., 2022). However, the relationships between microbial physiological traits and MNC under climate warming have remained unresolved.

Soil nutrient (i.e., N and P) availability might also be an important modulator of MNC dynamics. This is because N and P are essential nutrients for microbial growth, playing key roles in energy transfer, protein and nucleic acid synthesis, cell membrane structure, metabolic reactions, and signal transduction (Kuypers et al., 2018; Walton et al., 2023). Both nutrients therefore were shown to constrain the growth of microbes in many ecosystems. Recent studies on P effects have shown that the response of MNC to P addition varies across ecosystems, with increased MNC accumulation in a subalpine forest due to reduced decomposition (Luo et al., 2022), decreased accumulation in alpine grasslands due to enhanced decomposition (Ma et al., 2023), and increased recycling and MNC abundance in a tropical coastal forest (Yuan et al., 2021). These studies have primarily relied on fertilization experiments that artificially increase P availability through the addition of mineral P, but this may not accurately represent the conditions encountered by soil microbial communities in natural ecosystems. In addition, warming promotes the transformation of available P to occluded P (Siebers et al., 2017), and was shown to reduce soil total and labile P pools due to increased P outputs from soils via increased plant P uptake and downward transport of colloidal and particulate P (Tian et al., 2023b). However, the consistency of the relationship between MNC and soil P availability remains poorly understood when it comes to climate warming.

Soil extracellular enzyme activities (EEA) might also be important predictors of MNC dynamics by promoting MNC decomposition, therefore differing from the effects of microbial physiological traits and soil nutrients on MNC formation (Cao et al., 2023; Luo et al., 2022). MNC can be stabilized by interacting with the surfaces of soil minerals or aggregate formation, or it can be decomposed and utilized by live microorganisms (Buckeridge et al., 2022a; Kästner et al., 2021; Liang et al., 2019). Soil enzymes, such as N-acetylglucosaminidase (NAG), break down microbial residues like fungal-derived chitin and bacterial-derived peptidoglycan (Joergensen, 2018). Decomposition of MNC provides nutrients in favorable amounts due to its resemblance to microbial biomass in elemental and chemical composition (Buckeridge et al., 2022a; Whalen et al., 2022). Previous studies have

indicated that enzymes in colder regions exhibit greater sensitivity to temperature increases compared to those in warmer regions, with soil EEA at higher latitudes showing a stronger response to rising temperatures than enzymes at lower latitudes (German et al., 2012; Koch et al., 2007), but the actual relationship between MNC dynamics and soil enzymes in response to climate warming is still poorly understood.

To this end very little research has directly assessed the impacts of *in situ* warming on MNC contents and dynamics (Cai et al., 2023; Ding et al., 2019; Liang & Balser, 2012). For instance, Ding et al. (2019) found that the contribution of MNC to SOC increased with warming, due to facilitated microbial growth and proliferation in an alpine meadow on the Qinghai-Tibet Plateau. In contrast, warming decreased the contribution of MNC to SOC through accelerated degradation of amino sugars after 9-years warming in a Californian annual grassland ecosystem (Liang & Balser, 2012). These results clearly show that our knowledge on the warming response of MNC formation and stabilization are incomplete. Moreover, the few studies published were performed in grassland ecosystems (Cai et al., 2023; Ding et al., 2019; Liang & Balser, 2012), excluding forest ecosystems, with a predominant focus on shorter-term responses (Liang & Balser, 2012). However, short-term and long-term warming may be different in terms of their effect on soil nutrient availability, soil microbial community structure, and soil enzymes (Melillo et al., 2017; Romero-Olivares et al., 2017). For example, a 26-year long-term soil warming study conducted at the Harvard Forest LTER site (USA) revealed substantial reorganization of the soil microbial community, characterized by a decrease in the abundance of fungal biomarkers and a shift towards Gram-positive bacteria (Melillo et al., 2017; Metcalfe, 2017). Nonetheless, the roles of microbial traits (i.e., CUE, growth rates, and turnover), soil nutrient availability, and EEA in regulating MNC dynamics under long-term *in situ* warming have not yet been explored in temperate forests. Identifying these drivers may provide a more mechanistic understanding of how soil C sequestration can be enhanced under climate warming conditions.

Temperate forests encompass approximately 25% of the world's forested area and store around 22% of terrestrial forest soil C, making them crucial for regional soil C accounting (Bonan, 2008; Lal, 2005). The projected temperature increases of 1-2 °C from 1990 to 2050 in temperate forests, with the climate becoming warmer and drier, poses a significant threat to

the functioning of the soils in temperate forest ecosystems (Adams et al., 2019; Seidl et al., 2017). To our best knowledge, currently only two warming experiments have been operative in temperate forests for >10 years (Melillo et al., 2017; Tian et al., 2023a), but in none of those MNC dynamics were studied and published. To fill this knowledge gap, we investigated the response of MNC dynamics and the underlying processes to long-term soil warming (>14 years) in a temperate forest in Achenkirch, Austria. Our specific objectives were (1) to investigate how soil warming impacts the content of soil MNC, and (2) to identify the key factors and processes that underly the observed changes in MNC content. Our previous work found that long-term soil warming increased belowground plant C inputs (Heinzle et al., 2023; Kwatcho Kengdo et al., 2023) but decreased SOC content through increased EEA (Tian et al., 2023a) and decreased the soil P pools (Tian et al., 2023b). Therefore, we hypothesized that long-term warming reduced MNC as a matter of decreased soil P and soil microbial biomass and that warming promotes the decomposition of MNC by increased soil EEA.

## Materials and methods

### Experimental design

This study was conducted in the Achenkirch soil warming experiment, located in a temperate forest in the Austrian Alps (11°38′21″E; 47°34′50″N) at an altitude of 910 m. The area has a temperate continental climate, with an annual mean air temperature of 7 °C and mean annual precipitation of 1493 mm (from 1988 to 2017). The soils in the area are classified as shallow Rendzic Leptosols, developed on dolomite bedrock, and the dominant tree species in the ~130-year-old forest is Norway spruce (*Picea abies* L. H. Karst.), with European beech (*Fagus sylvatica* L.), and silver fir (*Albies alab* Mill.) admixed.

The soil warming experiment was designed in a paired plot design. Twelve 2 m × 2 m plots were grouped into six blocks (pairs), established in 2004 (n = 3 blocks) and 2007 (n = 3 blocks). Two treatments, ambient temperature (control) and warming by 4 °C, were assigned to the two plots of each block. Soil heating cables (Etherma, Salzburg, Austria) were installed at a soil depth of 3 cm, with 7.5 cm distance between cables, in the warming and the control plots (the control plots were not heated but cables installed to control for the disturbance

effect). Soil temperature in the warming plots was maintained at a constant 4 °C higher than in the paired control plots throughout the snow-free period (April-December). Soil temperatures were recorded at half-hourly intervals at depths of 5 and 15 cm below the soil surface. Further details about the site and the experimental setup can be found elsewhere (Kwatcho Kengdo et al., 2022; Schindlbacher et al., 2015; Tian et al., 2023b).

**Soil sampling, soil parameters and microbial biomass analysis**

Soil samples were collected from the control and the warmed plots at the Achenkirch soil warming experiment in May, August, and October 2019. Seven randomized soil cores per plot were taken from depths of 0-10 cm and 10-20 cm using a 2.5 cm wide hand auger. The soil depth increments within the same plot were combined and passed through a 2-mm sieve. Measurements of important soil physicochemical and biological properties (including microbial biomass, soil nutrients, soil enzymes, microbial growth, and turnover) were performed on the same samples, and the data published recently (Tian et al., 2023a, b) and used here. The measurement techniques are therefore only shortly depicted below.

Soil water content was determined gravimetrically by drying aliquots of 5 g of fresh soil at 105 °C for 48 hours. Soil pH was measured using an ISFET pH sensor (Sentron, The Netherlands) in a 1:5 (w:v) slurry of air-dried soil and ultra-pure water. To determine soil organic C, acid pretreatment (2 M HCl) was carried out to remove carbonates (dolomite), followed by CN analysis using an elemental analyzer (Carlo Erba EA1110, Thermo Fisher, USA). $NH_4^+$ and $NO_3^-$ were extracted with 1 M KCl (1:7.5 (w:v)) and determined colorimetrically. Dissolved organic N was calculated as the difference between total dissolved N (TDN, determined by a Shimadzu TOC/TN analyzer) and the sum of $NH_4^+$ and $NO_3^-$.

Soil microbial biomass C was determined by the chloroform-fumigation extraction method (Vance et al., 1987). Total dissolved organic C in 0.5 M $K_2SO_4$ extracts of fumigated and non-fumigated soils were measured using a dissolved organic C analyzer (Shimadzu TOC/TN analyzer), and microbial biomass C was calculated as the difference in dissolved organic C between the fumigated and unfumigated samples using a conversion factor (kc) of 0.45 (Joergensen, 1996).

To determine bioavailable phosphorus (P) in the form of Olsen inorganic P (Olsen Pi) and Olsen organic P (Olsen Po), soil bicarbonate extraction (0.5 M $NaHCO_3$, pH 8.5, 1:7.5 w:v) and the malachite green method were used (D'Angelo et al., 2001; Rowland & Haygarth, 1997), employing (or not) the acid persulfate digestion method for Olsen total P (Olsen Pt). The ignition method (450 °C for 5 hours) followed by 0.5 M $H_2SO_4$ extraction was used to determine soil total P (TP), total inorganic P (TIP), and total organic P (TOP) by difference (Kuo, 1996).

**Soil microbial activity**

Four hydrolytic enzymes (β-glucosidase (BG), N-acetylglucosaminidase (NAG), leucine-aminopeptidase (LAP), and acid phosphatase (AP)) were measured by the fluorescent substrate addition method described by Kaiser et al. (2010). Soil samples (1 g) were sonicated in sodium acetate buffer (100 mM, pH 5.5) and assayed with 4-methylumbelliferyl-β-D-glucopyranoside for BG, 4-methylumbelliferyl-N-acetyl-β-D-glucosaminide for NAG, L-leucine-7-amido-4-methylcoumarin hydrochloride for LAP, and 4-methylumbelliferyl-phosphate for AP.

Soil microbial CUE, microbial growth, respiration, and microbial turnover time were determined using the $^{18}O$-$H_2O$ incorporation into DNA method, as described in studies by Spohn et al., (2016) and Zheng et al. (2019). In brief, two aliquots (400 mg) of fresh soil were amended with $^{18}O$-labelled or unlabeled water and placed in 50 mL serum bottles. The head space was resampled to measure $CO_2$ accumulation by soil respiration over 24 hours using a portable IRGA system (EGM-4, PP systems, USA). Soil DNA was extracted from labeled and unlabeled soil using a DNA extraction kit (FastDNA™ SPIN Kit for Soil, MP Biomedicals, Germany). DNA quantity was determined by fluorescence measurement after staining with Quant-iT™ PicoGreen® assay (Life Technologies) and the O content and $^{18}O$:$^{16}O$ ratio of DNA determined using a Thermochemical Elemental Analyzer (TC/EA, Thermo Fisher) coupled to an IRMS (Delta V Advantage, Thermo Fisher, Germany). The amount of DNA that was produced during the incubation period (DNA produced) was calculated as follows:

$$DNA_{produced} = O_{Total} \times \frac{\%at_{excess}}{100} \times \frac{100}{\%at_{label}} \times \frac{100}{31.21} \quad (1)$$

where $O_{Total}$ is the total O content of the dried DNA extract, $\%at_{excess}$ is the at% excess $^{18}O$ and $\%at_{label}$ is the at% $^{18}O$ in the final soil solution. The average content (%) of O in DNA is 31.21 according to an average formula ($C_{39}H_{44}O_{24}N_{15}P_4$). A conversion factor ($f_{DNA}$) was calculated to represent the ratio of soil microbial biomass C ($C_{mic}$, μg $g^{-1}$ DW) to soil DNA content ($DNA_{mic}$, μg $g^{-1}$ DW):

$$f_{DNA} = \frac{C_{mic}}{DNA_{mic}} \quad (2)$$

and used to calculate microbial growth rates based on the dry soil mass ($C_{growth}$):

$$C_{growth} = \frac{f_{DNA} * DNA_{produced} * 1000}{DW * t} \quad (3)$$

where DW is the soil dry mass (g) and t is the incubation time (hours, h). Additionally, we calculated microbial C uptake ($C_{uptake}$) as the sum of microbial respiration ($C_{respiration}$) and C incorporation into microbial growth ($C_{growth}$):

$$C_{uptake} = C_{respiration} + C_{growth} \quad (4)$$

The microbial turnover time was determined by dividing microbial biomass C ($C_{mic}$) by microbial growth ($C_{growth}$).

$$M_{turnover} = \frac{C_{mic}}{C_{growth}} \quad (5)$$

$$CUE = \frac{C_{growth}}{C_{uptake}} = \frac{C_{growth}}{C_{respiration} + C_{growth}} \quad (6)$$

**Soil amino sugar analysis**

Soil amino sugar hydrolysis and quantification followed Zhang and Amelung (1996) and Salas et al. (2023). Aliquots (0.5 g) of air-dried soil were hydrolyzed with 10 mL 6 M HCl at 105 °C for 8 h. The hydrolysates were filtered through cellulose acetate filter membranes

(Sartorius, Goettingen, Germany) into 20 ml scintillation vials, evaporated to dryness with an $N_2$ dryer, and then re-dissolved in 12 mL Milli Q water. The hydrolysates were transferred into 50 mL falcon tube, and the pH was adjusted to 6.6-6.8 with 1 M KOH. The samples were then centrifuged (1600 *g*) for 15 minutes to remove iron precipitates and the supernatant freeze-dried. This residue was dissolved in 8 mL methanol and cleared by centrifugation (1600 *g*) for 10 min. The methanol supernatant was transferred to a 10 mL (BPA-free) cryovial (Simport, polypropylene T310-10A) and dried in a $N_2$ dryer. The samples were re-dissolved in 1 mL Milli Q water. Amino sugars in samples were prepared for LC-MS analysis via 1-methyl-3-phenyl-2-pyralozone (PMP) derivatization, as described by Salas et al. (2023). In brief, samples were derivatized using a 0.5 M PMP solution and the reaction was conducted in a water bath at 70°C. Following the reaction, formic acid was added for neutralization. To eliminate excess PMP, a liquid-liquid extraction with chloroform and water was performed. The resulting aqueous layer was carefully filtered through a 0.2 µm acetate membrane syringe filter (VWR International™). For analytical assessment, the filtered samples were introduced into a UPLC Ultimate 3000 system coupled to an Orbitrap Q Exactive HRMS system. Chromatographic separation was carried out on a Waters AccQ.Tag Ultra C18 column, and the mass spectrometer was operated in ESI positive mode, scanning a mass range from 150-1000 m/z.

We thereby quantified the microbial necromass biomarkers glucosamine (GluN) and muramic acid (MurA). GluN is present in both fungal and bacterial cell walls, and has a molecular weight of 179.2. MurA has a molecular weight of 251.2 and solely occurs in bacterial cell walls. Fungal necromass carbon (FNC), bacterial necromass carbon (BNC), and MNC were calculated as follows (Liang et al., 2019):

$$FNC = \left(\frac{GluN}{179.2} - 2 \times \frac{MurA}{251.23}\right) \times 179.2 \times 9 \qquad (7)$$

$$BNC = MurA \times 45 \qquad (8)$$

$$MNC = FNC + BNC \qquad (9)$$

Where 9 and 45 are the conversion factors from fungal GluN to FNC in equation (7) and from bacterial MurA to BNC in equation (8), respectively (Appuhn & Joergensen, 2006).

**Data analysis**

Statistical analysis was performed in R statistical software (version 4.2.3). Before conducting further analyses, we assessed the homoscedasticity and normality of the data for MNC, FNC, BNC, FNC to BNC ratio, and their contributions to SOC, and applied log or sqrt transformations if necessary. To investigate the main effects of season, depth, and warming and their interactions, we used mixed-effects models with warming, depth, and season as fixed factors, and block and warming duration as random factors. Given the significant interactions we identified between warming and depth for both FNC and MNC variables, we proceeded with pairwise comparisons. Additionally, we assessed the impact of warming on MNC, FNC, BNC and their contribution to SOC by using paired t-tests. For these tests, we set the significance level at $\alpha = 0.05$.

Residuals from a mixed effects model, considering season and depth as fixed factors and block and warming duration as random factors, were used to eliminate the influence of season and depth on soil N, soil P, microbial traits, EEA, and MNC. Only the residuals data were then employed for multiple regression models and linear regression analysis. We used multiple regression models to examine the combined effects of soil N, soil P, microbial traits, and EEA on MNC, as well as its two constituent components (BNC and FNC). To identify the most concise model that explains the variation in MNC best, we constructed four competing models, which consider an increasing level of biological complexity, to identify the set of predictors that provide the most parsimonious model for explaining the variation in MNC. (1) a "soil nutrient" model (includes soil $NH_4^+$, $NO_3^-$, dissolved organic N, total inorganic P, total organic P, Olsen organic P, and Olsen inorganic P); (2) a "microbial trait" model (includes microbial biomass C, CUE, and microbial turnover time); (3) a "EEA" model (includes three hydrolytic enzymes, BG, LAP, and AP); (4) full model (includes all the predictors).

Initially, we used a backward stepwise regression procedure using R software to determine the best-fitting models with the lowest AICc values. Starting with the full model, we successively removed variables that had the least significant impact on the AICc. Next, based on the best model selected from the initial models (1-4), we conducted a model-averaging procedure using AICc (with $\Delta AICc < 2$) to determine the parameter coefficients

for the most suitable final set of predictors for MNC. This procedure was performed using the "dredge" function in the R package Multi-Model Inference (MuMIn). All predictors and response variables were standardized prior to analysis, employing the Z-score method to interpret parameter estimates on a comparable scale. To assess the relative importance of the predictors as drivers of MNC, we calculated the relative effect of the parameter estimates for each predictor in comparison to the effect of all parameter estimates in the models. Finally, all figures were prepared by R statistical software (version 4.2.3) and/or Adobe Illustrator 2021.

## Results

### Soil microbial necromass carbon response to long-term soil warming

The linear mixed effects models revealed that long-term soil warming had significant negative effects on the bacterial necromass C (BNC), fungal necromass C (FNC), and MNC, but exerted no significant effect on the FNC to BNC ratio (Figure.1, Table 1). Both season and soil depth exhibited significant effects on BNC, FNC, MNC, and the FNC/BNC ratio. However, soil depth did not have a significant effect on BNC. Interestingly, none of the measured necromass parameters showed significant interactions between warming and season, highlighting that the observed warming effects were consistent across sampling periods. However, both FNC and MNC exhibited significant interactions between warming and soil depth suggesting that the effect of warming on FNC and MNC is contingent upon depth (Table 1). Pairwise comparisons revealed that warming had a more pronounced effect on FNC and MNC at 10-20 cm soil depth compared to 0-10 cm depth (Figure. 1). In the warming plots, the MNC content decreased by 11% (marginally significant, t=1.75, $p$=0.09) and BNC content dropped by 32% (t=3.53, $p$=0.002) at a soil depth of 0-10 cm, compared to the control plots (Figure. 1a, c). Conversely, at 10-20 cm soil depth, the content of BNC, FNC, and MNC declined by 30%, 36%, and 33%, respectively (Figure. 1e-g). The FNC to BNC ratio at 0-10 cm depth was 1.79 in the control and 2.22 in the warming treatment (Figure. 1d). In contrast, at 10-20 cm depth, the ratios were closely aligned, with 1.67 for the control and 1.53 for the warming plot (Figure. 1h).

Overall, the contribution of BNC to SOC (BNC/SOC) was significantly lower in warming plots than in control plots (t=3.11, $p$=0.006, Figure. 2a) at 0-10 cm depth. In contrast, soil warming did not affect FNC/SOC and MNC/SOC at 0-10 cm depth. At the 10-20 cm depth increment, the contribution of MNC to SOC decreased by 14% due to soil warming (t=1.98, $p$=0.04, Figure. 2b), but there were no observable effects of warming on FNC/SOC and BNC/SOC (Figure. 2b).

**Identification of biogeochemical predictors for microbial necromass carbon and its components**

We used two statistical approaches (multiple regression models and partial linear regression analysis) to identify the most important predictors of MNC, as well as of its two components, FNC and BNC. Among the parameters we tested microbial traits (microbial biomass C, CUE, and microbial turnover time), soil phosphorus (P) pools (total inorganic P, total organic P, Olsen organic P, and Olsen inorganic P), soil N pools ($NH_4^+$, $NO_3^-$, and dissolved organic N), and soil extracellular enzyme activities (EEA). Linear regression analysis showed that MNC, BNC, and FNC were positively correlated with SOC, soil pH, microbial biomass C, microbial turnover time, and total inorganic P, while negatively with soil N-acetylglucosaminidase (NAG) and leucine aminopeptidase (LAP) activity (Figure. 3 and Figure. S1). However, soil MNC, BNC, and FNC were not directly related to microbial CUE and Olsen organic P (Figure. 3 and Figure. S1).

The optimal multiple regression model explaining MNC included $NH_4^+$, total inorganic P, Olsen organic P, microbial biomass C, CUE, acid phosphatase (AP), and LAP (Figure. 4). Within the selected Akaike Information Criterion threshold ($\Delta$AICc$\leq$2), we found the full model to explain a high proportion of the variance in MNC (adjusted $R^2$=0.45, Figure.4 and Table S1). Soil N, soil P, microbial physiological traits, and EEA were responsible for 3.3%, 34.6%, 13.2%, and 48.9% of the explained variance in MNC, respectively (Figure.4). Both FNC and BNC shared similar predictors, though their relative importance differed (Figure. S2). For FNC and BNC, both the optimal models conferred to model structure 4 that includes soil P and EEA (Figure. 2a, b). The BNC model had TIP, OlsenPo, AP, and LAP as the strongest predictors, which explained 22% of the variation (Figure. 2a). Soil P and EEA were

responsible for 35% and 65% of the explained variance in BNC, respectively. In the FNC models, the strongest predictors were total inorganic P, Olsen organic P, β-glucosidase (BG), and LAP, which explained 24% of the variation (Figure. 2a). Soil P and EEA were responsible for 46% and 54% of the explained variance in the FNC model, respectively. Interestingly, we found that adding microbial traits to the multiple regression models did not improve the model performance in the BNC and FNC models (Figure. S2 and Table S1). We also statistically tested direct and indirect effects of warming on MNC through microbial functional traits using structural equation models (SEM), but all tested SEM models did not work out properly as the model structures used did not comply to the test parameter values commonly used to indicate a successful SEM (e.g. $\chi^2$ test, Standardized Root Mean Square Residual). However, we found a significant positive correlation between microbial CUE, microbial turnover time, and microbial biomass C (Figure. S3c, d). Microbial CUE was positively correlated with total organic P (Figure. S3a), while microbial turnover time was positively correlated with total inorganic P and total organic P (Figure. S3b). Therefore, part of the negative warming effects on MNC were likely indirect, through negative effects of soil P limitation on microbial biomass C and CUE and thereby on MNC.

**Discussion**

An improved mechanistic understanding of how longer-term soil warming affects MNC dynamics can be a cornerstone towards improved soil-C sequestration predictions. Our analysis considers the impact of long-term soil warming on soil microbial traits (microbial biomass C, CUE, and turnover time), soil nutrients (N and P), and soil EEA to provide a depth-informed understanding of MNC dynamics. Consistent with our hypotheses, we found that MNC and its components decreased (by 10-30%) at 0-10 cm and 10-20 cm soil depth under long-term soil warming (Figure. 1 and Table 1). This is in line with the findings of Liang et al (2015), who observed a 53% decrease in total amino sugar concentrations following nine years of experimental warming in a dry California annual grassland ecosystem. Long-term soil warming affected MNC in the studied temperate forest through two mechanisms (Figure. 5): (i) decreased soil available P limits microbial biomass production (growth), reducing CUE and microbial biomass C, leading to decreased MNC production;

and (ii) increased soil EEA promote the decomposition of soil organic matter and MNC, leading to increased MNC depolymerization and mineralization.

**Warming decreased microbial necromass carbon production by reducing available soil P**

Quantifying MNC production in soils presents significant challenges due to its diffuse nature and limitations of available methods (Buckeridge et al., 2022a; Camenzind et al., 2023; Kallenbach et al., 2016). However, microbial physiological traits, such as microbial turnover time, microbial biomass C and CUE, can serve as indirect indices of MNC production and provide valuable insights into MNC dynamics (Cotrufo et al., 2013; Kallenbach et al., 2016; Kallenbach et al., 2015; Prommer et al., 2020). In this study, linear regression and multiple regression models showed that MBC was positively related to MNC (Figure. 3b and Figure. 4), which is consistent with other studies (Jia et al., 2022; Prommer et al., 2020; Wang et al., 2021b). At our site, the microbial biomass C content declined by 22% after 14 years of soil warming (Tian, et al., 2023a), which indicates that the yield of MNC declined because MNC originates from the decomposition and breakdown of C-rich organic molecules in dead microbial cells (Camenzind et al., 2023). The decrease in microbial biomass C content observed in the warming plot was in part associated with a decline in CUE, as indicated by previous research at the site (Tian et al., 2023a). This relationship was corroborated by our regression analysis depicting a positive relationship between microbial biomass C and CUE (Figure. S3c). This suggests that soil microbes tend to channel more C toward respiration for energy provisioning rather than directing towards growth investments when environmental conditions disfavor growth and biomass accumulation, reducing microbial CUE and biomass concurrently.

Interestingly, the relationship between MNC and CUE displayed inconsistency in our regression analysis (Figure. 3d and Figure. 4). Linear regression analysis (Figure. 3d) did not reveal a significant correlation, while multiple regression models (Figure. 4) indicated a negative relationship. It was not surprising that CUE and MNC showed different or no relationships in both regression models, given that multiple regression models reflect the concurrent effects of multiple parameters and their interaction (direct and/or indirect effects)

on MNC. This further suggests that the effects of CUE on MNC may be indirect and influenced by other factors, such as soil P availability and soil EEA (see below for discussion). In addition, we observed that microbial physiological traits (microbial biomass C, CUE, and turnover time) were not included in the optimal model to explain specific BNC and FNC dynamics (Figure. S2b). Accordingly, microbial traits alone were not a good predictor for BNC and FNC dynamics in this study, which was also partially supported by linear regression analysis that showed no significant direct relationship of CUE with BNC or FNC. The inability of microbial physiological traits to account for variations in BNC and FNC implies that community-level parameters alone are insufficient to explain the dynamics of microbial necromass in temperate forests. This could partially be attributed to the differences in CUE between bacteria and fungi, with fungi generally exhibiting higher CUE than bacteria (Silva-Sánchez et al., 2019; Soares & Rousk, 2019), and fungi often being dominant in forest ecosystems. This result underscores the critical importance of evaluating microbial physiological traits at more refined than bulk microbial level to predict microbial necromass dynamics in future research.

Another possible reason for reduced MNC formation with warming could be the indirect effect of warming on soil available P. Several *in-situ* P addition experiments have examined the influence of soil-available P on MNC (Luo et al., 2022; Ma et al., 2023; Yuan et al., 2021). The results of these studies have produced inconsistent findings, largely because the impact of P addition on MNC was contingent upon the ecosystem type and the pre-existing soil P condition. Both linear regression and multiple regression models showed that MNC (Figure. 3b and Figure. 4), BNC (Figure. S1e and Figure. S2a), and FNC (Figure. S1e and Figure. S2b) were positively correlated with soil total inorganic P, while soil total inorganic P contents declined after 14 years soil warming (Tian et al., 2023b). This decrease in soil total P pools was likely due to long-term warming effects that increased net plant P uptake and enhanced the downward transportation of colloidal and particulate P, resulting in higher losses of P from soils (Tian et al., 2023b). These results indicate that soil available P plays a pivotal role in governing the reduced MNC formation under soil warming conditions. As mentioned above, there is a strong positive relationship between MNC and microbial biomass C, as shown here and elsewhere (Wang et al.,2021a). Additionally, soil P availability is an

important moderator of microbial growth. For example, the addition of P significantly increased the microbial biomass in old-growth tropical forests where P availability was low, while P addition had no effect on the microbial biomass in pine forests where P availability was high (Liu et al.,2012). Therefore, adequate P supply is essential for microorganisms due to its key roles in genetic encoding (DNA, RNA), energy transfer (e.g., ATP), cell structure (phospholipids), metabolism, and signaling (Kuypers et al., 2018; Walton et al., 2023). The critical role of P availability gains further substantiation from correlated research carried out at the same forest experimental site, indicating that sustained warming prompted a shift in soil microorganisms from being primarily C-limited to experiencing co-limitation by both C and P (Shi et al., 2023). This shift was attributed to an aggravation of abiotic P immobilization within warming soil environments and increased long-term soil P losses (Tian et al., 2023b). In addition, Luo et al. (2022) showed that P enhances the effectiveness of microbial N use and reduces the synthesis of N-acquiring enzymes, thereby decreasing unnecessary consumption and reducing the decomposition of microbial necromass. Conversely, reducing P availability appears to increase the synthesis of N-acquiring enzymes, potentially enhancing the decomposition of microbial necromass. In our study, soil warming reduced soil P availability, increased the activity of N- and P-acquiring enzymes (i.e., LAP and NAG, and AP) (Tian et al., 2023a, b) and thereby accelerated the decomposition of MNC, as discussed below. Moreover, thus far mining of MNC for nutrients has been mostly discussed in terms of N gain, due to the high N content of microbial cell wall fragments containing peptidoglycan and chitin, as well as cell wall bound proteins. However, microbial necromass does not only represent cell wall-bound residues (as indicated by e.g. amino sugars), but also substantial yet unknow contributions of intracellular and extracellular residues (Shi et al.,2024). Intracellular residues certainly come with a high content of DNA and RNA, though they are thought to turn over rapidly. Extracellular polymeric compounds (EPS) consist of proteins, polysaccharides, lipids and DNA (eDNA), with exopolysaccharides often colocalizing with eDNA in biofilms. Bacterial cell walls can also contain a substantial fraction of organic P in the form of teichoic acids, representing polymers consisting of repeating polyol phosphate units occurring in most Gram-positive bacteria (Shiraishi et al.,2016). Though not investigated in a targeted way thus far increased decomposition of

microbial (cellular, cell wall and extracellular) necromass may greatly benefit soil microbes in terms of P nutrition under P limiting conditions.

**Warming accelerates microbial necromass carbon decomposition by stimulating soil EEA**

In line with MNC production, the effects of warming on MNC decomposition received less attention due to limitations in methodological approaches (Buckeridge et al., 2022b; Wang et al., 2020). Hence, soil EEA frequently serve as an indicator for assessing the decomposition of MNC in numerous studies (Cai et al., 2023; Luo et al., 2022; Ma et al., 2023). For instance, increased soil EEA, such as β-glucosidase (BG), NAG and LAP, induced by nutrient addition (i.e., N and P), accelerated the decomposition of microbial necromass and hindered its accumulation in both an alpine grassland of the Tibetan Plateau (Ma et al., 2023) and in tropical forest ecosystems (Yuan et al., 2021). Warming-induced increases in soil EEA have been observed in numerous field experiments and in meta-analysis studies (Cai et al., 2023; Chen et al., 2018; Fanin et al., 2022). This result is supported by previous research conducted at the same site and during the same soil sampling campaigns (Tian et al., 2023a). We found a negative relationship between LAP and NAG activities and MNC (Figure. 3h, i and Figure. 4), as well as with its components BNC and FNC (Figure. S1h, i and Figure. S2). This result suggests an increased microbial effort towards decomposing microbial necromass under long-term soil warming. The stimulation of EEA can, in part, be attributed to soil microbes facing increased limitations in C and/or P in the warming plots compared to the ambient plots, as discussed earlier (Shi et al., 2023; Tian et al., 2023a). Consequently, microbes allocate more C to enzyme production for mining or recycling microbial necromass because microbial necromass exhibits lower C:nutrient ratios and higher nutrient contents compared to plant tissue, a phenomenon particularly evident under conditions of nutrient scarcity (Buckeridge et al., 2022a; Cui et al., 2020).

Furthermore, changes in soil pH may also play a role in reducing MNC stabilization (Buckeridge et al., 2022a; Cai et al., 2023; Ma et al., 2023). Lower pH levels can cause minerals to dissolve, diminishing their capacity to stabilize MNC (Buckeridge et al., 2022a; Kästner et al., 2021). This, in turn, leads to the presence of more unprotected MNC that can

be more readily decomposed and utilized by microbes than mineral-bound MNC. The positive correlation between MNC and pH supports this perspective, though the soil pH values varied across a small range only (pH 6.6-7.1) (Figure. 3c). Thus, whether lower pH levels in the warming plots (Tian et al., 2023a) can potentially enhance the desorption of mineral-associated MNC remains to be demonstrated. In addition, increased root biomass triggered by soil warming may enhance MNC decomposition through greater root activity and a 30% rise in root exudation, especially organic acids that can release carbon from mineral-bound MNC (Heinzle et al., 2023; Keiluweit et al., 2015; Kwatcho Kengdo et al., 2023; Kwatcho Kengdo et al., 2022). Organic acid exudation potentially accelerates MNC breakdown by stimulating rhizosphere priming processes (Buckeridge et al., 2022a; Kästner et al., 2021; Keiluweit et al., 2015).

**Warming reduced the microbial necromass carbon contribution to SOC**

In our study, the MNC contribution to SOC was found to decrease from 34-37% in control plots to 23-33% in warmed plots, with a more significant decline in the 10-20 cm layer compared to the 0-10 cm layer (Figure 2). This suggests that warming accelerated the decomposition of MNC more strongly than that of bulk soil organic matter. This phenomenon is likely influenced by multiple factors such as enhanced microbial mining of MNC for nutrients coupled with increased turnover rates of amino sugars and increased plant C inputs via root turnover leading to more plant-derived organic matter, which partly offset SOC losses. Firstly, as mentioned above, soil microbes in control plots were limited by C, which shifted towards C-P colimitation after 14 years of soil warming (Shi et al., 2023). In the context of nutrient scarcity, living microbes accelerate the mining of microbial necromass as a source of C and N (and P), due to its high proportions of lipids and proteins (Cui et al., 2020; Kögel-Knabner, 2002), and of nucleic acids (Makino et al., 2003). This process may consequently increase the turnover rate of microbial necromass biomarkers, such as amino sugars. For example, the turnover rate of the amino sugars was found to be faster under elevated $CO_2$ (Glaser et al., 2006). Secondly, our previous studies have confirmed enhanced plant root C input in warming plots, due to increased root growth/turnover and root exudation (Heinzle et al., 2023; Kwatcho Kengdo et al., 2023; Kwatcho Kengdo et al., 2022), indicating

a shift in the balance of plant- versus microbial-derived SOM under climate warming. Complementing this, Feng et al. (2008) reported an increased accumulation of cutin monomers in a mixed temperate forest in southern Ontario, Canada, due to enhanced litter degradation under warming. Consequently, the assumption that MNC belongs to the stable SOM pool under climate warming is challenged, despite its contribution of more than 30% to SOC in our study (Figure 2). Regardless, these findings align with the concept that the stability of SOC is not an inherent trait, but rather depends on ecosystem properties that vary with soil depth. This study offers essential insights into understanding the long-term fate of MNC relevant to C sequestration strategies.

There is evidence that warming preferentially increased the decomposition of BNC fractions in SOC compared to FNC at 0-10 cm depth. This can be attributed to the following reasons: First, in comparison to fungal necromass, which typically has an average C:N ratio of 10, microbes preferentially use bacterial necromass (average C:N of 4) (Paul, 2014). Bacterial necromass thus constitutes a more nutrient-rich resource (including N and P), making it nutritionally favorable for microbial growth (Paul, 2014; Sinsabaugh et al., 2016). Secondly, fungal cell walls are made from chitin and often have relatively high contents of melanin (Fernandez & Koide, 2014), a relatively recalcitrant organic compound class (Buckeridge et al., 2022a; Joergensen, 2018). These components can make fungal cell walls more resistant to decomposition in soils compared to bacterial cell walls. BNC accounted for approximately 30% of MNC in this study (Figure. 2). As a result, a decrease in BNC content, such as the observed 32% decline in the warming plots, would have a significant impact on its contribution to SOC.

**Conclusion**

Collectively, our results indicate that 14 years of soil warming at +4 °C in a temperate forest has significantly reduced the MNC content and its contribution to SOC, which is linked to changes in microbial traits, soil P availability, and EEA. Specifically, our results suggest that the reduction in MNC due to long-term soil warming is primarily attributed to a decrease in its production and an increase in its decomposition, driven by reduced soil available P limiting microbial biomass biosynthesis and CUE, coupled with enhanced soil EEA

indicating accelerated MNC decomposition. This demonstrates a decoupling of MNC production and decomposition, which represents a potential mechanism for reduced accumulation of MNC in temperate forest soil in a warming world. Overall, this is the first evidence of a causal link between microbial physiology, soil nutrient availability, soil enzymes and MNC dynamics in the context of climate warming.

## Conflict of interest

The authors have no conflicts of interest to declare.


## Funding

This study was funded by the Austrian Science Fund (FWF; project I 3745) and China Scholarship Council (CSC) Grant (202008350128).

## Acknowledgements

We sincerely thank Christian Holtermann for his invaluable contributions to maintaining the soil warming system in the field site.


## Author contributions

WW, AS, and WB designed the study. XF, JH, YT, SKK, WW, AS, and WB implemented the field experiment. XF, ES, and WW conducted the lab experiment. XF performed data analysis and wrote the manuscript, with the contributions of all co-authors.

## Reference


Adams, M. B., Kelly, C., Kabrick, J., & Schuler, J. (2019). Chapter 6 - Temperate forests and soils. In M. Busse, C. P. Giardina, D. M. Morris, & D. S. Page-Dumroese (Eds.), *Developments in Soil Science* (Vol. 36, pp. 83-108): Elsevier.

Appuhn, A., & Joergensen, R. G. (2006). Microbial colonisation of roots as a function of plant species. *Soil Biology and Biochemistry, 38*(5), 1040-1051. https://doi.org/10.1016/j.soilbio.2005.09.002

Bai, E., Li, S., Xu, W., Li, W., Dai, W., & Jiang, P. (2013). A meta-analysis of experimental warming effects on terrestrial nitrogen pools and dynamics. *New Phytologist, 199*(2), 431-440. https://doi.org/10.1111/nph.12252

Bonan, G. B. (2008). Forests and climate change: forcings, feedbacks, and the climate benefits of forests. *Science, 320*(5882), 1444-1449. doi:10.1126/science.1155121

Buckeridge, K. M., Creamer, C., & Whitaker, J. (2022a). Deconstructing the microbial necromass continuum to inform soil carbon sequestration. *Functional Ecology, 36*(6), 1396-1410. doi:10.1111/1365-2435.14014

Buckeridge, K. M., Mason, K. E., Ostle, N., McNamara, N. P., Grant, H. K., & Whitaker, J. (2022b). Microbial necromass carbon and nitrogen persistence are decoupled in agricultural grassland soils. *Communications Earth & Environment, 3*(1), 114. doi:10.1038/s43247-022-00439-0

Cai, M., Zhao, G., Zhao, B., Cong, N., Zheng, Z., Zhu, J., . . . Zhang, Y. (2023). Climate warming alters the relative importance of plant root and microbial community in regulating the accumulation of soil microbial necromass carbon in a Tibetan alpine meadow. *Global Change Biology, 29*(11), 3193-3204. doi:10.1111/gcb.16660

Camenzind, T., Mason-Jones, K., Mansour, I., Rillig, M. C., & Lehmann, J. (2023). Formation of necromass-derived soil organic carbon determined by microbial death pathways. *Nature Geoscience, 16*(2), 115-122. doi:10.1038/s41561-022-01100-3

Cao, Y. F., Ding, J. Z., Li, J., Xin, Z. M., Ren, S., & Wang, T. (2023). Necromass-derived soil organic carbon and its drivers at the global scale. *Soil Biology and Biochemistry, 181*, 109025. doi: 10.1016/j.soilbio.2023.109025

Chen, J., Luo, Y., Garcia-Palacios, P., Cao, J., Dacal, M., Zhou, X., . . . van Groenigen, K. J. (2018). Differential responses of carbon-degrading enzyme activities to warming: Implications for soil respiration. *Global Change Biology, 24*(10), 4816-4826. doi:10.1111/gcb.14394

Cotrufo, M. F., Wallenstein, M. D., Boot, C. M., Denef, K., & Paul, E. (2013). The Microbial Efficiency-Matrix Stabilization (MEMS) framework integrates plant litter decomposition with soil organic matter stabilization: do labile plant inputs form stable soil organic matter? *Global Change Biology, 19*(4), 988-995. doi:https://doi.org/10.1111/gcb.12113

Craig, M. E., Geyer, K. M., Beidler, K. V., Brzostek, E. R., Frey, S. D., Stuart Grandy, A., . . . Phillips, R. P. (2022). Fast-decaying plant litter enhances soil carbon in temperate forests but not through microbial physiological traits. *Nature Communications, 13*(1), 1229. doi:10.1038/s41467-022-28715-9

Cui, J., Zhu, Z. K., Xu, X. L., Liu, S. L., Jones, D. L., Kuzyakov, Y., . . . Ge, T. D. (2020). Carbon and nitrogen recycling from microbial necromass to cope with C:N stoichiometric imbalance by priming. *Soil Biology and Biochemistry, 142*, 107720. doi:10.1016/j.soilbio.2020.107720

D'Angelo, E., Crutchfield, J., & Vandiviere, M. (2001). Rapid, Sensitive, Microscale Determination of Phosphate in Water and Soil. *Journal of Environmental Quality, 30*(6), 2206-2209. doi: 10.2134/jeq2001.2206

Ding, X. L., Chen, S. Y., Zhang, B., Liang, C., He, H. B., & Horwath, W. R. (2019). Warming increases microbial residue contribution to soil organic carbon in an alpine meadow. *Soil Biology and Biochemistry, 135*, 13-19. doi:10.1016/j.soilbio.2019.04.004

Donhauser, J., Qi, W., Bergk-Pinto, B., & Frey, B. (2021). High temperatures enhance the microbial genetic potential to recycle C and N from necromass in high-mountain soils. *Global Change Biology, 27*(7), 1365-1386. doi:10.1111/gcb.15492

Fanin, N., Mooshammer, M., Sauvadet, M., Meng, C., Alvarez, G., Bernard, L., . . . Nottingham, A. T. (2022). Soil enzymes in response to climate warming: Mechanisms and feedbacks. *Functional Ecology, 36*(6), 1378-1395. doi:10.1111/1365-2435.14027

Feng, X., Simpson, A. J., Wilson, K. P., Dudley Williams, D., & Simpson, M. J. (2008). Increased cuticular carbon sequestration and lignin oxidation in response to soil warming. *Nature Geoscience*, 1(12), 836-839. doi:10.1038/ngeo361

Fernandez, C. W., & Koide, R. T. (2014). Initial melanin and nitrogen concentrations control the decomposition of ectomycorrhizal fungal litter. *Soil Biology and Biochemistry, 77*, 150-157. doi: 10.1016/j.soilbio.2014.06.026

German, D. P., Marcelo, K. R. B., Stone, M. M., & Allison, S. D. (2012). The Michaelis–Menten kinetics of soil extracellular enzymes in response to temperature: a cross-latitudinal study. *Global Change Biology, 18*(4), 1468-1479. doi: 10.1111/j.1365-2486.2011.02615.x

Glaser, B., Millar, N., & Blum, H. (2006). Sequestration and turnover of bacterial- and fungal-derived carbon in a temperate grassland soil under long-term elevated atmospheric $pCO_2$. *Global Change Biology*, 12(8), 1521-1531. doi:10.1111/j.1365-2486.2006.01186.x

Heinzle, J., Liu, X. F., Tian, Y., Kengdo, S. K., Heinze, B., Nirschi, A., . . . Schindlbacher, A. (2023). Increase in fine root biomass enhances root exudation by long-term soil warming in a temperate forest. *Frontiers in Forests and Global Change, 6*. doi:10.3389/ffgc.2023.1152142

Jia, S. X., Liu, X. F., Lin, W. S., Li, X. J., Yang, L. M., Sun, S. Y., . . . Yang, Y. S. (2022). Tree roots exert greater influence on soil microbial necromass carbon than above-ground litter in subtropical natural and plantation forests. *Soil Biology and Biochemistry, 173*, 108811. doi: 10.1016/j.soilbio.2022.108811

Joergensen, R. G. (1996). The fumigation-extraction method to estimate soil microbial biomass: calibration of the k EC value. *Soil Biology and Biochemistry, 28*(1), 25-31. https://doi.org/10.1016/0038-0717(95)00102-6

Joergensen, R. G. (2018). Amino sugars as specific indices for fungal and bacterial residues in soil. *Biology and Fertility of Soils, 54*(5), 559-568. doi:10.1007/s00374-018-1288-3

Kaiser, C., Koranda, M., Kitzler, B., Fuchslueger, L., Schnecker, J., Schweiger, P., . . . Richter, A. (2010). Belowground carbon allocation by trees drives seasonal patterns of extracellular enzyme activities by altering microbial community composition in a beech forest soil. *New Phytologist, 187*(3), 843-858. doi:https://doi.org/10.1111/j.1469-8137.2010.03321.x

Kallenbach, C. M., Frey, S. D., & Grandy, A. S. (2016). Direct evidence for microbial-derived soil organic matter formation and its ecophysiological controls. *Nature Communications, 7*(1), 13630. doi:10.1038/ncomms13630

Kallenbach, C. M., Grandy, A. S., Frey, S. D., & Diefendorf, A. F. (2015). Microbial physiology and necromass regulate agricultural soil carbon accumulation. *Soil Biology and Biochemistry, 91*, 279-290. doi:10.1016/j.soilbio.2015.09.005

Kästner, M., Miltner, A., Thiele-Bruhn, S., & Liang, C. (2021). Microbial Necromass in Soils—Linking Microbes to Soil Processes and Carbon Turnover. *Frontiers in Environmental Science, 9*. doi:10.3389/fenvs.2021.756378

Keiluweit, M., Bougoure, J. J., Nico, P. S., Pett-Ridge, J., Weber, P. K., & Kleber, M. (2015). Mineral protection of soil carbon counteracted by root exudates. *Nature Climate Change, 5*(6), 588-595. doi:DOI 10.1038/nclimate2580

Koch, O., Tscherko, D., & Kandeler, E. (2007). Temperature sensitivity of microbial respiration, nitrogen mineralization, and potential soil enzyme activities in organic alpine soils. *Global Biogeochemical Cycles, 21*(4). doi.org/10.1029/2007GB002983

Kögel-Knabner, I. (2002). The macromolecular organic composition of plant and microbial residues as inputs to soil organic matter. *Soil Biology and Biochemistry*, 34(2), 139-162. doi.org/10.1016/S0038-0717(01)00158-4

Kuo, S. (1996). Phosphorus. In *Methods of Soil Analysis* (pp. 869-919).

Kuypers, M. M. M., Marchant, H. K., & Kartal, B. (2018). The microbial nitrogen-cycling network. *Nature Reviews Microbiology, 16*(5), 263-276. doi:10.1038/nrmicro.2018.9

Kwatcho Kengdo, S., Persoh, D., Schindlbacher, A., Heinzle, J., Tian, Y., Wanek, W., & Borken, W. (2022). Long-term soil warming alters fine root dynamics and morphology, and their ectomycorrhizal fungal community in a temperate forest soil. *Global Change Biology, 28*(10), 3441-3458. doi:10.1111/gcb.16155

Kwatcho Kengdo, S., Ahrens, B., Tian, Y., Heinzle, J., Wanek, W., Schindlbacher, A., & Borken, W. (2023). Increase in carbon input by enhanced fine root turnover in a long-term warmed forest soil. *Science of the Total Environment, 855*, 158800. doi:10.1016/j.scitotenv.2022.158800

Lal, R. (2005). Forest soils and carbon sequestration. *Forest Ecology and Management, 220*(1), 242-258. doi.org/10.1016/j.foreco.2005.08.015

Liang, C., Amelung, W., Lehmann, J., & Kastner, M. (2019). Quantitative assessment of microbial necromass contribution to soil organic matter. *Global Change Biology, 25*(11), 3578-3590. doi:10.1111/gcb.14781

Liang, C., & Balser, T. C. (2012). Warming and nitrogen deposition lessen microbial residue contribution to soil carbon pool. *Nature Communications, 3*, 1222. doi:10.1038/ncomms2224

Liang, C., Gutknecht, J. L., & Balser, T. C. (2015). Microbial lipid and amino sugar responses to long-term simulated global environmental changes in a California annual grassland. *Frontiers in microbiology, 6*, 385. doi:10.3389/fmicb.2015.00385

Liu, L., Gundersen, P., Zhang, T., & Mo, J. (2012). Effects of phosphorus addition on soil microbial biomass and community composition in three forest types in tropical China. *Soil Biology and Biochemistry, 44*(1), 31-38. doi:10.1016/j.soilbio.2011.08.017

Luo, R., Kuzyakov, Y., Zhu, B., Qiang, W., Zhang, Y., & Pang, X. (2022). Phosphorus addition decreases plant lignin but increases microbial necromass contribution to soil organic carbon in a subalpine forest. *Global Change Biology, 28*(13), 4194-4210. doi:10.1111/gcb.16205

Ma, T., Yang, Z. Y., Shi, B. W., Gao, W. J., Li, Y. F., Zhu, J. X., & He, J. S. (2023). Phosphorus supply suppressed microbial necromass but stimulated plant lignin phenols accumulation in soils of alpine grassland on the Tibetan Plateau. *Geoderma, 431*, 116376. doi: 10.1016/j.geoderma.2023.116376

Makino, W., Cotner, J. B., Sterner, R. W., & Elser, J. J. (2003). Are bacteria more like plants or animals? Growth rate and resource dependence of bacterial C : N : P stoichiometry. Functional Ecology, 17(1), 121-130. doi.org/10.1046/j.1365-2435.2003.00712.x

Melillo, J. M., Frey, S. D., DeAngelis, K. M., Werner, W. J., Bernard, M. J., Bowles, F. P., . . . Grandy, A. S. (2017). Long-term pattern and magnitude of soil carbon feedback to the climate system in a warming world. *Science, 358*(6359), 101-105. doi:10.1126/science.aan2874

Metcalfe, D. B. (2017). Microbial change in warming soils. *Science, 358*(6359), 41-42. doi: 10.1126/science.aap7325

Paul, E. A. (2014). *Soil microbiology, ecology and biochemistry*: Academic press.

Prommer, J., Walker, T. W. N., Wanek, W., Braun, J., Zezula, D., Hu, Y., . . . Richter, A. (2020). Increased microbial growth, biomass, and turnover drive soil organic carbon accumulation at higher plant diversity. *Global Change Biology, 26*(2), 669-681. doi:10.1111/gcb.14777

Purcell, A. M., Hayer, M., Koch, B. J., Mau, R. L., Blazewicz, S. J., Dijkstra, P., . . . Hungate, B. A. (2022). Decreased growth of wild soil microbes after 15 years of transplant-induced warming in a montane meadow. *Global Change Biology, 28*(1), 128-139. doi:10.1111/gcb.15911

Romero-Olivares, A., Allison, S., & Treseder, K. (2017). Soil microbes and their response to experimental warming over time: A meta-analysis of field studies. *Soil Biology and Biochemistry, 107*, 32-40.

Rowland, A. P., & Haygarth, P. M. (1997). Determination of Total Dissolved Phosphorus in Soil Solutions. *Journal of environmental quality, 26*(2), 410-415. doi.org/10.2134/jeq1997.00472425002600020011x

Salas, E., Gorfer, M., Bandian, D., Wang, B., Kaiser, C., & Wanek, W. (2023). A rapid and sensitive assay to quantify amino sugars, neutral sugars and uronic acid necromass biomarkers using pre-column derivatization, ultra-high-performance liquid chromatography and high-resolution mass spectrometry. *Soil Biology and Biochemistry, 177*, 108927. doi:10.1016/j.soilbio.2022.108927

Schindlbacher, A., Schnecker, J., Takriti, M., Borken, W., & Wanek, W. (2015). Microbial physiology and soil CO2 efflux after 9 years of soil warming in a temperate forest - no indications for thermal adaptations. *Global Change Biology, 21*(11), 4265-4277. doi:10.1111/gcb.12996

Seidl, R., Thom, D., Kautz, M., Martin-Benito, D., Peltoniemi, M., Vacchiano, G., . . . Reyer, C. P. O. (2017). Forest disturbances under climate change. *Nature Climate Change, 7*(6), 395-402. doi:10.1038/nclimate3303

Shi, C., Urbina-Malo, C., Tian, Y., Heinzle, J., Kwatcho Kengdo, S., Inselsbacher, E., . . . Wanek, W. (2023). Does long-term soil warming affect microbial element limitation? A test by short-term assays of microbial growth responses to labile C, N and P additions. *Global Change Biology, 29*(8), 2188-2202. doi:10.1111/gcb.16591

Shi, K., Liao, J., Zou, X., Chen, H. Y. H., Delgado-Baquerizo, M., Yan, Z., . . . Ruan, H. (2024). Accumulation of soil microbial extracellular and cellular residues during forest rewilding: Implications for soil carbon stabilization in older plantations. *Soil Biology and Biochemistry*, 188, 109250. doi: 10.1016/j.soilbio.2023.109250

Shiraishi, T., Yokota, S., Fukiya, S., & Yokota, A. (2016). Structural diversity and biological significance of lipoteichoic acid in Gram-positive bacteria: focusing on beneficial probiotic lactic acid bacteria. *Bioscience of Microbiota, Food and Health*, 35(4), 147-161. doi:10.12938/bmfh.2016-006

Siebers, N., Sumann, M., Kaiser, K., & Amelung, W. (2017). Climatic Effects on Phosphorus Fractions of Native and Cultivated North American Grassland Soils. *Soil Science Society of America Journal, 81*(2), 299-309. doi: 10.2136/sssaj2016.06.0181

Silva-Sánchez, A., Soares, M., & Rousk, J. (2019). Testing the dependence of microbial growth and carbon use efficiency on nitrogen availability, pH, and organic matter quality. *Soil Biology and Biochemistry, 134*, 25-35. doi:10.1016/j.soilbio.2019.03.008

Sinsabaugh, R. L., Turner, B. L., Talbot, J. M., Waring, B. G., Powers, J. S., Kuske, C. R., . . . Follstad Shah, J. J. (2016). Stoichiometry of microbial carbon use efficiency in soils. *Ecological Monographs, 86*(2), 172-189. https://doi.org/10.1890/15-2110.1

Soares, M., & Rousk, J. (2019). Microbial growth and carbon use efficiency in soil: Links to fungal-bacterial dominance, SOC-quality and stoichiometry. *Soil Biology and Biochemistry, 131*, 195-205. doi:10.1016/j.soilbio.2019.01.010

Spohn, M., Klaus, K., Wanek, W., & Richter, A. (2016). Microbial carbon use efficiency and biomass turnover times depending on soil depth-Implications for carbon cycling. *Soil Biology and Biochemistry, 96*, 74-81. doi:10.1016/j.soilbio.2016.01.016

Tian, Y., Schindlbacher, A., Malo, C. U., Shi, C., Heinzle, J., Kwatcho Kengdo, S., . . . Wanek, W. (2023a). Long-term warming of a forest soil reduces microbial biomass and its carbon and nitrogen use efficiencies. *Soil Biology and Biochemistry, 184*, 109109. doi.org/10.1016/j.soilbio.2023.109109

Tian, Y., Shi, C., Malo, C. U., Kwatcho Kengdo, S., Heinzle, J., Inselsbacher, E., . . . Wanek, W. (2023b). Long-term soil warming decreases microbial phosphorus utilization by increasing abiotic phosphorus sorption and phosphorus losses. *Nature Communications, 14*(1), 864. doi:10.1038/s41467-023-36527-8

Vance, E., Brookes, P., & Jenkinson, D. (1987). An extraction method for measuring soil microbial biomass C. *Soil Biology and Biochemistry, 19*(6), 703-707. https://doi.org/10.1016/0038-0717(87)90052-6

Walker, T. W. N., Kaiser, C., Strasser, F., Herbold, C. W., Leblans, N. I. W., Woebken, D., . . . Richter, A. (2018). Microbial temperature sensitivity and biomass change explain soil carbon loss with warming. *Nature Climate Change, 8*(10), 885-889. doi:10.1038/s41558-018-0259-x

Walton, C. R., Ewens, S., Coates, J. D., Blake, R. E., Planavsky, N. J., Reinhard, C., . . . Pasek, M. A. (2023). Phosphorus availability on the early Earth and the impacts of life. *Nature geoscience, 16*(5), 399-409. doi:10.1038/s41561-023-01167-6

Wang, B. R., An, S. S., Liang, C., Liu, Y., & Kuzyakov, Y. (2021a). Microbial necromass as the source of soil organic carbon in global ecosystems. Soil Biology and Biochemistry, 162, 108422. doi:10.1016/j.soilbio.2021.108422

Wang, C., Qu, L., Yang, L., Liu, D., Morrissey, E., Miao, R., . . . Bai, E. (2021b). Large-scale importance of microbial carbon use efficiency and necromass to soil organic carbon. *Global Change Biology, 27*(10), 2039-2048. doi:10.1111/gcb.15550

Wang, C., Wang, X., Pei, G. T., Xia, Z. W., Peng, B., Sun, L. F., . . . Bai, E. (2020). Stabilization of microbial residues in soil organic matter after two years of decomposition. *Soil Biology and Biochemistry, 141*, 107687. doi:10.1016/j.soilbio.2019.107687

Whalen, E. D., Grandy, A. S., Sokol, N. W., Keiluweit, M., Ernakovich, J., Smith, R. G., & Frey, S. D. (2022). Clarifying the evidence for microbial- and plant-derived soil organic matter, and the path toward a more quantitative understanding. *Global Change Biology, 28*(24), 7167-7185. doi:10.1111/gcb.16413

Yuan, Y., Li, Y., Mou, Z., Kuang, L., Wu, W., Zhang, J., . . . Liu, Z. (2021). Phosphorus addition decreases microbial residual contribution to soil organic carbon pool in a tropical coastal forest. *Global Change Biology, 27*(2), 454-466. doi:10.1111/gcb.15407

Zhang, Q., Qin, W., Feng, J., & Zhu, B. (2022). Responses of soil microbial carbon use efficiency to warming: Review and prospects. *Soil Ecology Letters, 4*(4), 307-318. doi:10.1007/s42832-022-0137-3

Zhang, X. D., & Amelung, W. (1996). Gas chromatographic determination of muramic acid, glucosamine, mannosamine, and galactosamine in soils. *Soil Biology and Biochemistry, 28*(9), 1201-1206. doi:Doi 10.1016/0038-0717(96)00117-4

Zheng, Q., Hu, Y., Zhang, S., Noll, L., Bockle, T., Richter, A., & Wanek, W. (2019). Growth explains microbial carbon use efficiency across soils differing in land use and geology. *Soil Biology and Biochemistry, 128*, 45-55. doi:10.1016/j.soilbio.2018.10.006

**Table 1** Results of three-way ANOVA analysis of the factors warming, soil depth, and season on microbial (fungal and bacterial) necromass carbon, its components, and fungi to bacterial necromass ratios

| | BNC | | FNC | | MNC | | FNC/BNC | |
|---|---|---|---|---|---|---|---|---|
| | F | P | F | P | F | P | F | P |
| Warming | 28.708 | **<0.001** | 6.105 | **0.016** | 24.644 | **<0.001** | 0.795 | 0.376 |
| Season | 4.474 | **0.015** | 65.611 | **<0.001** | 70.563 | **<0.001** | 18.224 | **<0.001** |
| Depth | 1.479 | 0.228 | 18.376 | **<0.001** | 20.301 | **<0.001** | 6.107 | **0.016** |
| Warming×Season | 1.347 | 0.267 | 0.071 | 0.931 | 0.492 | 0.614 | 1.133 | 0.328 |
| Warming×Depth | 0.430 | 0.514 | 8.002 | **0.006** | 4.981 | **0.029** | 3.176 | 0.079 |
| Season×Depth | 7.484 | **0.001** | 10.684 | **<0.001** | 11.382 | **<0.001** | 6.423 | **0.003** |
| Warming×Season×Depth | 0.258 | 0.773 | 2.238 | 0.115 | 1.706 | 0.189 | 1.469 | 0.237 |

Note: BNC, bacterial necromass carbon; FNC, fungi necromass carbon; MNC, microbial necromass carbon.

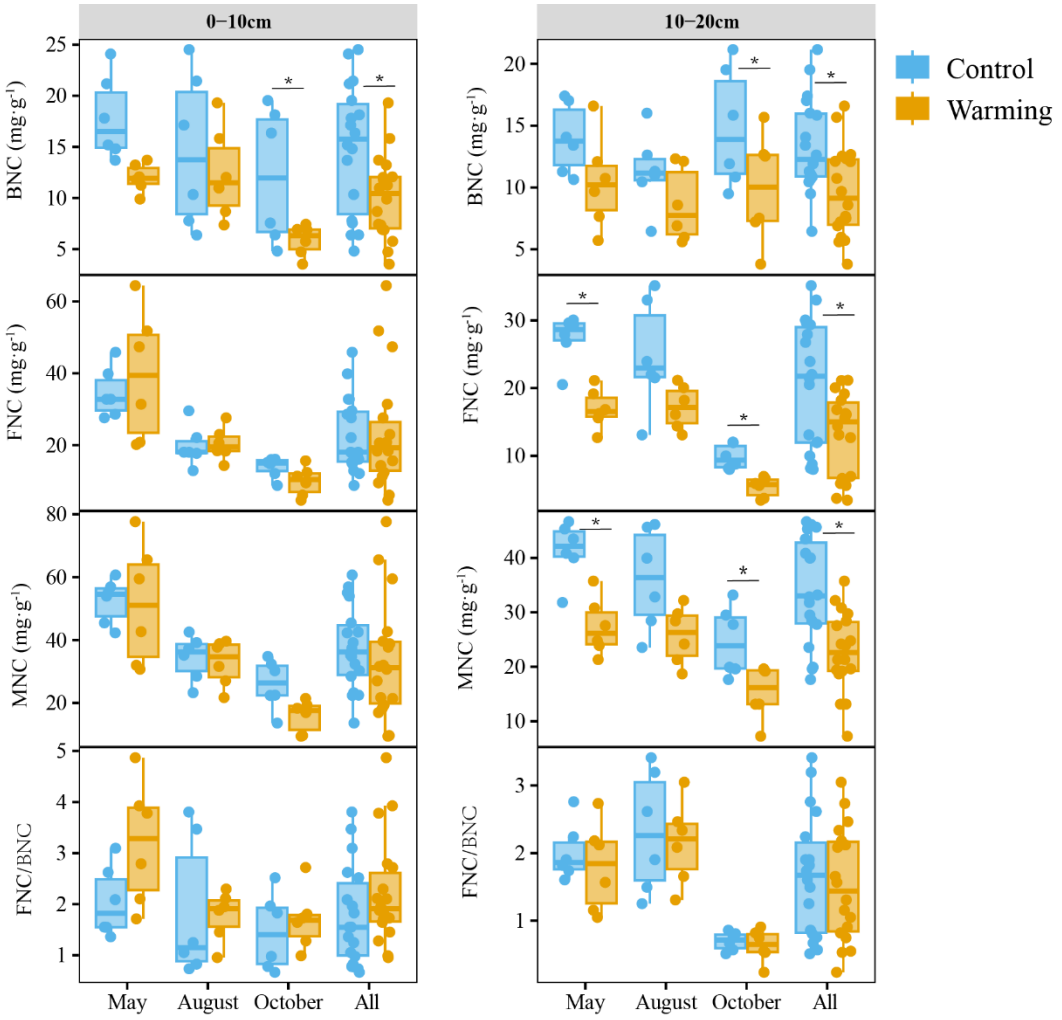


**Figure 1** Content of microbial necromass carbon (MNC), fungal necromass carbon (FNC), bacterial necromass carbon (BNC), and the ratio of FNC to BNC in the control and warming plots at 0-10 cm and 10-20 cm soil depth. Mean indicates the average of the corresponding data in May, August, and October. The lines inside the boxes represent the median values, while the box edges indicate the 25th and 75th percentiles (n=6). The whiskers extend up to 1.5 times the interquartile range in both the upper and lower directions. Stars above boxplots indicate significant differences in the control and warming plots at $p < 0.05$.

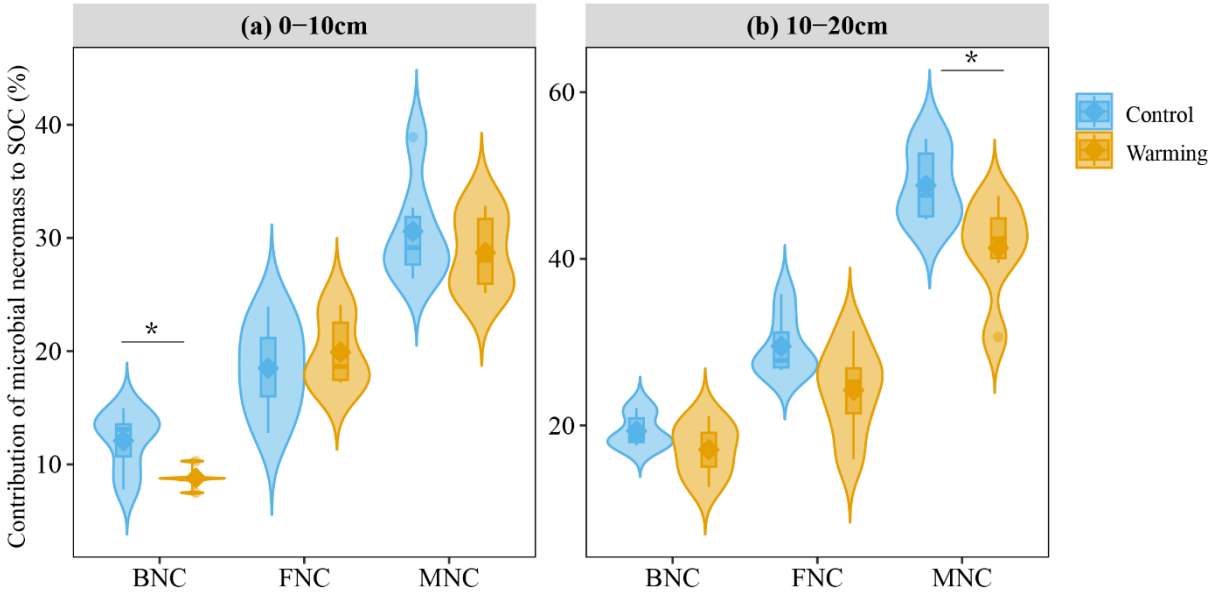


**Figure 2** Contribution of microbial necromass carbon (MNC), fungal necromass carbon (FNC), and bacterial necromass carbon (BNC) to soil organic carbon (SOC) in the control and warming plots at 0-10 cm (a) and 10-20 cm (b) soil depth. The lines inside the boxes represent the median values, while the box edges indicate the 25th and 75th percentiles (n=6). The whiskers extend up to 1.5 times the interquartile range in both the upper and lower directions. The violins represent kernel density plots, visualizing the distribution of the numerical data. Stars above boxplots indicate significant differences in the control and warming plots at $p < 0.05$.

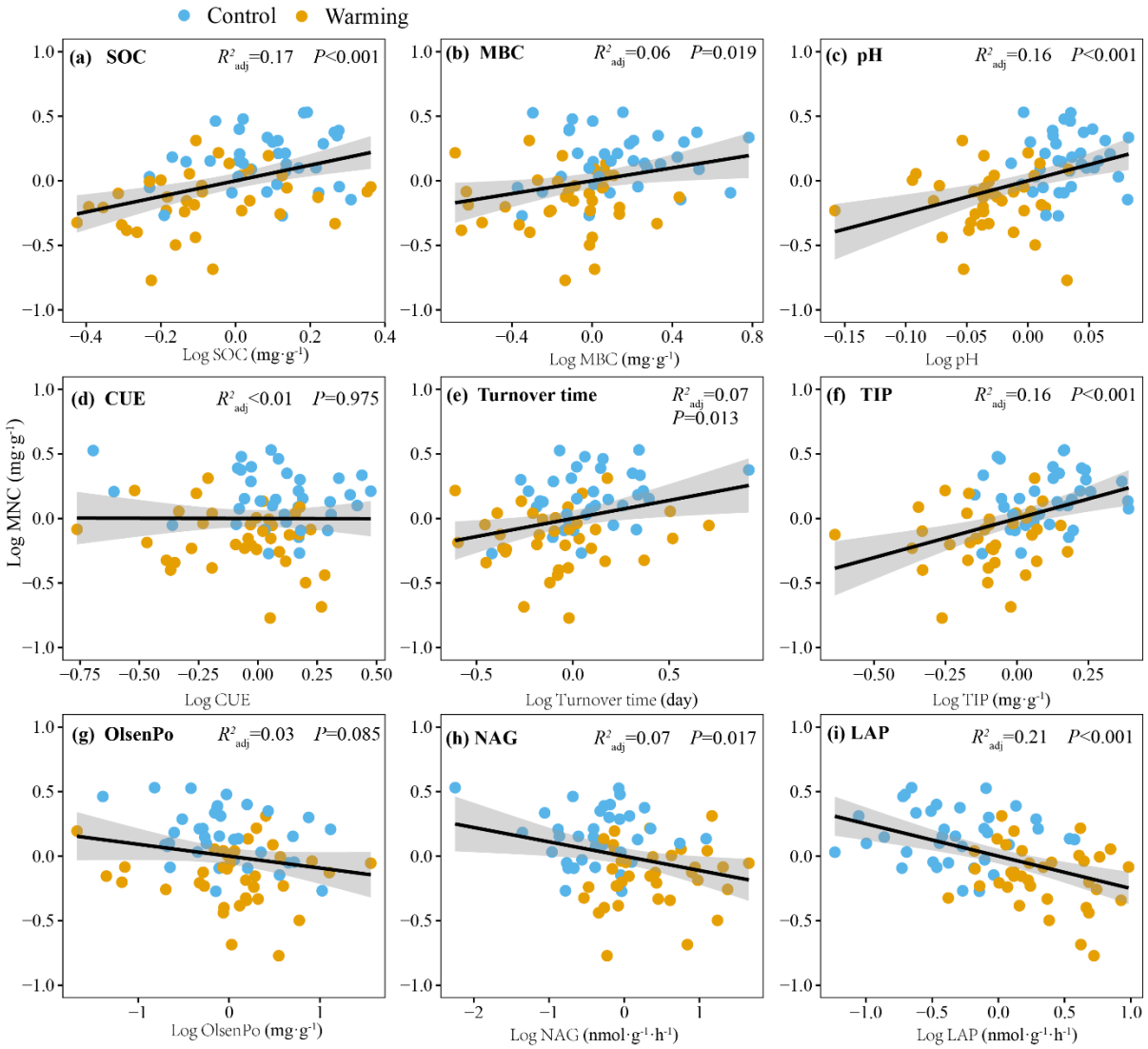


**Figure 3** Partial residual plots of the variability of microbial necromass carbon (MNC) explained by soil pH, microbial traits (MBC, CUE, and turnover time), soil phosphorus (TIP and OlsenPo), and extracellular enzyme activities (NAG and LAP). Partial residual plots permit the evaluation of the effect of warming on a full model after correcting for effects of season, depth, and their interactions. Colored areas indicate 95% confidence intervals. All variables were Log-transformed. Abbreviations: SOC (soil organic carbon), MBC (microbial biomass C), CUE (microbial C use efficiency), TIP (total inorganic P), OlsenPo (Olsen organic P), NAG (N-acetylglucosaminidase), and LAP (leucine-aminopeptidase).

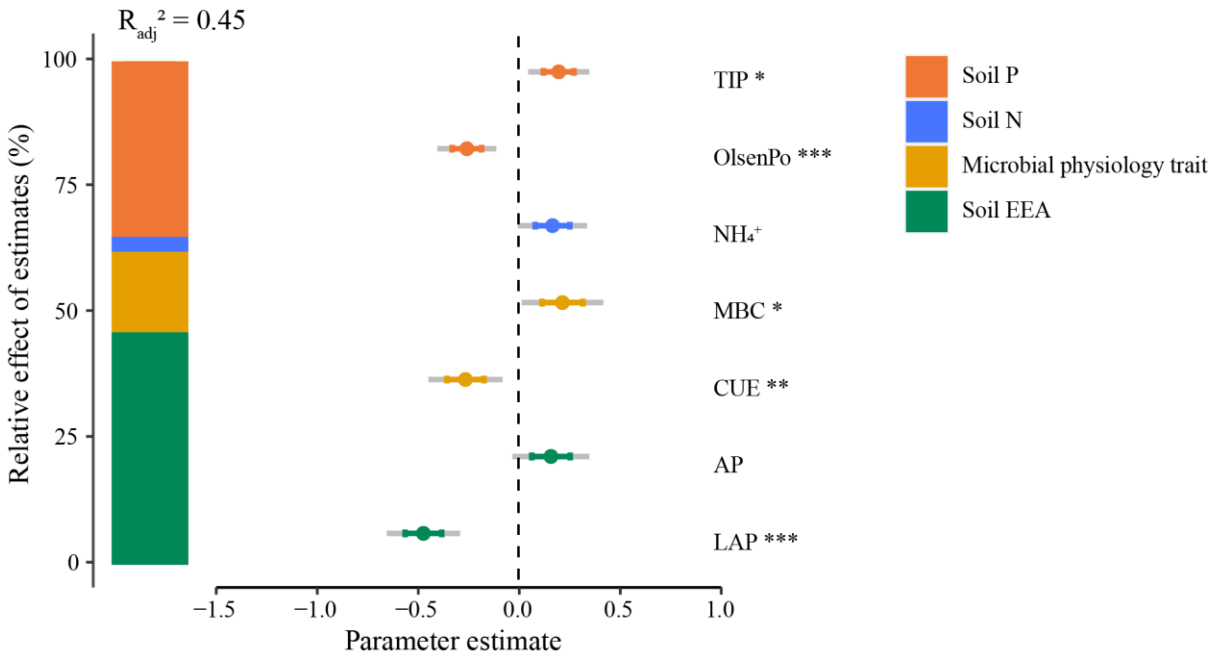


**Figure 4** Relative effects of multiple predictors of MNC. The averaged parameter estimates (standardized regression coefficients) of the model predictors are shown with their associated standard error (n=72, color line) and 95% confidence intervals (gray line) along with the relative importance of each predictor, expressed as the percentage of explained variance. The graph represents the best model selected based on the AICc. The relative effect of the predictors, and their interactions, was calculated as the ratio between the parameter estimate of the predictor and the sum of all parameter estimates, and is expressed as a percentage. Soil N includes $NH_4^+$, $NO_3^-$, and DON; Soil P includes TIP, TOP, OlsenP, and OlsenPi; Microbial traits include MBC, CUE, and turnover time; EEA include AP, BG, and LAP. *P < 0.05; **P < 0.01; ***P < 0.001. Abbreviations: DON (dissolved organic N), TIP (total inorganic P), TOP (total organic P), OlsenPo (Olsen organic P), OlsenPi (Olsen inorganic P), MBC (microbial biomass C), CUE (microbial C use efficiency), AP (acid phosphatase), β-glucosidase (BG), and LAP (leucine-aminopeptidase).

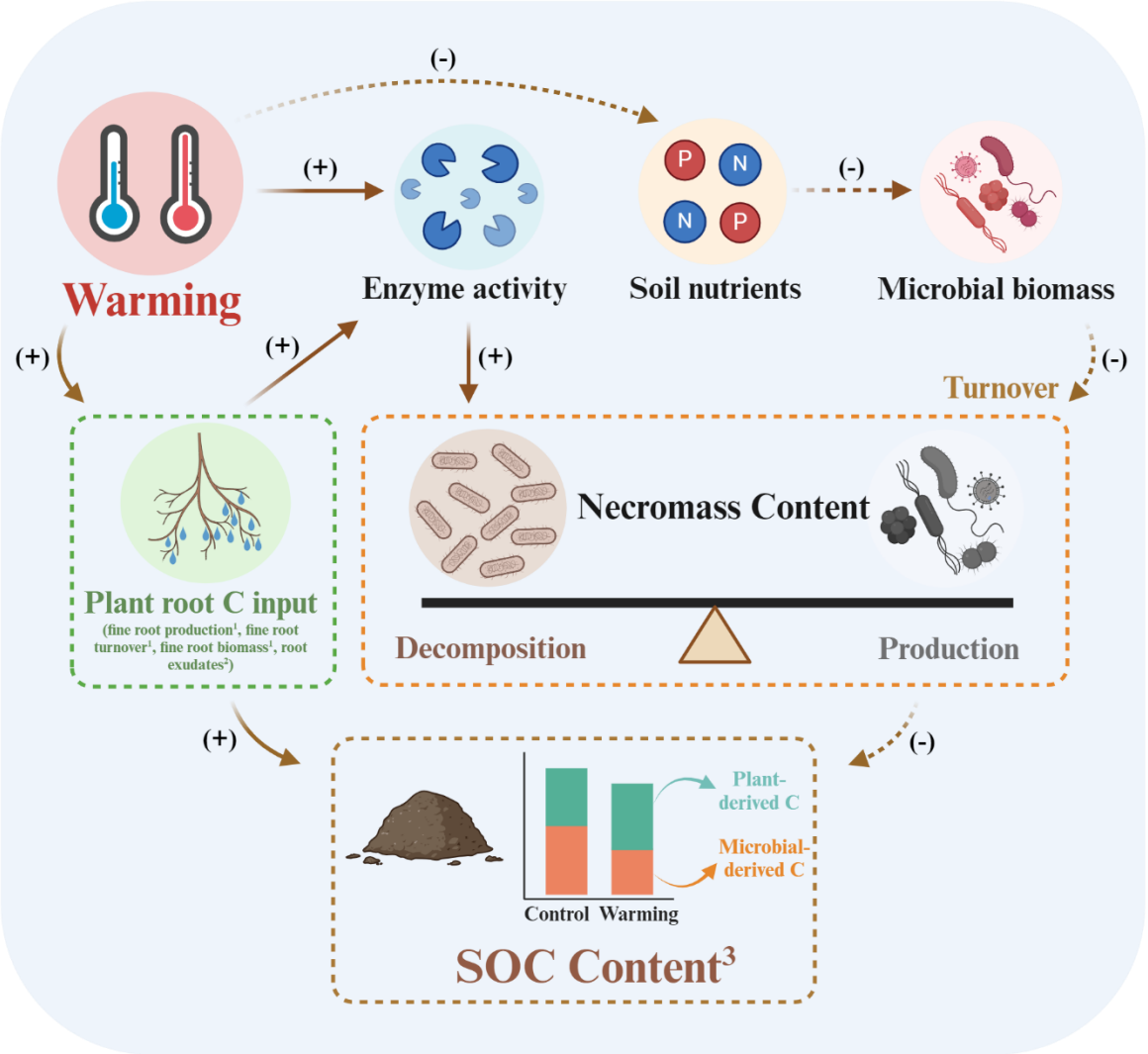


**Figure 5** Conceptual model depicting the mechanisms mediated by microbes, soil nutrients, and enzyme activity that influence the formation and decomposition of microbial necromass carbon (MNC) under long-term warming. The symbols (+) and (-) indicate whether long-term warming has an increasing or decreasing effect on the parameters, respectively. Plant root C input data are from studies conducted at the same site: [1]Kengdo et al. (2022) and [2]Heinzle et al. (2023). Similarly, SOC content data is from studies conducted at the same site: [3]Tian et al. (2023a).

## Supplementary Material

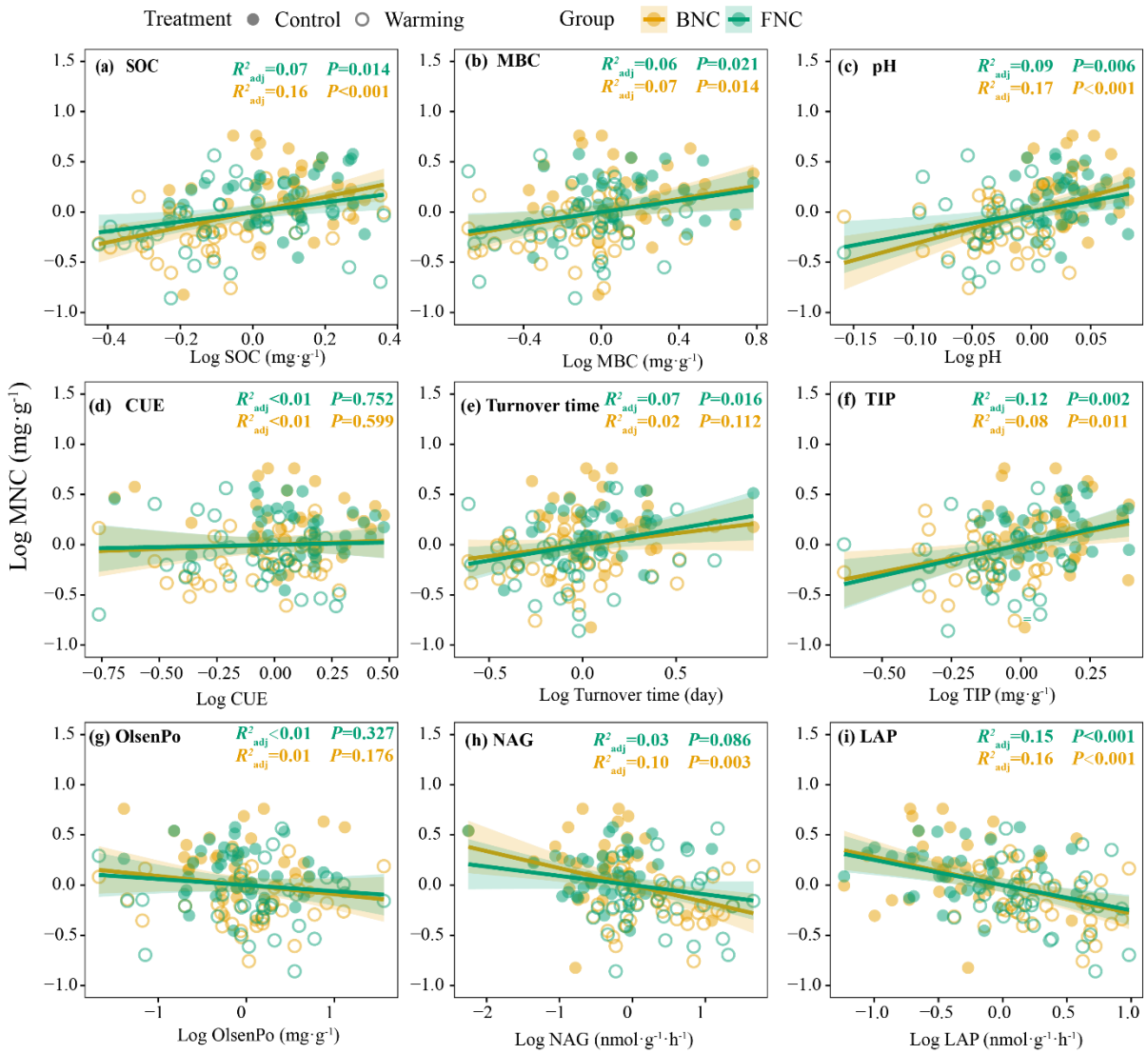


**Figure S1** Partial residual plot of the variability of microbial necromass carbon (FNC and BNC) explained by microbial traits (MBC, CUE, and turnover time), soil phosphorus (TIP and OlsenPo), and extracellular enzyme activities (NAG and LAP). Partial residual plots permit the evaluation of the effect of warming on a full model after correcting for effects of season, depth, and their interactions. Colored areas indicate 95% confidence interval. All variables were Log-transformed. Abbreviations: SOC (soil organic carbon), MBC (microbial biomass C), CUE (microbial C use efficiency), TIP (total inorganic P), OlsenPo (Olsen organic P), NAG (N-acetylglucosaminidase), and LAP (leucine-aminopeptidase).

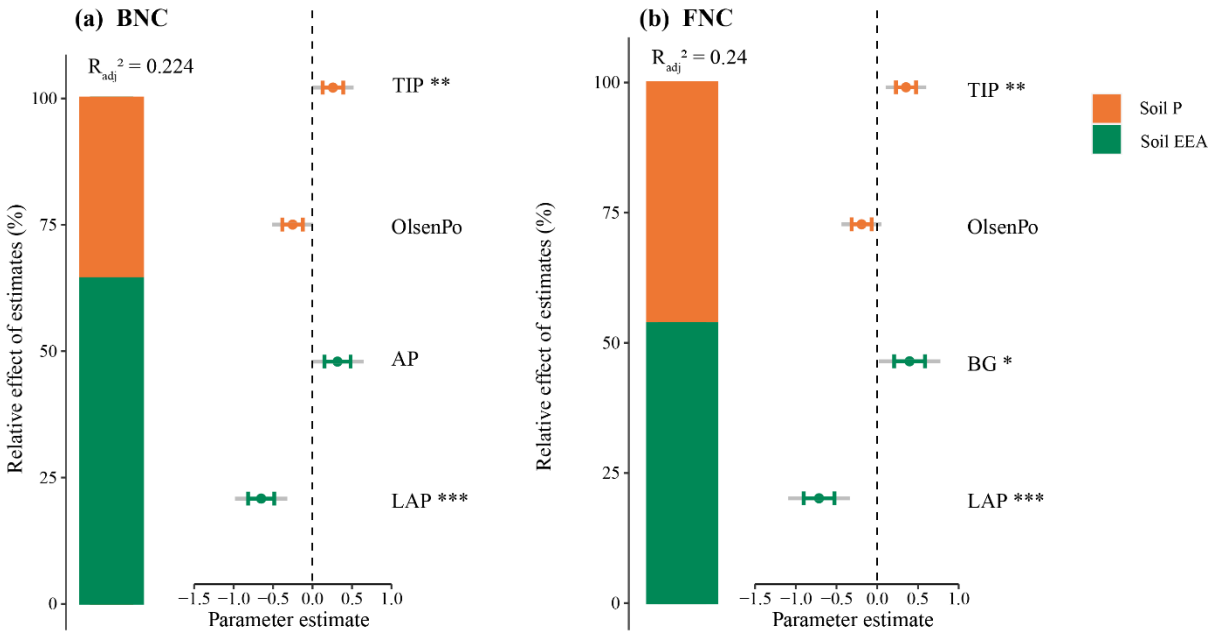


**Figure S2** Relative effects of multiple predictors of BNC (a) and FNC (b). The averaged parameter estimates (standardized regression coefficients) of the model predictors are shown with their associated standard error (n=72, color line) and 95% confidence intervals (gray line) along with the relative importance of each predictor, expressed as the percentage of explained variance. The graph represents the best model selected based on the AICc. The relative effect of the predictors, and their interactions, was calculated as the ratio between the parameter estimate of the predictor and the sum of all parameter estimates, and is expressed as a percentage. Soil P include TIP, TOP, OlsenP, and OlsenPi; EEA include BG, AP, and LAP. *P < 0.05; **P < 0.01; ***P < 0.001. Abbreviations: TIP (total inorganic P), TOP (total organic P), OlsenPo (Olsen organic P), OlsenPi (Olsen inorganic P), AP (acid phosphatase), β-glucosidase (BG), and LAP (leucine-aminopeptidase).

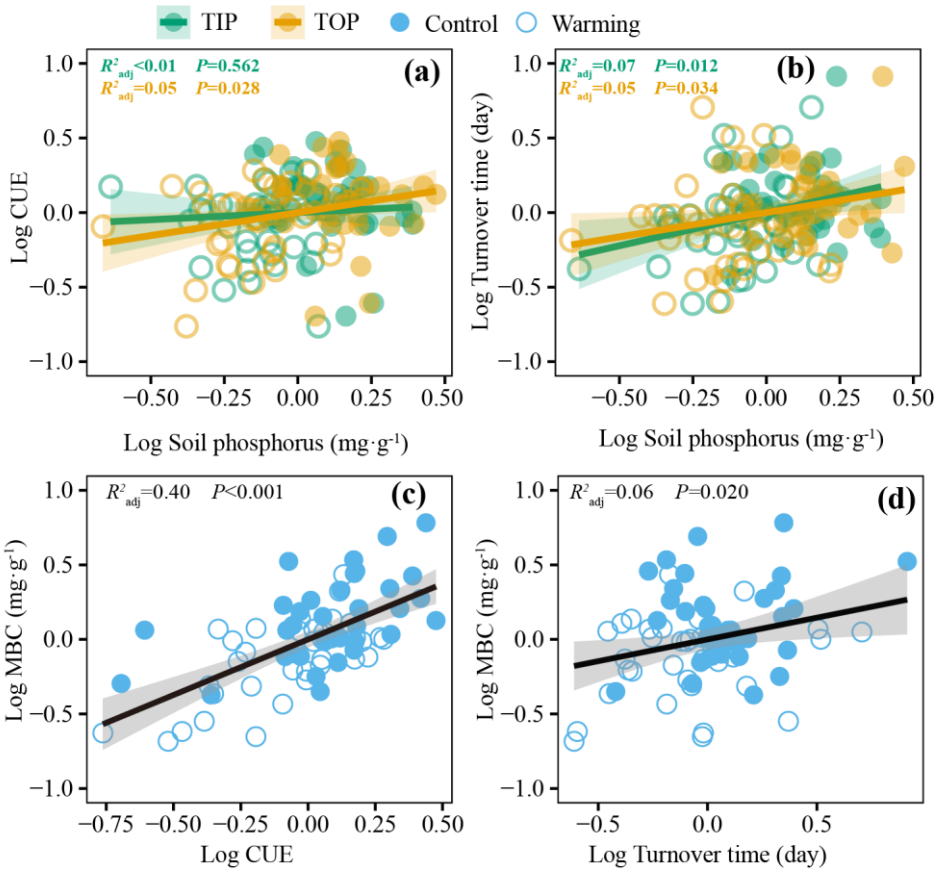


**Figure S3** Relationships between soil P (TIP, TOP) content and CUE (a) and turnover time (b), and relationship between CUE and MBC (c) and turnover time and MBC (d). All variables were Log-transformed. Abbreviations: TIP (total inorganic P), TOP (total organic P), MBC (microbial biomass C), and CUE (microbial C use efficiency).

**Table S1**

Results of model selection including results for Akaike Information Criterion (AICc and △AICc) of the best selected models for MNC, BNC, and FNC. Model 1 included soil nutrients. Model 2 included microbial traits. Model 3 included soil EEA. Model 4 represents the full model including all three parameter groups. We indicated with colors when parameters were selected in the models. Light blue represents soil nutrient variables, light orange represents soil microbial trait variables, light green represents soil extracellular enzyme activity variables. We present the Model $R^2$, *adj*.$R^2$ and AICc values for all the selected models with ΔAICc ⩽2.

| | | MNC | | | | BNC | | | | FNC | | | |
|---|---|---|---|---|---|---|---|---|---|---|---|---|---|
| | Model comparison | Model 1 | Model 2 | Model 3 | Model 4 | Model 1 | Model 2 | Model 3 | Model 4 | Model 1 | Model 2 | Model 3 | Model 4 |
| Models Parameters | $R^2$ | 0.26 | 0.17 | 0.26 | 0.50 | 0.16 | 0.08 | 0.21 | 0.33 | 0.18 | 0.12 | 0.20 | 0.31 |
| | *Adj* $R^2$ | 0.23 | 0.13 | 0.24 | 0.45 | 0.13 | 0.06 | 0.18 | 0.28 | 0.16 | 0.09 | 0.18 | 0.26 |
| | AICc | 192.6 | 200.7 | 189.9 | 173.8 | 199.5 | 203.4 | 195.4 | 190.4 | 197.6 | 202.6 | 195.6 | 190 |
| | ΔAICc | 18.8 | 26.9 | 16.1 | 0 | 11.7 | 15.6 | 7.6 | 0 | 7.6 | 12.6 | 5.6 | 0 |
| Soil Nutrient | $NH_4^+$ | | | | | | | | | | | | |
| | $NO_3^-$ | | | | | | | | | | | | |
| | DON | | | | | | | | | | | | |
| | TIP | | | | | | | | | | | | |
| | TOP | | | | | | | | | | | | |
| | OlsenPo | | | | | | | | | | | | |
| | OlsenPi | | | | | | | | | | | | |
| Microbial trait | MBC | | | | | | | | | | | | |
| | CUE | | | | | | | | | | | | |
| | Turnover rate | | | | | | | | | | | | |
| Extracellular enzyme activity | BG | | | | | | | | | | | | |
| | LAP | | | | | | | | | | | | |
| | AP | | | | | | | | | | | | |

Abbreviations: DON (dissolved organic N), TIP (total inorganic P), TOP (total organic P), OlsenPo (Olsen organic P), OlsenPi (Olsen inorganic P), MBC (microbial biomass C), CUE (microbial C use efficiency), AP (acid phosphatase), β-glucosidase (BG), and LAP (leucine-aminopeptidase).

# Chapter V

# Summary

**Summary**

This Ph.D. project, conducted in a temperate forest in Achenkirch, Austria, in the European Alps, investigated the effects of long-term soil warming over a period extending beyond 14 years. It focused on understanding the impact of warming on primary metabolites (organic acids, amino acids, and sugars) in both root tissues and root exudates, as well as on microbial necromass C dynamics. It offers a thorough insight into how prolonged soil warming influences the metabolism of tree root tissues and root exudates, as well as the behavior of microbial necromass C, thereby contributing to a better understanding of temperate forest responses to climatic warming.

In Chapter 2, I investigated the response of primary metabolites in root tissues to long-term soil warming across three seasons (spring, summer, and autumn) and two years (2020 and 2021). We quantified 44 different metabolites, including 19 amino acids, 12 organic acids, and 13 sugars. The results showed that sugars dominated the primary metabolites. Soil warming significantly increased the total concentration of primary metabolites, and of total amino acids and sugars, but had no effect on total organic acids. Interestingly, primary metabolite profiles varied notably across different seasons and years, with less variation observed between warmed and control treatments. This indicates that changes in metabolite profiles were not driven by the responses of single or a few compounds to warming, but rather followed a general up- or downregulation of most primary metabolites, and therefore of primary metabolism. Additionally, a comprehensive metabolite pathway analysis revealed significant impacts of soil warming on several key metabolic pathways, most notably those involved in starch and sucrose metabolism, galactose metabolism, and amino acid metabolisms. These changes in metabolic pathways may aid roots in adapting to stressful environments, providing osmoprotectants or aiding in thermal acclimation, and enabling the roots to better match nutrient uptake and assimilation requirements under warming. Overall, this chapter provides valuable insights into how long-term soil warming affects primary metabolites in root tissues, highlighting the complex interplay between climatic conditions and plant metabolism. This underscores the importance of understanding these dynamics in the context of ongoing climate change and its impact on forest ecosystems.

In Chapter 3, I focused on the effects of long-term soil warming on root exudates in a temperate forest, specifically examining the quantity and composition of primary metabolites. The results indicate that organic acids are predominant in root exudates, contrasting the

metabolite composition in root tissues which was dominated by sugars. The results highlight those seasonal variations impacted root exudation rates more than soil warming did, with the highest rates of total primary metabolites and sugars observed in summer 2021, and amino acids peaking in autumn 2021. Non-parametric dissimilarity analyses and NMDS analysis revealed that primary metabolite profiles in root exudates changed significantly across sampling dates but remained consistent between warmed and control treatments, demonstrating their resilience to warming. A notable finding is that root tissues contain a broader variety of metabolites compared to root exudates, with Principal Component Analysis showing distinct segregation between their metabolite profiles. There was a strong positive correlation between individual metabolites in root tissues and exudates, though their profiles differed. This challenges the previous assumption that soil warming increases metabolite exudation, suggesting instead that root exudate responses to environmental changes are complex and may involve physiological adjustments like increased root biomass and specific compound concentrations. The study emphasizes the importance of further research into root exudation compounds, especially secondary metabolites, to better understand their roles in relation to rhizosphere microbial communities, plant growth strategies, and adaptation to climate warming.

In Chapter 4, I examined the impact of long-term soil warming on soil microbial necromass C dynamics at different soil depths and explored the underlying mechanisms, such as the formation and decomposition of microbial necromass. The results indicate that long-term warming significantly reduced bacterial necromass C, fungal necromass C, and microbial necromass C, though it did not significantly affect the fungal necromass C to bacterial necromass C ratio. Specifically, soil warming led to an 11% reduction in microbial necromass C at 0-10 cm depth and a 33% reduction at 10-20 cm depth. This reduction in microbial necromass was due to a warming-induced decrease in microbial necromass formation and an increase in microbial necromass decomposition. The study attributes the reduction in microbial biomass C and microbial C use efficiency primarily to a decline in soil phosphorus content caused by warming which reduced microbial growth. Interestingly, warming also increased the activity of soil extracellular enzymes, such as N-acetylglucosaminidase and leucine aminopeptidase, thereby accelerating MNC decomposition. Overall, the findings suggest that long-term soil warming leads to a significant decrease in microbial necromass C, primarily due to phosphorus limitations and increased soil enzyme activity. This could have substantial effects on soil organic C content

in temperate forest ecosystems. The study highlights the complexity of soil carbon dynamics under climate warming and its potential broader impacts on forest ecosystems, emphasizing the decoupling of microbial necromass carbon formation and decomposition processes.

Overall, this Ph.D thesis contributed novel insight into long-term soil warming effects on the concentration and composition of primary metabolites of tree root tissues and root exudates, and also on soil microbial necromass C dynamics. Soil warming significantly increased amino acids (15%) and sugars (21%) in root tissues, while not affecting organic acids. This indicates stimulated root growth, respiration, and nutrient uptake under warming conditions, with a general up- or downregulation of primary metabolites (Chapter 2). Root exudation rates and exudate profiles did not significantly respond to warming but varied seasonally, indicating intricate interactions between root metabolism and environmental factors. The profiling of primary metabolites in root tissues and exudates differed, yet the positive relationship between these primary metabolites in root tissues and exudates remained unchanged, reflecting a complex but consistent metabolic interplay (Chapter 3). Soil warming also led to a reduction in microbial necromass carbon by 11% in the upper soil layer (0-10 cm) and 33% in the lower soil layer (10-20 cm), primarily due to decreased microbial biomass and carbon use efficiency, compounded by limited soil phosphorus for microbial growth. Increased activity of soil extracellular enzymes under warming conditions further accelerated microbial necromass decomposition (Chapter 4). These findings highlight the multifaceted effects of climate warming on tree root metabolism and microbial necromass C dynamics, underscoring the complex responses of temperate forest ecosystems to environmental changes.